HOKKAIDO UNIVERSITY

Title	Seismic Performance of Base-isolated Bridges under Low Temperature in Snow Cold Region
Author(s)	干, 治平
Degree Grantor	北海道大学
Degree Name	博士(工学)
Dissertation Number	甲第12462号
Issue Date	2016-09-26
DOI	https://doi.org/10.14943/doctoral.k12462
Doc URL	https://hdl.handle.net/2115/63436
Type	doctoral thesis
File Information	Gan_Zhiping_.pdf

Hokkaido University Collection of Scholarly and Academic Papers : HUSCAP

2016 Doctor Thesis

Seismic Performance of Base-isolated Bridges under Low Temperature in Snow Cold Region

積雪寒冷地における低温時免震橋梁の地震応答性状に関する研究

Gan Zhiping

Laboratory of Bridge and Structural Design Engineering

Graduate School of Engineering

Hokkaido University

ABSTRACT

Base isolation system is one of the most effective technologies for protecting structures from damages in earthquakes. It has been extensively used worldwide in recent years, considering the increasing threat of great earthquakes. The basic strategy of base isolation system is that a structure can be uncoupled from the damaging effects of the ground movement in a strong earthquake, by taking advantage of the flexibility of base isolation devices, which provides flexibility through its ability to deform and move but return to its original position, i.e., restoring ability.

Base isolation devices, which are mainly made of material rubber, have temperature dependence behavior due to its material characteristics as an elastomer type of polymer. The thermal effect, when applied to polymers, induce a transition from a elastomeric, rubbery phase to a brittle, glassy solid amorphous phase on cooling. Consequently, the stiffness of polymer trends to increase with the decreasing temperature. With the increment of stiffness of rubber material, the flexibility of base isolation devices is deteriorated and therefore its seismic protection capability will be weakened.

For engineering purposes, cold regions are defined as any region where cold temperatures, unique terrain, and snowfall significantly affect engineering structures for one month or more each year. About one quarter of the earth's land mass may be termed severely cold. Since the area of cold regions unavoidably overlap with seismic zone, i.e. Hokkaido Island of Japan, it is necessary to take account of the low temperature effect on base isolation system in seismic response analysis.

This study conducts a three-dimensional non-linear numerical analysis to evaluate the seismic performance of curved grillage girder viaducts equipping base isolation system when it is applied in severe cold environment. For this purpose, a finite element modeling is adopted to examine the seismic response of bridge system in detail under the action of near-fault earthquake ground motions. Various base isolation systems which represent various temperature conditions are systematically compared and discussed. Temperature effect and temperature variation is taken into account particularly. And for the practicability and preciseness, a dynamic bearing property definition method is introduced to carry out the temperature and performance variation process of base isolation system during earthquake.

The temperature effect on lead rubber bearing (LRB) base isolation system is the main focus of this study, since it has been widely applied. Anylytical cases of high-damping bearing (HDR) bearings are also added as comparison. For practice and accuracy, the parameters of commercial products are adopted, which have been proved to be proper design under room temperature in previous studied. Nonlinear dynamic analysis is performed to obtain structural responses of the viaducts under the input earthquake waves which are obtained from 1995 Kobe earthquake which supposed an inflection point in seismic design of highway bridges in Japan, and 2003

Tokachi-oki earthquake which has a much longer duration to raise the temperature of bearings higher.

The main object of this study is to confirm the necessity of considering low temperature effect of base isolation system in seismic response analysis. In order to achieve this, a series of numerical results are carried out. Base-isolation bearings with energy dissipation capacity, demonstrate to be very effective in suppressing excessive force responses acting on bridge piers when subjected to strong earthquakes. Based on the dynamic analysis results, it is found that these types of bearing systems may prevent structural damage during a seismic event, because their demand-reduction features provide a significant reduction in the seismic forces that the bridge structure must resist. Moreover, due to an appropriate selection of the design parameters of these bearing systems, moderate deformations of isolator devices are observed. This result is significant in that it indicates that LRB base-isolation systems are capable of controlling peak deck displacement response. Whereas cold region factors conspicuously weaken this base isolation function, which is the main conclusion of this study. In this study, by adopting dynamic bearing property definition method and examining the numerical results, the necessity of considering low temperature effect, not only in a short-duration earthquake, but also in a long-duration earthquake, has been clearly indicated.

On the other hand, high damping rubber (HDR) bearing system, which are expected to be an improvement of LRB system, still keep relatively large area of hysteresis loops under low temperature. This is because the yield force of HDR is much lower than LRB with a lead plug inside. Then HDR could take more advantage of stiffness after yield stage, achieving an overall low stiffness.

Temperature dependence performance of base-isolation systems of highway viaducts offers many possibilities for further research. In the present study, additional investigation has been conducted to study the response of variable performance of base isolation system, which is time and temperature dependence. In particular, application of heat conduction technology to different types of base isolation systems, acquiring the accurate temperature value in specified time and finally putting a dynamic properties definition of base isolation systems into use in the seismic analysis.

A further area for research concerns more detailed evaluation of HDR bearing system in cold region, which has better performance than LRB system in this study. As mentioned above, seismic protection capacity should be balanced with deformation, which may be the main problem of application of HDR bearing system.

It is also suggested to develop more temperature independence isolator devices. Since additional constant temperature equipment for base isolation systems is obviously inefficient, temperature independence materials and structures could be a better idea. And this is actually being studied by several manufacturers.

DEDICATION

I make a special dedication to my parents, Gan Minfeng and Wu Sufen. Thanks to their love, patience, and sacrifice, I could achieve one of my greatest dreams.

ACKNOWLEDGEMENTS

First of all, I would like to extend my sincere gratitude to my supervisor, Professor Hayashikawa, not only for his instructive advice and helpful suggestions on my thesis, but also for his kindness and niceness to all the students. I will never even forget my first meeting with you, I was so nervous, so anxious, so afraid in this brand new world as a foreign student. But your smile and humorous talking smash my worry, as well as your instructions bring me deeply into the world of science. I am deeply grateful of your help in the completion of my doctor course.

Every result described in this thesis was accomplished with the help and support of professors and fellow lab-mates from the Laboratory of Bridge and Structural Engineering. I wish to express my cordial appreciation to Professor Matsumoto, whose advice, motivation and encouragement always created the best environment in our laboratory. I extend many thanks to my colleagues and friends, especially Dr. Sun Liangming, Dr. Tian Qin and Dr. Deng Pengru for the many helpful comments and suggestions to improve the results of this thesis. I am greatly indebted to the research members of the laboratory, for their support and the excellent research environment and advanced facilities provided in the laboratory. I gratefully acknowledge funding by Hokkaido University, Hokkaido International Exchange and Cooperation Center and Japan Student Services Organization for the financial supports providing me this precious opportunity and therefore making all of this possible.

High tribute shall be paid to Mr. Yoshino, as my first supporter, you helped me dealing with all the complicated procedures. It's really hard for a foreigner to understand this system immediately, your patience overcame them pretty well. And even more fortunately, your advice and notes of study helps my research very much.

I am also deeply indebted to all the other tutors and teachers in doctor course for their direct and indirect help to me. The lectures you gave were greatly impressive, and your methods of study inspired me.

Special thanks should go to my Japanese friends who belong to Hokkaido University hiking circle Amazon. They kindly shared much precious time and experience with me. I will never forget the exciting hiking activities with them.

Finally, I am really really appreciated to my parents for their continuous support and encouragement. Without your hard push, I would never achieve this.

July 2016
Gan Zhiping

CONTENTS

ABSTRACT
DEDICATION
ACKNOWLEDGEMENTS
CONTENTS
CHAPTER 1: GENERAL INTRODUCTION
1.1 Statement of the Problem 1
1.1.1 Seismic damage of highway viaducts 2
1.1.2 Seismic protection strategy 4
1.1.3 Seismic design in cold region 5
1.2 Brief Review of Previous Research 6
1.2.1 Study on seismic isolation system 7
1.2.2 Low temperature effect in dynamic analysis 8
1.3 Object and Scope of Study 9
1.4 Organization of the Thesis 10
References 11
CHAPTER 2: DESCRIPTION OF HIGHWAY VIADUCT
2.1 Introduction 16
2.2 Superstructure 18
2.3 Substructure 19
2.3.1 Design horizontal seismic coefficient 20
2.3.2 Allowable stress evaluation 21
2.2.3 Cross section fiber element model 22
2.4 Bearing Supports 23
2.4.1 Lead-rubber bearings 24
2.4.2 Low temperature effect on LRB 25
2.5 Input Earthquake Ground Motions 26
2.5 Conclusion 28
References 28
CHAPTER 3: NONLINEAR DYNAMIC ANALYSIS
3.1 Introduction 30
3.2 Natural Vibration Analysis Formulation 31
3.3 Three-dimensional Fiber Beam Element Formulation 34
3.3.1 Strain displacement relations 35
3.3.2 Equilibrium condition 36
3.3.3 Finite element formulation 37
3.3.4 Solution technique of non-linear equilibrium equation 38
3.4 Non-linear Dynamic Equilibrium Equation of Motion 41
3.4.1 Dynamic equilibrium equation 41
3.4.2 Consistent mass matrix 41

3.4.3 Damping mechanism 42
3.4.4 Integration of dynamic equilibrium equation 43
3.5 Energetic Analysis 46
3.6 Conclusions 47
References 48
CHAPTER 4: SEISMIC RESPONSE OF HIGHWAY VIADUCTS EQUIPPED WITH LRB UNDER LOW TEMPERATURE
4.1 Introduction 50
4.2 Lead-rubber Bearing Isolation System 51
4.2.1 LRB analytical model 52
4.2.2 Radial restraint configurations of LRB isolation system 53
4.2.3 Low temperature effect on LRB 54
4.2.4 Heat production and temperature variation analysis 55
4.2.5 Application of dynamic bearing property definition 58
4.3 Numerical Results Considering Low Temperature Effect 56
4.3.1 Natural vibration analysis 59
4.3.2 Shear force-displacement response at bearing 61
4.3.3 Bending moment-curvature response 62
4.3.4 Energy-time history 64
4.3.5 Displacement-time history at top of pier 65
4.4 Conclusions 67
References 68
CHAPTER 5: EVALUATION AND DISCUSSION OF LONG DURATION EARTHQUAKE CASES
5.1 Introduction 71
5.2 2003 Tokachi-Oki Earthquake 72
5.3 Analytical Cases 74
5.4 Numerical Results of Long Duration Earthquake Cases 76
5.4.1 Natural vibration analysis 76
5.4.2 Shear force-displacement response at bearing 77
5.4.3 Bending moment-curvature response 78
5.4.4 Energy-time history 79
5.4.5 Displacement-time history at top of pier 80
5.5 Conclusions 81
References 82
CHAPTER 6: TEMPERATURE-DEPENDENT BEHAVIOR OF HIGH DAMPING RUBBER BEARING
6.1 Introduction 83
6.2 High-Damping Rubber Bearing Isolation System 84
6.2.1 Thermal analysis 84
6.2.2 Time-varying temperature of HDR 85
6.2.3 Behavior variation with temperature 86
6.2.4 HDR modeling 87
6.3 Numerical Results of HDR Cases 88

6.3.1 Natural vibration analysis 88
6.3.2 Shear force-displacement response at bearing 90
6.3.3 Bending moment-curvature response 92
6.3.4 Energy-time history 93
6.3.5 Displacement-time history at top of pier 94
6.4 Conclusions 95
References 95
CHAPTER 7: CONCLUSIONS
7.1 Summary of the Present Study 96
7.2 Recommendations for Further Research 99

CHAPTER 1

GENERAL INTRODUCTION

1.1 Statement of the Problem

Highway viaducts are extremely important components in modern transportation networks. Bridges play the role of critical lifeline facilities due to their significance in the economic development of a nation and their importance in supporting the daily functions and needs. Unfortunately, such essential systems often become the victims of earthquakes. Society suffers a tremendous cost and inconvenience due to the collapse of a bridge. Even non-collapsed, the temporary lost of post-earthquake serviceability of important bridges may cause very costly disruption to vehicle traffic on major transportation arteries and is simply unacceptable [1, 2]. In the immediate aftermath of an earthquake, closure of a bridge can impair emergency response operations. Additionally, the direct economic loss, attributed to replacement or repair cost of the damaged bridges, forms only a minor portion of the total losses. The major cost, which is often difficult to estimate accurately, is associated with the disruption of vehicular movement immediately following the earthquakes and during the long re-construction phase [3]. In order to ensure the functionality and operationally of highway bridges, it is therefore essential to design them to safely withstand the devastating forces of earthquake ground motions.

The tragic examples of bridge seismic damage during past earthquakes have served as full-scale laboratory tests and have forced engineers to reconsider design principles and philosophies. Ideally, earthquake-resistant constructions should be designed to have regular configurations so that their behaviour is simple to conceptualize and analyze. This ideal is often not achievable in bridge structures due to the irregularities imposed by site conditions and traffic flow requirements. In practice, it is generally accepted the fact that bridges with irregular configurations complicate and potentially magnify the seismic responses.

Base isolation system is one of the most effective technologies for protecting structures from damages in earthquakes. It has been extensively used worldwide in recent years, considering the increasing threat of great earthquakes. The basic strategy of base isolation system is that a structure can be uncoupled from the damaging effects of the ground movement in a strong earthquake, by taking advantage of the flexibility of base isolation devices, which provides flexibility through its ability to deform and move but return to its original position, i.e., restoring ability.

Base isolation devices, which are mainly made of material rubber, have temperature dependence behavior due to its material characteristics as an elastomer type of polymer. The thermal effect, when applied to polymers, induce a transition from a elastomeric, rubbery phase to a brittle, glassy solid amorphous phase on

cooling. Consequently, the stiffness of polymer trends to increase with the decreasing temperature. With the increment of stiffness of rubber material, the flexibility of base isolation devices is deteriorated and therefore its seismic protection capability will be weakened.

1.1.1 Seismic damage of highway viaducts

The widely recognized susceptibility to earthquake damage of curved highway viaducts is substantially amplified with the irregularity originated by the rupture of continuity of the deck superstructure at expansion joints. Long bridges are constructed as multiple spans separated by joints in the superstructure to accommodate thermal expansions and contractions without inducing large forces to the bridge components. Recent strong earthquakes have repeatedly demonstrated that during an earthquake, adjacent spans often vibrate out-of-phase, causing three main types of displacement problems. The first type is the catastrophic damage that occurs when the seismically induced separation at the expansion joint is excessively large. This major change in the bridge geometry is absorbed by the deformation capacity of steel roller bearing supports located under the joint. In case of extreme ground earthquakes, the induced relative displacements to roller bearings can exceed the seat width at the pier top, causing the dislodgement of the rollers from the bearing assembly and the subsequent collapse due to deck superstructure unseating [4-7]. Unseating of simply-supported bridge spans is the most common seismic damage and it has been observed to be considerably magnified by complex bridge configurations like curved deck geometries. Unseating of simply-supported deck superstructures has occurred during all major earthquakes. Dramatic examples are the collapse of the Showa Bridge in the 1964 Niigata Earthquake [8] and the collapsed upper and lower decks of the eastern portion of the San Francisco-Oakland Bay Bridge in the 1989 Loma Prieta Earthquake [9]. The second type of damage at expansion joints is the one caused by adjacent spans pounding together at the joints. In addition to the expected local damage at colliding girders, the impact character of pounding forces can potentially contribute to the loss of stability of bridge decks due to fracture of bearing supports [10]. The third type of damage is related to residual horizontal and vertical separations of damaged expansion joints that may substantially disrupt the post-earthquake serviceability of a bridge.

The last type of irregularity is found at the weak connection between deck superstructure and substructure members. This link is considerably fragile due to the vulnerability of steel bearing supports. Failure of steel bearings can cause substantial damage to superstructures, large differences in levels of the road surface and damaged superstructure ends, which impede the vehicle flow. The deficient seismic performance of steel bearings is generally identified as a consequence of their brittle behaviour. Failure of bearings in an earthquake can cause redistribution of internal forces, which may overload either the superstructure or substructure, or both. The 1995 Hyogoken Nanbu Earthquake provides several examples of steel bearing failures [11]. One of them is the severe damage sustained by the Hamate Bypass, a

double-deck elevated roadway comprising steel box girders on either fixed or expansion steel bearings. Another example is provided by the Nishinomiya-ko Bridge in which the fixed-end bearings failed, apparently causing the unseating of the adjacent approach span.

Japan is one of the most seismically prone countries in the world and has often suffered significant damage from large earthquakes. More than 3,000 highway bridges have sustained seismic damage since the 1923 Kanto Earthquake [12]. Important progresses in seismic design provisions for highway bridges have been developed based on research findings and lessons learned from past earthquakes. In Japan, seismic design of highway bridges started in 1924, one year after the 1923 Great Kanto Earthquake. In 1971 the modem Specifications for Seismic Design of Highway Bridges [13], which introduced design methods for soil liquefaction and unseating prevention devices, were published. In 1980 the Specifications were revised and integrated as "Part V: Seismic Design" in the Design Specifications of Highway Bridges including the check method for ductility of reinforced concrete piers. In 1990 it was further modified to recommend a detailed ductility check method for reinforced concrete piers, soil liquefaction, dynamic response analysis, and design detailing [14]. The 1995 Hyogoken Nanbu Earthquake supposed an inflexion point in seismic design of highway bridges in Japan. This earthquake dramatically changed the perception of the way in which highway bridges respond to seismic ground shaking. The Hyogoken Nanbu Earthquake has been extensively studied and analyzed, mainly in Japan but also elsewhere in the world, because it is the first real case of a strong earthquake affecting a large and densely populated metropolitan area. The seismic vulnerability of simply-supported bridges was made evident by the failure due to deck unseating of many of these structures. Lifeline systems were heavily disrupted during the earthquake, and the collapse of major infrastructures such as viaducts of elevated highways and railway tracks during the earthquake was an unprecedented shock. As a favorable fact, the Hyogoken Nanbu Earthquake provided a stimulus to investigate the seismic response of highway bridges.

Immediately, in response to the serious damages to bridges observed after the earthquake, the 1990 Specifications were completely revised and new comprehensive Design Specifications of Highway Bridges [15] were published in 1996. A major revision of the 1996 Specifications was the introduction of explicit two-level seismic design consisting of the seismic coefficient method and the ductility design method. The last modification of the Japanese Seismic Specifications in 2002 included the performance-base principles of bridge seismic design.

Based on the above considerations, it is clear how the necessity of an accurate design of new bridges and the seismic evaluation of existing structures have become deeply felt issues. It is broadly recognized that curved bridges are complex and unique structures, which can be subjected to different vibration movements during an earthquake. Therefore, a realistic prediction of the bridge seismic response should consider the adoption of refined three- dimensional finite-element models. On the other hand, the considerable complexity associated with the analysis of highway viaducts, particularly under the extreme ground motions generated by Level II

earthquakes, imposes the obligatory adoption of dynamic time-history analysis with considerations of geometrical and material non-linearities. Moreover, the strong motion data from the Hyogoken Nanbu Earthquake [16] provides an exceptional set of near-fault measurements of strong shaking that invite to investigate the bilateral directivity excitation effects, which greatly contribute to increase the damage sustained by simply-supported bridges during near-fault seismic excitations.

1.1.2 Seismic protection strategy

Bridges consist of many structural components, which contribute to the overall resistance ability of the system. The safety of highway bridges and the functional capability of the associated emergency transportation routes in the aftermath of a major earthquake are essentially dependent upon their seismic resistance. With the rapid development of highway systems, steel bridge piers have become widely adopted to support highway viaducts in urban areas in Japan, being considered specially advantageous in regions of high seismic activity [17]. However, in the 1995 Hyogoken Nanbu Earthquake, thin-walled steel bridge piers suffered severe seismic damage in the form of local buckling for the first time in world history [18]. This fact emphasizes the need for increasingly sophisticated analysis technique capable to provide predictable performance of steel bridge piers that could be subjected in the future to earthquake ground motions more severe than anticipated by design codes. On the other hand, the disastrous consequences that a bearing failure can cause on the overall earthquake performance of a bridge highlight the idea that the bearing support is one of the essential structural members of a bridge. Therefore, the concept, in which the bearing supports are regarded as a fuse or as having a fuse-like function for alleviating the potential damage to the whole bridge, should be avoided.

The increasing need for safer bridges has stimulated the adoption of a common earthquake protection strategy consisting in the replacement of the vulnerable steel bearing supports with seismic isolation devices [19]. An isolation system placed between the bridge superstructure and its supporting substructure is generally capable of increasing both flexibility and energy dissipation. Flexibility in the horizontal plane will lower the fundamental frequency of the bridge below the range of the most-damaging frequencies, which dominate general earthquake input so that the earthquake-induced acceleration will be decreased. The energy-dissipating capacity of isolation bearings is used to considerably reduce the damaging energy exerted to the bridge piers. Moreover, when isolation bearings are installed at the top of the piers, the lateral force of a superstructure can be distributed to each substructure, and thus the concentration of lateral force to several specific substructures can be avoided.

Many different types of seismic isolation devices have been developed and tested for seismic applications over the last three decades, and more are still being investigated. Among the great variety of seismic isolation systems, lead-rubber bearings (LRB) have found wide application in bridge structures [20]. This is due to their simplicity and the combined isolation-energy dissipation function in a single compact unit. LRB bearings are steel reinforced elastomeric bearings in which a lead

plug is inserted to provide hysteretic damping as well as rigidity against minor earthquakes, wind and service loads. The lead plug yields at relatively low shearing stress resulting in significant dissipation of seismic energy and reduction of earthquake response. By using hydraulic jacks, the superstructure of the bridge can be lifted to remove the original bearings, easily replacing them with suitable LRB bearings. In practice, isolated bridges with LRB bearings have been proven to perform effectively reducing the bridge seismic response during earthquake shaking. The Thjorsa River Bridge in Iceland survived two major earthquakes of moment magnitudes (M_w) 6.6 and 6.5 without serious damage and was open for traffic immediately after the earthquakes as reported by Bessason and Haflidason [21].

Seismic isolation systems provide an alternative to conventional earthquake resistance design, and have the potential for significantly reducing seismic risk without compromising safety, reliability, and economy of bridge structures. Furthermore, with the adoption of new performance-based design criteria, seismic isolation technologies will be the choice of more structural engineers because they offer economical alternatives to traditional earthquake protection measures. Although installation of isolation devices is generally favorable, the reduction in seismic forces may be accompanied by an increase in displacement demand that shall be accommodated within the isolation system and any adjacent structures [22]. This consideration could be critical in case of curved isolated structures due to the effects of asymmetric response in horizontal displacements. Therefore, seismic response of isolated curved bridges needs to be precisely investigated; evaluating the probable increase of pounding of simply-supported isolated bridges subjected to strong earthquake shaking. In order to design safer isolated structures, capable of resisting Level II earthquakes, accurate modeling of isolation bearing supports needs to be explored, developing new and more comprehensive concepts for realistic prediction of the isolation behaviour under strong ground motions.

1.1.3 Seismic design in cold region

Cold regions are part of the earth system characterized by the presence of snow and ice at least part of the year [23], as shown in **Fig. 1.1**. Roughly divided into polar and sub-polar regions, historically a majority of these cold regions is sparsely populated with minimum human impact to nature. Due both to the pressure of population and economic development, this picture is changing. Global warming may accelerate the pace of change. The theme on cold regions science and technology is developed to cover a cross-section of topics in fundamental science and practical engineering for cold regions. Climate change has modified the distribution of cold regions around the world. These modifications also come from economic developments. Human activities, especially those of grand scales, have potential to greatly impact cold regions environment. Science and technology development in and for the cold regions can only come from scientific understanding of many inter-related processes. Synthesis of these processes using sophisticated mathematical modeling is often needed. Issues discussed in this theme demonstrate the breadth of knowledge required to address the natural phenomena and engineering challenges in cold regions.

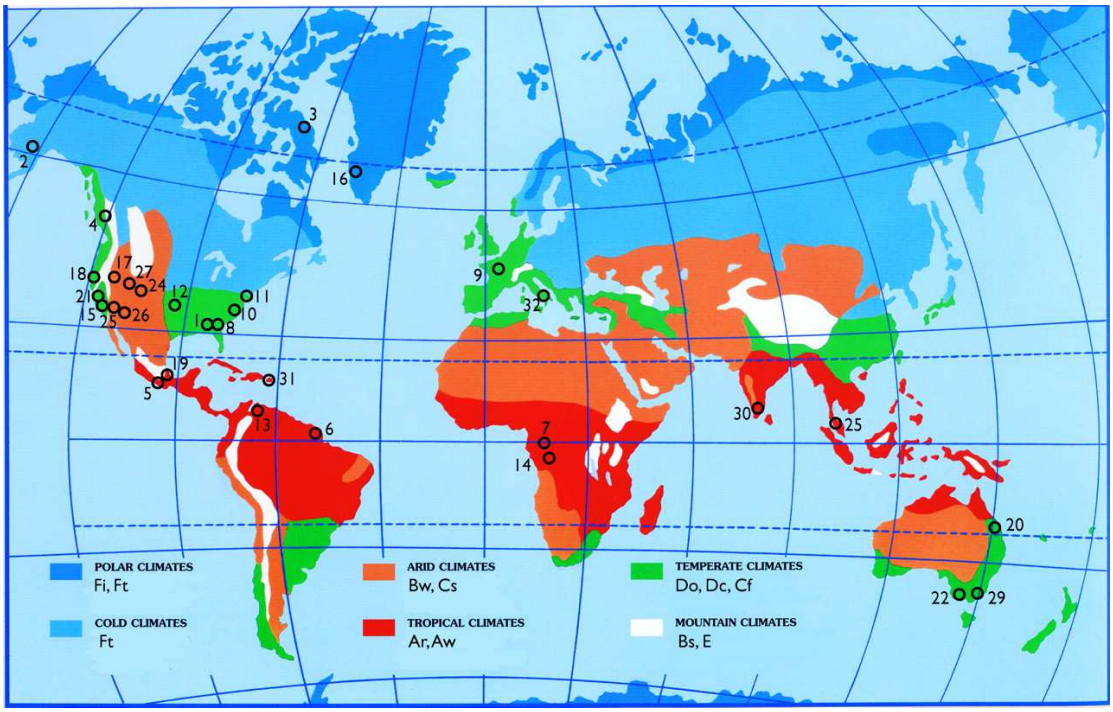


Fig. 1.1: Cold Region Classification

Seismic design encounters a major problem in cold region: low temperature. As mentioned above, the application of base isolation system has been proved to be a quite sensible seismic strategy to improve safety, stability and survivability of bridges in an earthquake event. The main material of base isolation devices is rubber, whose performance is temperature dependence. The elasticity of a rubber increases as temperature increases [24]. This material characteristics of rubber results in the performance variation of base isolation devices under low temperature. With the increment of stiffness of rubber material, the flexibility of base isolation devices is deteriorated and therefore its seismic protection capability will be weakened [25]. However, even after years of practice, the temperature dependence behavior of base isolation devices is still a less understand issue.

1.2 Brief Review of Previous Research

Contrary to straight bridges, a very limited documentation on the study of horizontal curved bridges has been made available. This fact severely narrows the literature regarding the effects of seismic activities on horizontally curved bridge superstructures. In 1976, experimental studies on the seismic response of high curved over crossings were performed by Williams and Godden. [26]. Their experiments are related to seismic resistance of large multi-span curved over crossings similar of the type, which suffered heavy damage during the 1971 San Fernando Earthquake. In New Zealand, Buckle [27] conducted in-situ response evaluation of two bridges subjected to earthquake loads, one straight and the other curved and continuous over many spans. Time histories of acceleration and displacement were collected and

analyzed using spectral analysis. Abdel-Salam and Heins. [28] carried out a study on the seismic response of curved bridges. They examined moments and shear occurring at abutments, bents, and column bases of their model by analyzing the response history of the bridge. Chen [29] presented the effects of various modeling and analysis methods on seismic responses of curved bridges. Important system parameters such as bridge length, soil-structure interactions and bridge skews were examined. DesRoches and Fenves [30], in 1997, evaluated the earthquake response of a curved highway bridge. They developed a three-dimensional calibrated bridge model to investigate and compare the significant differences between uniform free-field and non-uniform input motion. More recently, a study by Hayashikawa et al. [31] evaluated in detail the influence of various bearing conditions on curved bridges. This investigation showed that the effects of steel bearing support conditions dramatically affect the seismic behavior of curved bridges.

1.2.1 Study on seismic isolation system

The idea of seismic isolation dates back to the late nineteenth century, but its application was delayed by the lack of suitable commercial isolation components. Since the middle 1980s,substantial development has occurred and seismic isolation for certain types of civil structures in now considered a highly viable design option by the seismic engineering community for moderate to extreme seismic excitation. Extensive reviews on historical developments and recent literature on isolation systems have been provided by Kelly [32] and Buckle and Mayes [33]. In the recent years, several studies have been carried out in order to understand the performance of seismic isolation devices and systems. A variety of isolation devices, including elastomeric bearings, frictional/sliding bearings and roller bearings have developed and used practically for seismic design of bridges. The lead rubber bearing (LRB) system was invented and developed by Robinson in the 1970s to achieve high damping and initial rigidity when a lead core is inserted in the laminated rubber system. Firstly, LRB bearings were applied to the seismic isolation of bridge structures in New Zealand since 1978 [34] when installed to the Toetoe Bridge. The Sierra Point Overhead highway bridge was the first bridge to be seimically isolated with LRB bearings in the United States in 1985. One year later, in 1986, the Carafone bridge was constructed the first Italian bridge supported on LRB isolators, while in Japan, the Miyagawa bridge, built in 1991, was the first bridge in Japan to be isolated using LRB bearings. Since then, mechanical properties and analytical models have been investigated and proposed by different authors, being specially remarkable those carried out by Kikuchi and Aiken [35], Huang and Chiou [36],and Mori et al. [37]. Additionally, a number of experimental studies have been reported on the load deformation behaviour of LRB isolation devices in the past. Kelly et al. [38] and Buckle and Kelly [39] studied quarter-scale models of straight and skewed bridge decks mounted on plain and LRB bearings subjected to earthquake ground motions using a shaking table. The deck response was compared to determine the effectiveness of mechanical energy dissipaters in isolation systems and investigate the mode of

failure of isolated bridges. Wei et al. [40] evaluated the effectiveness of LRB bearings for aseismic design of bridges by earthquake simulation test of a bridge model. In New Zealand, Robinson [41] carried out studies on seismic isolation for new and retrofitted bridges. A special lead-extrusion damper and LRB bearings were developed for this specific purpose. Igarashi and Iemura [42] studied the effects of the implementation of LRB bearings as seismic isolators of highway bridge structures under seismic loads using the substructure hybrid loading (pseudo-dynamic) test method. The effectiveness of the isolation system was investigated based on acceleration and displacement amplifications using earthquake response results. Ando et al [43] conducted forced and free vibration tests on the Ohito Viaduct, scismically isolated with LRB bearings.

There had been several analytical studies in the past to demonstrate the effectiveness of seismic isolation with LRB bearings for earthquake-resistant design of bridge structures. An identification algorithm to investigate the dynamic properties of an isolated bridge equipped with LRB bearings was carried out by Tan & Huang [44] Chaudhary et al. [45] evaluated the performance of the Yama-age bridge with high damping rubber bearings, using recorded seismic data. Jankowski et al. [46] studied the pounding of superstructure segments in isolated elevated bridge with high damping rubber bearings during earthquakes. Wang et al. [47] and Mutobe and Cooper [48] studied the seismic response of bridges isolated with friction pendulum bearings, and Wilde et al. [49] developed a base-isolation system for elevated highway bridges using shape memory alloy device. Few studies have been earned out in order to evaluate the performance of various base-isolation systems for the same model of bridge structure. The most remarkable works include a comparative study on seismic performance of different base-isolation systems for multi-span continuous bridges was presented by Park et al. [50], and investigation about responses of bridges subjected to near-fault ground motions under different base-isolation conditions carried out by Jangid and Kelly [51]. The results of previous research earned out by Ruiz and Hayashikawa [52] indicate that a number of parameters of seismic isolation bearings can have a great impact on seismic response of bridge structures.

1.2.2 Low temperature effect in dynamic analysis

The temperature dependent mechanical behavior of rubber material was first investigated by Gough and Joule in 1805. They concluded that due to the entropy elasticity property of rubber, the elastic response changes with the absolute temperature of the material. Moreover, in the recent past, several experimental investigations of thermo-mechanical behavior of rubber materials have been conducted by some authors [53]. The conclusions from these experimental investigations have been made that the rate-independent behavior of rubber material is weakly dependent on the temperatures, whereas the rate-dependent behavior is very sensitive to the ambient temperature of the material. Some authors carried out experimental studies of the temperature dependence of rubber bearing based on sinusoidal loading tests, and a large scale experimental scheme was being conducted

to investigate the thermo-mechanical behavior of rubber bearings at different temperatures ranging from -30℃ to +40℃ [30]. The experimental results have been presented to prove the necessity of considering the temperature dependence in the rheology model. Based upon these experimental results, some practical computation models have been proposed to approach temperature effect on base isolation system, as shown in **Fig. 1.2**.

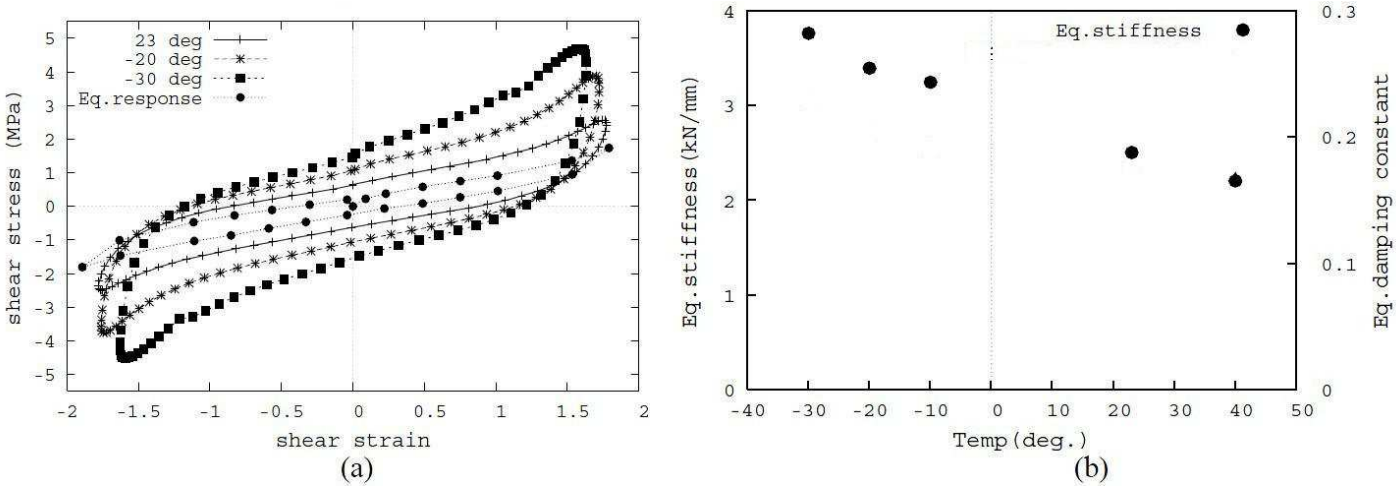


Fig. 1.2: Temperature Effect on LRB

In previous study by authors, a simplified bearing property modeling under low temperature which adopted only a fixed value was used to evaluate the low temperature. And the results clearly showed us the negative influence of low temperature [54].

1.3 Object and Scope of Study

The goal of design bridge structures in areas of high seismicity, implies that such structures should not only remain standing but should also be usable after a very large earthquake. Accomplishing this task requires an understanding of the behaviour of bridge structures, a knowledge of parameters affecting their seismic response, and an ability to predict their response to different types of earthquake loading.

Engineers and researchers have long recognized the importance of isolating bridges from earthquake loads. In spite of the recognition of the importance and role of seismic base-isolation in reducing seismic damage of bridges, it is evident that research orientated to obtain a higher level of performance for this isolator devices is required.

The primary objective of the present investigation is to assess the possible advantages and problems that various types of base-isolation bearings have on the performance of curved highway viaducts, under the action of great earthquake ground motions in cold region.

A secondary objective of this study is to optimize design of these seismic isolation systems affected by cold region factor to ensure the most appropriate response of highway viaducts subjected to earthquakes, determining what trends

occurs in the seismic response of a base-isolated bridge structure as the seismic isolation devices characteristics are modified.

The successful accomplishment of this main objective is achieved in three progressive stages. The first specific stage consists in developing a sophisticated three-dimensional analytical computer program capable of simulating and predicting the bridge structural behaviour in severely inelastic response under strong earthquake excitations. This is accomplished by the development of a realistic three-dimensional modeling of highway viaduct, which plenty represents the essential mechanical and structural properties of real bridge structures. The next stage starts with the accurate estimation of Level II earthquake demands on this curved viaduct model under room temperature condition. Posteriorly, the benefits on seismic performance with the adoption of seismic isolation bearings are evaluated. The final third stage further discusses a comprehensive measurement of cold region factor, how it affects and the solution of these problems.

The present study combines the use of a non-linear dynamic analysis methodology with a precise non-linear modeling of the entire bridge structural system in order to ensure stability of the global bridge performance under the action of Level II earthquake ground motions in cold region. Non-linear three-dimensional fiber elements are used to model the bridge piers and bearing supports, whereas the superstructure is represented as a planar grillage beam system. Cold region factor is introduced in this model and thermal analysis is conducted as well. In order to perform a complete investigation the non-linear viaduct seismic responses have been accurately analyzed to provide a refined estimation of seismic demands on critical bridge components with particular emphasis focused on the three-dimensional expansion joint behaviour and its interaction with the remaining structure. With the adoption of a three-dimensional viaduct analytical model, seismically induced forces and displacements acting on individual bearing supports can be calculated. This supposes a good approximation to the real response of the bridge under the action of earthquakes.

1.4 Organization of the Thesis

The thesis contents are organized in seven chapters, which are further divided into several sections and subsections. The chapters have individual introduction, which give brief orientations of the subject under investigation. For a detailed discussion of various aspects of the subject, many references have been included. The specific objectives of each chapter are as follows:

Chapter 1 provides the general introduction and motivating objectives of this research.

In **Chapter 2** the comprehensive three-dimensional analytical model of the highway viaduct object of this research is presented. The effects of the analytical model assumptions are investigated in detail using non-linear seismic time-history analysis. In order to ensure a realistic prediction of the bridge seismic response, an evaluation three-dimensional analytical model of the highway viaduct is

systematically performed. Simultaneously, the three-axiality effects of Level II earthquake ground motions on the response and performance of highway viaducts are discussed.

Chapter 3 presents the theoretical approach for a sophisticated three-dimensional analytical program capable of simulating structural behaviour in severely inelastic response and accurately predicting seismic response of bridges. The theoretical foundation of the non-linear finite element formulation includes the best features of several previous studies. A three-dimensional element, capable of modeling geometric and material non-linearities, is developed based on the fiber element model. An incremental-iterative method based on the Newmark direct integration method and the Newton-Raphson method is employed for obtaining the solutions of the non-linear dynamic equilibrium equations. The energetic analysis formulation and natural frequency analysis of the problem are also presented.

Nonlinear dynamic analysis is performed in **Chapter 4, Chapter 5** and **Chapter 6** to determine the structural response for the bridge members under the action of the input earthquake waves with temperature effect on base isolation systems. The overall structural performance of the model of highway viaduct is compiled, systematically compared and discussed for seismic performance of multi-span continuous viaducts for the four types of bearing support systems and three earthquake ground motions. The non-linear response comparison has been accomplished by extensive parametric studies conducted by varying those bearing design parameters, which have major influence on the overall bridge response. The most important notion of these two chapter is, low temperature effect on base isolation systems has been introduced, as additional design parameter, to evaluate its influence on the behaviour of seismically isolated viaducts subjected to great earthquake ground motions in cold region.

Finally, the significant findings and general conclusions in this research are summarized in **Chapter 7**. Specific recommendations are made for designing new bridges and also for retrofitting of existing structures.

References

[1] Zhang, R.: Chapter 41: Seismic isolation and supplemental energy dissipation. In: Chen, W. F., and Duan, editors. *Bridge Engineering Handbook*, Boca Raton, CRC Press, 1999.

[2] Hashimoto, S., Abe, M., and Fujino, Y.: Damage analysis of Hanshin Expressway viaducts during 1995 Kobe earthquake. III: Three-span continuous girder bridges, *Journal of Bridge Engineering ASCE*, Vol. 10, No. 1, pp. 61-68, 2005.

[3] Rose, A., and Lim, D.: Business interruption losses from natural hazards: conceptual and methodological issues in the case of the Northridge earthquake, *Environmental Hazards*, Vol. 4,pp. 1-14, 2002.

[4] DesRoches, R., Choi, E., Leon, R. T., Dyke, S. J., and Aschheim, M.: Seismic response of multiple span steel bridges in central and southeastern United States. I: As built, *Journal of Bridge Engineering ASCE*, Vol. 9, No. 5, pp. 464-472,2004.

[5] Moehle, J. P., and Eberhard, M. O.: Chapter 34: Earthquake damage to bridges. In: Chen, W. F., and Duan, editors. *Bridge Engineering Handbook*, Boca Raton, CRC Press, 1999.

[6] Pamuk, A., Kalkan, E., and Ling, H. I.: Structural and geotechnical impacts of surface rupture on highway structures during recent earthquakes in Turkey, *Soil Dynamics and Earthquake Engineering*, Vol. 25,No. 7-10, pp. 581-589,2005.

[7] Choi, E., DesRoches, R., and Nielson, B.: Seismic fragility of typical bridges in moderate seismic zones, *Engineering Structures*, Vol. 26, No. 2, pp. 187-199,2004.

[8] Bhattacharya, S., and Bolton, M.: Buckling of piles during earthquake liquefaction, *Proceedings of 13th World Conference on Earthquake Engineering*, Paper No. 95, Vancouver, Canada, 1-6 August, 2004.

[9] Duan, L., and Chen, W. F.: Chapter 18: Bridges. In: Chen, W. F., and Scawthom, C., editors. *Earthquake Engineering Handbook*, Boca Raton, CRC Press, 1999.

[10] Tanimura, S., Sato, T., Umeda, T., Mimura, K. and Yoshikawa, O.: A note of dynamic fracture of the bridge bearing due to the great Hanshin-Awaji earthquake, *International Journal of Impact Engineering*, Vol. 27, No. 2, pp. 153-160, 2002.

[11] Wilson, J. C.: Repair of new long-span bridges damaged by the 1995 Kobe earthquake, *Journal of Performance of Constructed Facilities ASCE*, Vol. 17, No. 4, pp. 196-205, 2003.

[12] Unjoh, S.: Chapter 44: Seismic design practice in Japan. In: Chen, W. F., and Duan, editors. B*ridge Engineering Handbook*, Boca Raton, CRC Press, 1999.

[13] Japan Road Association (JRA), Guide Specifications for Seismic Design of Highway Bridges, Tokyo (Japan), Maruzen, 1971.

[14] Japan Road Association (JRA), Design Specifications of Highway Bridges — Part V Seismic Design, Tokyo (Japan), Maruzen, 1990.

[15] Japan Road Association (JRA), Specification for Highway Bridges - Part V Seismic Design, Tokyo (Japan), Maruzen, 1996.

[16] Megawati, K., Higashihara, H., and Koketsu, K.: Derivation of near-source ground motions of the 1995 Kobe (Hyogo-ken Nanbu) earthquake from vibration records of the Akashi Kaikyo Bridge and its implications, *Engineering Structures*, Vol. 23, pp.1256-1268, 2001.

[17] Usami, T. and Kumar, S.: Inelastic seismic design verification method for steel bridge piers using a damage index based hysteretic model, *Engineering Structures*, Vol. 20, No. 4-6, pp. 472-480,1998.

[18] Watanabe, E., Sugiura, K., Nagata, K. and Kitane, Y.: Performances and damages to steel structures during the 1995 Hyogoken-Nanbu earthquake, *Engineering Structures*, Vol. 20, No. 4-6, pp. 282-290,1998.

[19] Kunde, M. C. and Jangid, R. S.: Seismic behavior of isolated bridges: A-state-of-the-art review, *Electronic Journal of Structural Engineering*, Vol. 3, pp. 140-170, 2003.

[20] Kelly, J. M.: Aseismic base isolation: review and bibliography, *Soil Dynamics and Earthquake Engineering*, Vol. 5, No. 4, pp. 202-216, 1986.

[21] Bessason, B., and Haflidason, E.: Recorded and numerical strong motion response of a base-isolated bridge, *Earthquake Spectra*, Vol. 20, No. 2, pp. 309-332, 2004.

[22] Ruiz Julian, D., Hayashikawa, T. and Sato, K.: Effect of bearing supports on nonlinear seismic behaviour of highway viaducts, *Proceedings of the Ninth Asia-Pacific Conference on Structural Engineering and Construction (EASEC-9)*, Bali, Indonesia, December 16-18, 2003.

[23] Bates, R.E., and Bilello, M.A.: Defining the cold regions of northern hemisphere. Hanover, NH: CRREL, Technical Report 179.

[24] Oshima, T., Mikami, S., Yamazaki, T., Ikenaga, M., Matsui, Y., and Kubo, K.: Experimental of functional confirmation on lead rubber bearing (LRB) under low temperature, *J. Struct. Eng*, 44A, pp.753-760, 1998.

[25] Hayashikawa,T.: Bridge Engineering. Asakura Publishing Co., Ltd, 2000.

[26] Williams, D., and Godden, W. G.: Experimental model studies on the seismic response of high curved overcrossings, Report No, 76/18 UCB/EERC, Earthquake Engineering Research Center, University of California at Berkeley, 1976.

[27] Buckle, I.G.: Field tests of a curved box girder bridge using simulated earthquake loads, *Proceedings of the 8th European Conference on Earthquake Engineering*, Lisbon, Portugal, Vol. 4, pp. 1-8,1986.

[28] Abdel-Salam, M. N. and Heins, C. P.: Seismic response of curved steel box girder bridges, *Journal of Structural Engineering*, Vol. 114, pp. 2790-2800,1988.

[29] Chen, Y.: Effects of modeling and analysis methods on seismic responses of curved bridges, Engineering Mechanics: Proceedings of the 10th Conference, Colorado, USA, Vol. 2, pp. 1078-1081,1995.

[30] DesRoches, R., and Fenves, G. L.: Evaluation of recorded earthquake response of a curved highway bridge, *Earthquake Spectra*, Vol. 3, No. 3, pp. 363-386, 1997.

[31] Hayashikawa, T., Otake, A., and Nakajima, A.: Nonlinear behavior of curved viaducts subjected to three-dimensional earthquake ground motions, Paper No. Gl-20, *The 10th Earthquake Engineering Symposium Proceedings*, Architectural Institute of Japan, Tokyo, Japan, Vol. 2, pp. 2391-2396,1998.

[32] Kelly, J. M.: A seismic base isolation: Review and bibliography, *Soil Dynamics and Earthquake Engineering*, Vol. 5, pp. 202-216,1986.

[33] Buckle, J. G., and Mayes, R. L.: Seismic isolation: History, application and performance - A world overview, *Earthquake Spectra*, Vol.6, No.2, pp. 161-202,1990.

[34] Protective Systems Research Group: List of seismically-isolated bridges, Web-Site of Earthquake Engineering Research Center, University of California at Berkeley. Available from: http://nisee.berkelev.edu/prosvs/nzbridges.html

[25] Kikuchi, M., and Aiken, I. D.: An analytical hysteresis model for elastomeric seismic isolation bearings, *Earthquake Engineering and Structural Dynamics*, Vol. 26,pp. 215-231,1997.

[26] Huang, J. S., and Chiou, J. M.: An equivalent linear model of lead-rubber seismic isolation bearings, *Engineering Structures*, Vol. 18, No. 7, pp. 528-536,1996.

[27] Mori, A., Carr, A. J., Cooke, N., and Moss, P. J.: Compression behavior of bridge bearings used for seismic isolation, *Engineering Structures*, Vol. 18, No. 5, pp. 351-362,1996.

[38] Kelly, J. M., and Tsztoo, D. F.: Energy absorbing devices in structures under earthquake loading, *Proceedings of the 6th World Conference on Earthquake Engineering*, New Delhi, India, Vol. 2, pp. 1369-1374,1977.

[39] Buckle, I.G., and Kelly, J. M.: Shake table studies of base isolated bridge superstructures with energy dissipators, *Proceedings of the 8th European Conference on Earthquake Engineering*, Lisbon, Portugal, Vol. 5, pp. 55-61,1986.

[40] Wei, Z., Kai, Q., Weihua, Z., and Zhengxin, R.: Test and analysis of bridge vibration isolation, *Proceedings of the 10th World Conference on Earthquake Engineering*, New Delhi, India, Vol. 4, pp. 739-752, 1992.

[41] Robinson, W. H.: Seismic isolation of bridges in New Zealand, *Proceedings of the Second U. S. - Japan Workshop on Earthquake Protective Systems for Bridges*, Japan, pp. 185-194,1993.

[42] Igarashi, A., and Iemura, H.: Experimental and analytical evaluation of seismic performance of highway bridges with base isolation bearings, *Proceedings of the 11th World Conference on Earthquake Engineering*, Acapulco, Mexico, Paper No. 553,1996.

[43] Ando, Y., Sakakibara, M., Yamandoe, S. I., and Ohbo, N.: Seismic evaluation of actual bridge with isolators by vibration tests, *Proceedings of the Second World Conference on Structural Control*, Kyoto, Japan, Vol. 1, pp. 913-922,1998.

[44] Tan, R. Y., and Huang, M. C.: System identification of a bridge with lead-rubber bearings, *Computers and Structures*, Vol. 74, pp. 267-280,2000.

[45] Chaudhary, M. T. A., Abe, M., Fujino, Y., and Yoshida, J.: System identification of two base-isolated bridges using seismic records, *Journal of Structural Engineering ASCE*, Vol. 126, pp. 1187-1195, 2000.

[46] Jankowski, R., Wilde, K., and Fujino, Y.: Pounding of superstructure segments in isolated elevated bridge during earthquakes, *Earthquake Engineering and Structural Dynamics*, Vol. 27, pp. 487-502,1998.

[47] Wang, Y. P., Chung, L. L., and Liao, W. H.: Seismic response analysis of bridges isolated with friction pendulum bearings, *Earthquake Engineering and Structural Dynamics*, Vol. 27, pp. 1069-1093,1998.

[48] Mutobe, R. ML, and Cooper, T. R.: Nonlinear analysis of a large bridge with isolation bearings, *Computers and Structures*, Vol. 72, pp. 279-292,1999.

[49] Wilde, K., Gardoni, P., and Fujino, Y.: Base isolation system with shape memory alloy device for elevated highway bridges, *Engineering Structures*, Vol. 22, pp. 222-229, 2000.

[50] Park, K. S., Jung, H. J., and Lee, I. W.: A comparative study on seismic performances of base isolation systems for multi-span continuous bridge, *Engineering Structures*, Vol. 24, pp. 1001-1013,2002.

[51] Jangid, R. S., and Kelly, J. M.: Base isolation for near-fault motions, *Earthquake Engineering and Structural Dynamics*, Vol. 30, pp. 691-707, 2001.

[52] Ruiz Julian, D., and Hayashikawa, T.: Hardening effect of lead-rubber bearings on nonlinear seismic behaviour of highway viaducts with piers of unequal heights, *International Workshop on Structural Health Monitoring of Bridges/Colloquium on Bridge Vibration*, Kitami, Japan, pp. 141-148,1-2 September, 2003.

[53] Khan, A.S., and Lopez-Pamies, O.: Time and temperature dependent response and relaxation of a soft polymer, *Intl. J. Plast*, 8, pp 1359-1372, 2002.

[54] Gan, Z.P., Hayashikawa, T., Matsumoto, T., and He, X.W., Study on seismic response analysis of curved grillage girder viaducts with base isolation system under low temperature, *Proceeding of Hokkaido Chapter of JSCE*, Vol.69, No.A-53, 2013.2.

CHAPTER 2

DESCRIPTION OF HIGHWAY VIADUCT

2.1 Introduction

A typical type of curved highway viaduct in Japan has been selected for analysis in the presented study. The composite continuous superstructure is supported by various bearing systems at top of four box-section steel bridge piers. Different types of base-isolation devices are used to improve the seismic response of the viaduct, isolating the bridge structure from seismic ground motions.

In recent years, horizontally curved steel viaducts have become an important component in modem highway systems as the most viable option at complicated interchanges or river crossings where geometric restrictions and constraints of limited site space make extremely complicated the adoption of standard straight superstructures. Curved alignments offer, in addition, the benefits of aesthetically pleasing, traffic sight distance increase, as well as economically competitive construction costs with regard to straight bridges. On the contrary, steel viaducts with curved configurations may sustain severe seismic damage owing to rotation of the superstructure or displacement toward the outside of the curve line due to complex vibrations occurring during strong earthquake ground motions.

Seismic design of bridge structures has greatly evolved in the past few years in response to serious damage to bridges observed in the 1995 Hyogoken-Nanbu earthquake. Damages to highway structures caused by this earthquake show especially the high vulnerability of simply supported structures to seismic forces, and enhance the desirable adoption of multi-span continuous bridges [3]. Providing continuity to a series of simple spans improves the seismic resistance of the bridge, and in addition, the number of bearings is decreased, expansion joints in the deck are eliminated and maintenance problems are reduced.

Steel bridge piers are widely used to support highway bridges in urban areas in Japan, being considered advantageous in regions of high seismic activity [1, 2]. In modem highway systems, it is also considered suitable the selection of continuous superstructures supported on seismic isolation bearings as long as the ground characteristics and another factors allow for the construction of this type of highway viaducts.

For a multi-span continuous type bridge on good ground conditions and having short natural period, adoption of seismic-isolation design is desirable. From the experiences of recent great earthquakes, it is probable that steel bearing supports will be damaged by impact seismic forces, and unexpected behaviour for the bridge can occur when a support is broken. During the Hyogoken-Nanbu earthquake, there were some cases where vehicle flow was impeded by superstructure falling onto the surface of the substructure, large differences in levels of the road surface, or damaged superstructure ends, as a result of failures of steel bearing supports. Therefore, following the recommendations of the Japan Road Association [3], base isolation bearings that absorb energy are adopted in this study.

The analytical model of the viaduct is shown in **Fig. 2.1**. The bridge is discretized in 71 nodal points which geometric coordinates are given in **Table 2.1**. Superstructure and piers are modeled as beam-column elements, and spring elements are introduced to represent the bearing supports for each pier.

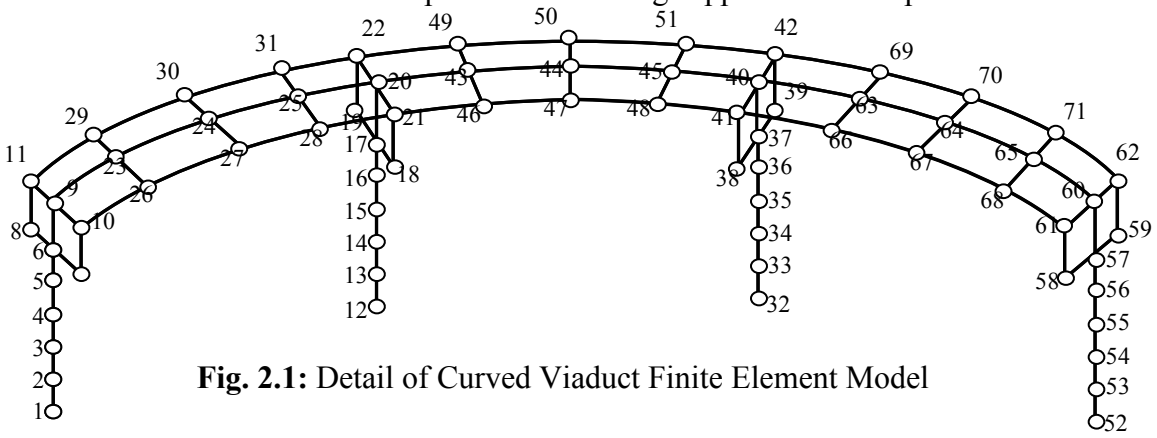


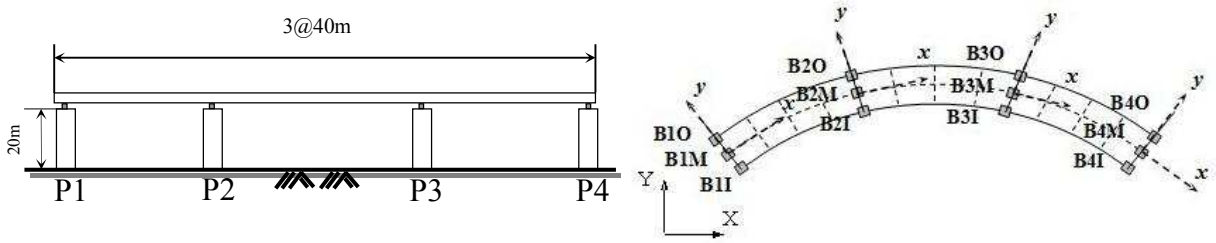
Fig. 2.1: Detail of Curved Viaduct Finite Element Model

Table 2.1: Coordinates of Nodal Points of Finite Element Model [m]

節点番号	X	Y	Z	節点番号	X	Y	Z
1	0.000	0.000	0.000	37	76.332	15.470	20.000
2	0.000	0.000	4.000	38	75.915	13.412	20.000
3	0.000	0.000	8.000	39	76.749	17.528	20.000
4	0.000	0.000	12.000	40	76.332	15.470	20.500
5	0.000	0.000	16.000	41	75.915	13.412	20.500
6	0.000	0.000	20.000	42	76.749	17.528	20.500
7	1.186	−1.733	20.000	43	46.482	16.965	20.500
8	−1.186	1.733	20.000	44	56.465	17.464	20.500
9	0.000	0.000	20.500	45	66.449	16.964	20.500
10	1.186	−1.733	20.500	46	46.692	14.875	20.500
11	−1.186	1.733	20.500	47	56.465	15.364	20.500
12	36.598	15.472	0.000	48	66.239	14.874	20.500
13	36.598	15.472	4.000	49	46.692	19.055	20.500
14	36.598	15.472	8.000	50	56.465	19.564	20.500
15	36.598	15.472	12.000	51	66.239	19.054	20.500
16	36.598	15.472	16.000	52	112.929	0.000	0.000
17	36.598	15.472	20.000	53	112.929	0.000	4.000
18	37.015	13.414	20.000	54	112.929	0.000	8.000
19	36.181	17.530	20.000	55	112.929	0.000	12.000
20	36.598	15.472	20.500	56	112.929	0.000	16.000
21	37.015	13.414	20.500	57	112.929	0.000	20.000
22	36.181	17.530	20.500	58	111.743	−1.733	20.000
23	8.522	5.224	20.500	59	114.115	1.733	20.000
24	17.623	9.572	20.500	60	112.929	0.000	20.500
25	26.913	12.999	20.500	61	111.743	−1.733	20.500
26	9.529	3.381	20.500	62	114.115	1.733	20.500
27	18.441	7.638	20.500	63	86.017	12.996	20.500
28	27.534	10.993	20.500	64	95.407	9.568	20.500
29	7.515	7.067	20.500	65	104.407	5.220	20.500
30	16.805	11.506	20.500	66	85.396	10.990	20.500
31	26.292	15.005	20.500	67	94.589	7.634	20.500
32	76.332	15.470	0.000	68	103.400	3.377	20.500
33	76.332	15.470	4.000	69	86.638	15.002	20.500
34	76.332	15.470	8.000	70	96.225	11.502	20.500
35	76.332	15.470	12.000	71	105.414	7.063	20.500
36	76.332	15.470	16.000				

2.2 Superstructure

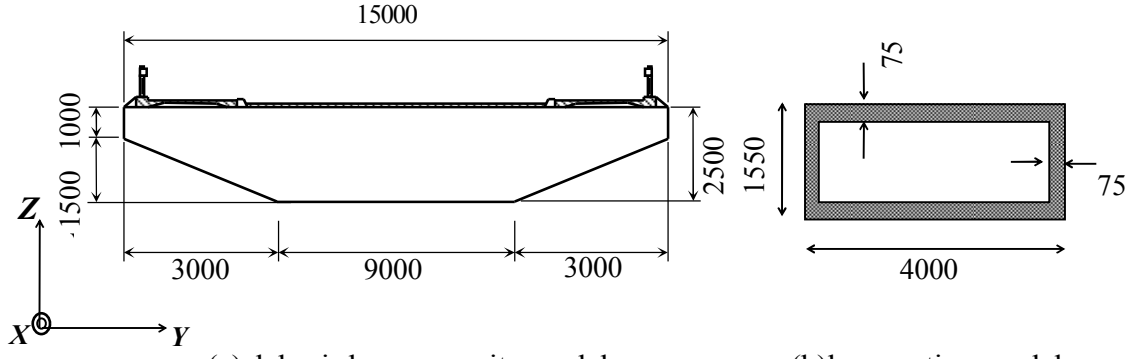
The elevated curved highway viaduct considered in the analysis is a three-span-continuous bridge having an overall length of 120.0 m with equal spans of 40.0 m and supported on four steel piers of 20.0 m of height. The bridge alignment is horizontally curved in a circular arc and the radius of curvature is 100m. And the total weight of superstructure is 8.82MN. Four types of bearing systems are considered to support the continuous steel reinforced concrete box girder. The basic model of viaduct with steel bearings is configurated with fixed bearings. To improve the seismic response, the bridge is equipped with three different types of base isolation bearings with different size, stiffness and deformation capacity on top of each pier. In this study the effect of abutments as well as soil-structure interaction type are not taken into account, and piers are considered as fixed on the soil. The side view and plan view of the bridge, are shown in **Fig. 2.2**.



(a) Side view of the viaduct (b) Plain view of the viaduct

Fig. 2.2: Side and Plan Views of Curved Highway Viaduct Model

The slab-girder composite model of the superstructure is represented in **Fig. 2.3(a)**. The area of composite section is 0.8 m^2. The cross section moment of inertia about y axes is 0.35492m^4, about z axes is 1.5185m^4. And the torsional constant is 4.01786m^4. Therefore the equivalent box cross section model is calculated to obtain approximately same values of area and moment of inertia, as shown in **Fig. 2.3(b)**.



(a)slab-girder composite model (b)box section model

Fig. 2.3: Cross Section of Superstructure (mm)

2.3 Substructure

During the Hyogoken-Nanbu earthquake, piers of many highway bridges, were seriously damaged, and steel bridge piers suffered earthquake damage for the first time since their adoption. According to the "Interim report on the damage of highway bridges by the Hyogoken-Nanbu earthquake" published by the Ministry of Construction on 30 March 1995 [4],about 1% of the steel bridge piers of national roads, the Hanshin Expressway, and national expressways collapsed or were severely damaged or deformed. This figure was small compared to 3% for reinforced concrete (RC) bridge piers, but about a half of the steel bridge piers investigated were damaged to some degree, compared to 30% for the RC bridge piers.

Box-section steel bridge piers of cantilever-type are widely used to support highway bridges in urban areas of Japan [5]. The use of steel box sections for bridge pier construction is common and is considered advantageous in urban areas of high seismic activity [6] because these sections possess high strength/mass ratios and significant ductility, which greatly enhance their structural performance during strong earthquakes.

During a seismic event, the piers are subjected to the combined action of the dead load of the superstructure and the lateral load due to the earthquake. This produces damage in the form of local buckling in the component plates near the base, where the bending moment is large. The local buckling increases with an increase in the top deformation or due to low cycle fatigue under repeated cycling. This is turn degrades the strength and stiffness of the piers, thereby leading to collapse [7].

In the presented study, the highway viaduct is supported by four thin-walled steel hollow box section piers, having the same height of 20.0 m. Cross-section geometry dimensions (**Fig. 2.4**) of piers are calculated based on the stability criteria under static loading. Size and thickness of the pier plate elements are selected considering that width/thickness ratios of the members must not exceed specified limits for box-section design, usually achieved by welding transverse to the thin-walled plates.

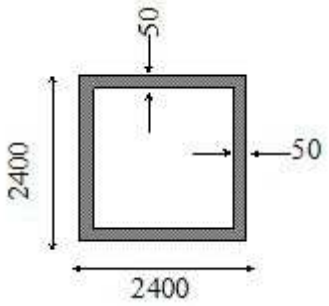


Fig. 2.4: Cross Section of Bridge Piers

Although steel box sections possess high flexural capacity, their cross-sections, composed of thin-walled plates, are susceptible to local buckling if the members are not adequately proportioned or detailed. The parameters governing the structural behaviour of members composed of thin-walled plates are the width/thickness ratios of the plates and the pier slenderness parameter [8].

The seismic design of the bridge piers is based on the seismic coefficient method given in the Specifications for Highway Bridges in Japan (Part II) [9]. Firstly, the design horizontal seismic coefficient is calculated.

2.3.1 Design horizontal seismic coefficient

The response of a bridge to earthquake motion varies according to the strength of the earthquake motion, its periodicity and duration, the ground type, structural type of the bridge, and particularly the structure of its foundation. The standards for the design horizontal seismic coefficient are established accounting for these elements and are also in accordance with the stipulations concerning seismic design in the previous Specification for Seismic Design (February 1990) [9]. The standard values for the design horizontal seismic coefficient have been established by integrating past practices and experience, and are based on the results, accounting for the acceleration response spectrum curves by ground type found through analysis of the strong motion records of 394 components observed in Japan, the characteristics of bridge damage caused in recent earthquakes, and other facts obtained through observations and experimental studies.

The design horizontal seismic coefficient is calculated by the following equation

$$k_h = C_Z \cdot C_G \cdot C_I \cdot C_T \cdot C_E \cdot k_{h0}$$

k_{h0}:	standard horizontal seismic coefficient for design	=0.25
C_Z:	zone factor	=1.0
C_G:	ground condition factor	=0.8
C_I:	importance factor	=1.0
C_T:	natural period factor	=1.25
C_E:	damping constant factor	=1.00

The design horizontal seismic coefficient is taken, $k_h = 0.25$.

The equivalent lateral force P, acting at the top of the pier and representing the effect of earthquake loads is calculated. This lateral force depends on the weight of the superstructure $W = 8.82$ MN, and it is expressed as

$$P = k_h \cdot W = 0.25 \times 8.82 = 2.205\text{MN} = 2.205 \times 10^6\ \text{N}$$

The bending moment, maximum at the base of the bridge pier, depends on the pier height H and it is calculated using following equation

$$M = P \cdot L = 2.205 \times 10^6 \times 20 = 44.10 \times 10^6\ \text{Nm}$$

The compressive stress, σ_c, and the bending compressive stress, σ_b, are calculated

$$\sigma_b = \frac{M}{I} y = \frac{44.10 \times 10^6}{0.4328} \times 1.20 = 122.27 \times 10^6\ \text{N/m}^2 = 122.27\text{N/mm}^2$$

$$\sigma_c = \frac{R}{A} = \frac{3.234}{0.4700} = 6.88\text{MN/m}^2 = 6.88\text{N/mm}^2$$

where M is the bending moment at the pier base previously calculated, I is the cross-section moment of inertia (0.4328 m^4), y is the distance to the external cross-sectional fiber (1.20 m), R is the axial compressive load (3.234 MN), and A is the cross-sectional area (0.4700m^2).

2.3.2 Allowable stress evaluation

The allowable stress is evaluated based on the criteria,

$$\sigma_a \geq \sigma$$

The allowable axial compressive stress without local budding is calculated using

$$\sigma_{cag} = 140 - 0.82\left(\frac{l}{r} - 20\right) = 140 - 0.82 \times \left(20 - \frac{16}{0.9596}\right) = 137.27\text{N/mm}^2$$

where r is the radius of gyration (0.9596 m) and l is the effective length of the pier (16 m).

The local buckling allowable stress, σ_{cal}, is

$$\sigma_{cal} = 140\text{N/mm}^2$$

The upper limit of the allowable axial compressive stress without local buckling is

$$\sigma_{cao} = 140\text{N/mm}^2$$

And the allowable axial compressive stress is calculated by using

$$\sigma_{ca} = \frac{\sigma_{cag} \bullet \sigma_{cal}}{\sigma_{cao}} = \frac{137.27 \times 140}{140} = 137.27\text{N/mm}^2$$

$$\sigma_{bag} = 134.8\text{N/mm}^2$$

The allowable Euler buckling stress is calculated using

$$\sigma_{ea} = 980000\theta\left(\frac{r}{l}\right)^2 = 3525.06\text{N/mm}^2$$

And finally verifications stipulated in the Specifications [10] for the geometrical characteristics of pier cross-section is carried out by using following equation

$$\frac{\sigma_c}{\sigma_{ca}} + \frac{\sigma_b}{\sigma_{bag}\left(1 - \frac{\sigma_c}{\sigma_{ea}}\right)} \leq 1$$

$$\sigma_c + \frac{\sigma_b}{1 - \frac{\sigma_c}{\sigma_{ea}}} \le \sigma_{cal}$$

And numerically,

$$\frac{6.88}{137.27} + \frac{122.27}{134.8 \times \left(1 - \frac{6.88}{3525.06}\right)} = 0.9588 < 1$$

$$6.88 + \frac{122.27}{1 - \frac{6.88}{3525.06}} = 129.40 \le 140 \text{N/mm}^2$$

The yield moment of the pier, M_{eo}, is calculated through following equation

$$M_y = \frac{4\sigma_y}{3a}\left[\, a^3 b - (a - 2t_1)^3 (b - 2t_2) \,\right]$$
$$= 84.8 \text{ (MNm)}$$

where σ_y is the yield stress (235 MN) and a, b, t_1 and t_2 are geometrical properties represented in **Fig. 2.5**.

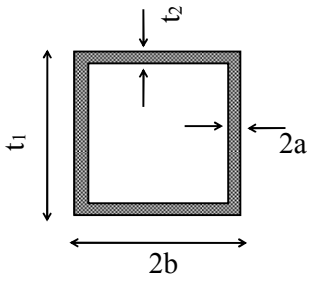


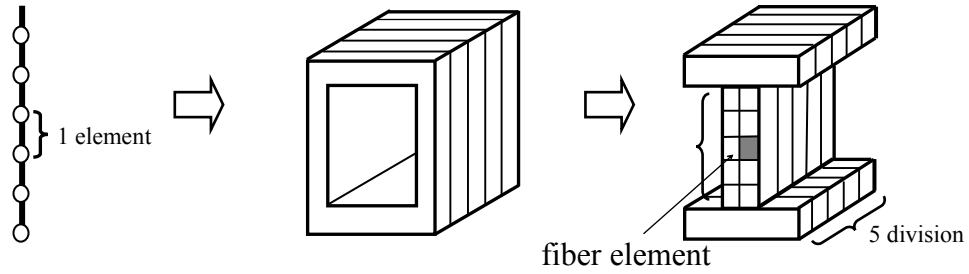
Fig. 2.4: Geometrical Properties of Pier Cross Section

2.3.3 Cross section fiber element model

The fiber element modelization is actually considered an accurate and practical technique for computing the response of steel pier sections. Dynamic analysis presented in this study is based on the fiber element modelization of the structural members. The fiber element model of an element cross-section entails discretization of the section into many small regions (fibers) for which constitutive model is based on uniaxial stress- strain relationship to describe the members response. Each region represents a fiber of material running longitudinally along the member, and it is assigned bilinear nonlinear model.

The fiber element developed for characterization of structural bridge elements in this study is shown in **Fig. 2.21**. In the fiber element model of this study, the

element is subdivided into a discrete number of longitudinal and transversal fibers. The element is divided in 5 longitudinal parts (**Fig. 2.21-b**), which, as well are subdivided in 12 transversal divisions (**Fig. 2.21-e**). The geometric characteristics of each fiber are its location in the local reference system and the fiber area.



(a) Column model (b) Box section (c) I section

Fig. 2.21 Cross Section Fiber Element

The accuracy of the element response and, consequently, that of the entire structure are affected by the mesh selection that is the number of sections used in the discretization of a given member, and by the number of fibers in a section. A large number of fibers certainly gives better results, but computational cost increases with it, since the history variables necessary to track the behaviour of each fiber must be stored at each iteration. The selected number of divisions is considered appropriate and optimum in the model of this study.

Inelasticity of the flexure element is accounted for by the division of the cross-section into a number of fiber zones with uniaxial plasticity defining the normal stress- strain relationship for each zone. The element stress resultants are determined by integration of the fiber zone stresses over the cross section of the element. The nonlinear behaviour of the fiber element derives entirely from the nonlinear behaviour of the fibers. The steel stress-strain behaviour is described by a bilinear nonlinear model. The yield stress is 235.4 MPa, the Young's modulus is 200 GPa, and the strain hardening in plastic area is 0.01.

2.4 Bearing Supports

Bearing devices are designed to transmit loads from superstructure to substructure, providing for expansion, contraction and rotation capacity to the deck superstructure. Bridge bearings are also able to accommodate movements of the structure that result from loads, temperature changes, deflection, impact and centrifugal force, and their design tends to be in such a way that the bearings are easy to maintain and require a minimum of maintenance

In the presented study the role of bearings supports, considered as one of the most important structural elements of a bridge structure, is emphasized. The Hyogoken-Nanbu earthquake, and others that preceded it and have occurred since, clearly showed poor performance of bearings supports and the disastrous consequences

that a bearing failure can have on the overall performance of a bridge. The concept, in which the bearing supports are regarded as a fuse or as having a fuse-like function for alleviating the potential damage to the whole bridge, is avoided, and therefore, it is considered appropriate to introduce in this study the basic concept that the bearing support is one of the essential structural members of a bridge [3].

2.4.1 Lead-rubber bearings

Many innovative devices and systems are being developed for the purpose of seismic isolation of bridges [11]. One of the most widely adopted isolation system is the lead-rubber bearing (LRB) shown in **Fig. 2.5**. This type of elastomeric bearing protects the bridge from the destructive effects of earthquake ground motions increasing the structure fundamental period beyond the energy-containing periods of earthquakes and also by dissipation of seismic energy through the additional hysteretic damping due to yielding of the lead plug [12].

Under normal conditions, LRB bearings behave like regular bearings. However, in the event of a strong earthquake, with the utilization of this base-isolation system, the superstructure of a bridge is decoupled from its substructure, and the response of the superstructure to the dynamic seismic loading is altered favorably and the seismic dynamic energy transferred to the superstructure is reduced. Thus seismic inertial loads are reduced and the seismic damage the structure acquires is drastically reduced.

Although base-isolation is an effective technology for improving the seismic performance of a bridge, there are certain limitations on its usage. Seismic base-isolation improves the performance of a bridge under seismic loading partially by increasing the fundamental vibration period. Thus the vibration period of a bridge is moved away from the high-energy seismic ground period and seismic energy transfer to the structure is minimized. Therefore usage of seismic base-isolation on soft or weak soil conditions, where high period ground motion is dominant, reduces the benefits offered by the technology. The base-isolation system has a relatively high vibration period compared to a conventional structure. Due to the principle of dynamic resonance, a larger difference between the dynamic vibration frequencies of the isolation system and the superstructure results in a minimized seismic energy transfer to the superstructure. Therefore, seismic base-isolation is most effective in relatively rigid structural systems and will provide limited benefits for highly flexible bridges.

Another consideration is related to the large deformations that may occur in the seismic base-isolation bearings during a major seismic event, which causes large displacements in a deck. This may result in an increased possibility of collision between deck and abutments, and in the adoption of large expansion joints for the bridge with cause noise, vibration and maintenance problems.

The force displacement behaviour of LRB bearings is either bilinear or trilinear hysteretic. The bilinear model has been extensively accepted as analytical model for LRB bearings due to its simplicity and accuracy to identify the force- displacement relationship of the bearings. However, a trilinear analytical model (**Fig. 2.6**) is introduced in this study to represent the strain hardening of the hysteresis curve at a high shear strain,and thus to accurately reproduce the hysteresis loop obtained from experimental tests on LRB bearings.

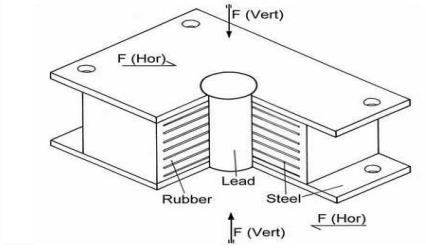


Fig. 2.5: LRB Device

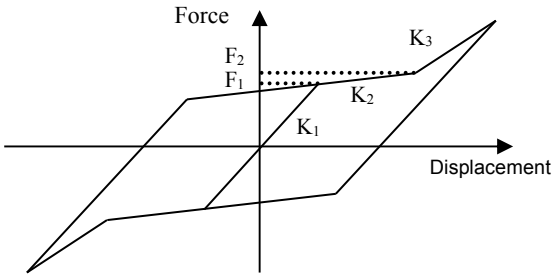


Fig. 2.6: Analytical Model of LRB

This bilinear model is characterized by three parameters: the elastic stiffness of the lead core K_1, the post-yield stiffness of the rubber material K_2, and the yield force of the lead core F_1. The parameters of the trilinear model are five, the three corresponding to those of the bilinear model plus two others for characterizing the hardening behaviour of the bearing, the stiffness of rubber at high strain levels K_3,and the second yield displacements, F_2. Values selected for structure characteristics of LRB bearing supports are summarize in **Table 2.2**.

2.4.2 Low temperature effect on LRB

Since LRB is mainly made of rubber, some characteristics of rubber conspicuously influence the performance of LRB. Such as strain hardening effect which has been discussed above, and the stiffness increment under low temperature.

High stiffness basically is not a favorable property of LRB, it may cause intensive vibration and more response transferred to superstructure. Stiffness increase under low temperature may lead to problems, as well as strain hardening does. Thus, it is necessary to evaluate the temperature effect on LRB.

Base on the experiment results, for the case of a long-term low temperature accumulation, the equivalent stiffness of LRB increases about 30%. The configuration of LRB considered in this study is summarized in **Table 2.2**. It should be remarked, dynamic bearing property cases (temperature increasing during earthquake) are the main focus of this study, while fixed low temperature cases are also introduced as a reference value.

Table 2.2 Configuration of LRB (K(MN/m) F(MN))

Case	LRB	K_1	K_2	K_3	F_1	F_2	Temperature
1	s200	1.489	0.212	0.549	0.063	0.125	+20℃, fixed
2	s200l-d	2.055	0.293	0.758	0.102	0.203	-30℃, increasing
3	s200l-f	2.055	0.293	0.758	0.102	0.203	-30℃, fixed
4	s350	2.662	0.380	0.984	0.096	0.191	+20℃, fixed
5	s350l-d	3.674	0.524	1.358	0.155	0.309	-30℃, increasing
6	s350l-f	3.674	0.524	1.358	0.155	0.309	-30℃, fixed
7	s500	3.850	0.550	1.425	0.138	0.275	+20℃, fixed
8	s500l-d	5.313	0.759	1.966	0.224	0.446	-30℃, increasing
9	s500l-f	5.313	0.759	1.966	0.224	0.446	-30℃, fixed

2.5 Input Earthquake Ground Motions

The 17th of January 1995 at 5.46 a.m. a violent earthquake, 7.2 on the Richter scale, struck Kobe, a highly developed and congested modem city in Japan. The depth of its epicenter was 14 km below ground level. Since the earthquake motion progressed toward the faults directly below Kobe, the HN Earthquake caused severe damage and destruction to a large number of structures throughout the Hanshin-Awaji areas [13]. In addition to the collapse of buildings, many public works that form the urban infrastructure also suffered extensive damage. In particular, damage to highway bridges was unprecedented, both in scale and quantity [14].

Based on the damage surveys, to ensure seismic performance against a direct-type urban earthquake, the Ministry of Construction took the lead in revising the seismic standard of bridges, and issued new specifications in December 1996 [3]. On the other hand, the Japan Society of Civil Engineers (JSCE) issued the "Proposal on Earthquake Resistance for Civil Engineering Structures" [15], in which two types of earthquake ground motions were defined for earthquake resistant design of structures. One type, referred to as Level I (L-1), represents ground motions of moderate intensity, which are likely to be experienced by the structures once or twice during their lifetime. The other is Level II (L-II) ground motion of extreme intensity rarely experienced during their lifetime. L-II ground motions represent the near-fault earthquakes, with accelerograms modified from direct-inland-stricken type earthquake records characterized by a short duration, high intensity, pulse-like shaking like the devastating 1995 HN Earthquake.

Japanese Seismic Specifications were revised to performance-based design in 2000 [16]. According to the performance-based philosophy, a structure should satisfy requirements to assess the seismic performance under different specified levels of seismic excitation. L-II motions are of special interest since they can drive the bridge structure to its ultimate limit state design stage, resulting in the highest damage potential. Consequently, L-II motions are basically used to check the ultimate capacity of structures beyond their elastic limits. L-II motions generated by active inland faults are, in principle, determined based on identification of threatening active faults and estimation of their fault mechanism. Geological data of active faults in Japan is extensive. However, there are many hidden faults not included in the present fault data and they are threatening to cause inland earthquakes anywhere in Japan. Therefore, consideration on L-II motions is needed even in an area where significant active faults are not mapped until today [17].

The near-fault region of an earthquake is considered to be the area within several kilometers of the extension to the ground surface of the fault rupture plane. Near-fault earthquake ground motions contain large, rapid pulses, which result in large ground displacements, generally exceeding 0.5 m, which take place at rapid ground velocities, usually on the order of 1 m/sec, duration in the range of 1-3 sec, and significant long-period content.

In order to evaluate the seismic performance of the viaduct, the non-linear model is subjected to three different sets of earthquake records. The input ground motions are accelerograms obtained during the HN Earthquake (M_w= 6.9) at JR Takatori Station (TAK). The large magnitude records used in this study, classified as near-fault motions, are characterized by the presence of high peak accelerations and

strong velocity pulses with a long period component as well as large ground displacements. These exceptionally strong earthquakes have been selected due to the destructive potential of long duration pulses on structures that can lead to large deformations, probably exciting the bridge into its nonlinear range as well as inducing significant opening and pounding phenomenon at the expansion joint. Acceleration histories, including the three earthquake components, are shown in **Fig. 2.7**. The longitudinal component (L) of the earthquake record is selected to exclusively shake the highway viaduct parallel to the X-axis of the global coordinate system in case of 1-component earthquake excitation. This longitudinal component corresponds to the strike normal component, characterized by large pulses of motion oriented in the direction perpendicular to the fault strike, which is significantly larger than the strike- parallel or transverse component. On the other hand, in order to assess the effect of 3- components excitation the transverse (T) and vertical (V) components are added to the longitudinal component acting simultaneously in the Y- and Z-axes, respectively.

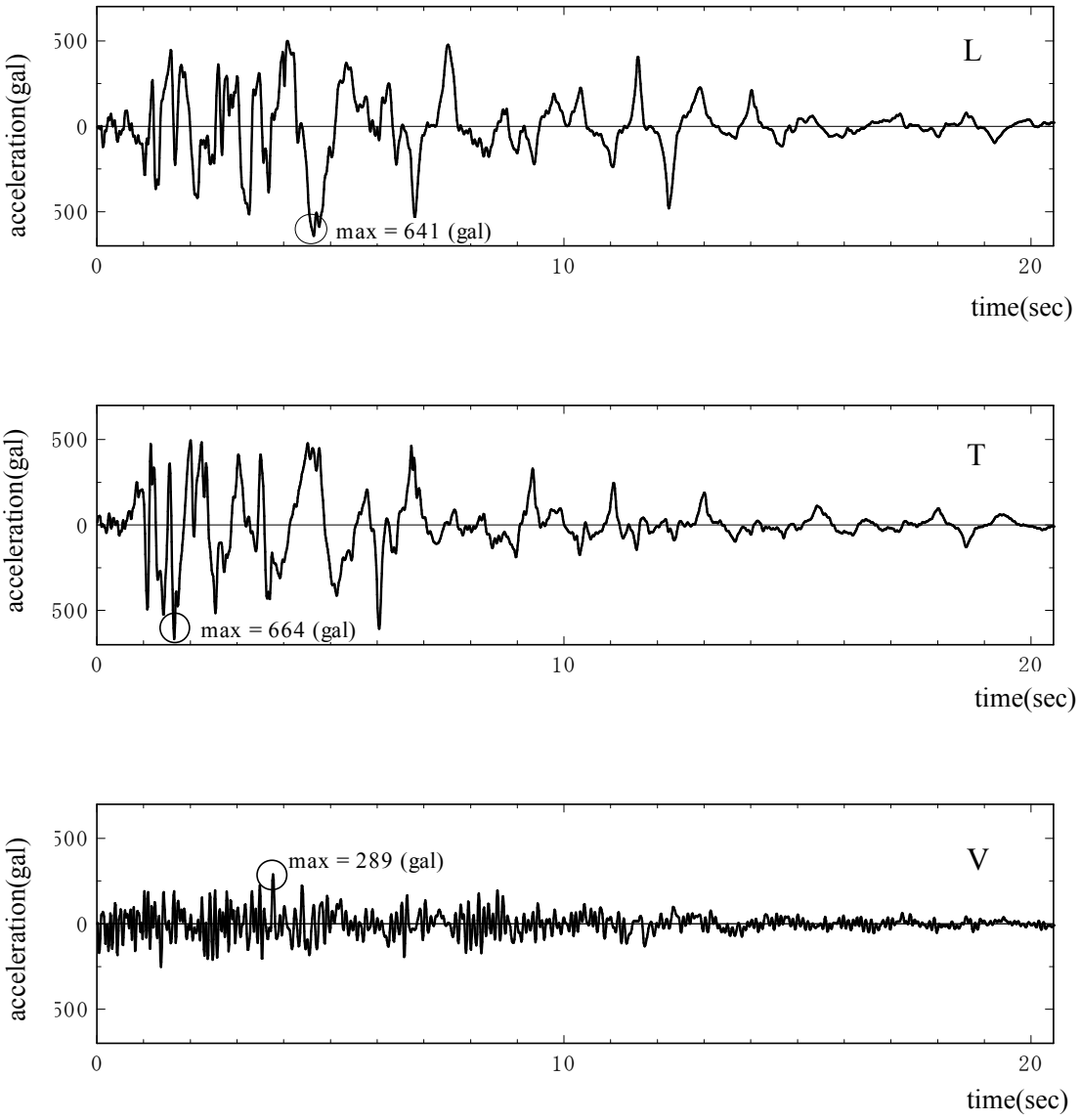


Fig. 2.7 Input Earthquake Accelerations

2.6 Conclusions

In this chapter, the analytical model of the highway viaduct object of this study is presented. This viaduct can be identified as one of the many existing elevated highway bridges typical in urban areas of Japan, which were seriously damaged during the Hyogoken-Nanbu earthquake of 1995. The model is a three-span continuous viaduct having equal spans of 40.0 m, with 100 m radius curvature, and supported on four steel piers of 20.0 m of height.

Bridge members are modeled using analytical models which plenty represent their mechanical and structural characteristics, and are also adequate for their implementation in the finite element analysis. Cross-sectional properties of the nonlinear elements are prescribed using fiber elements which are considered as the most promising models for nonlinear analysis of structural members.

The continuous bridge superstructure is modeled with a box cross-section element which represents the composite effect of the continuous steel reinforced concrete deck and the steel girders, identified as a homogeneous material.

Cross-section geometry dimensions of the steel hollow box section piers are calculated based on the stability criteria under static loading. Size and thickness of the pier plate elements are selected under the considerations specified for seismic design of bridge piers based on the seismic coefficient method.

Especial attention is paid in this chapter to bearing supports, considered as one of the most important structural elements of the bridge. The concept of base-isolation to protect the bridge by reducing inertia loads transmitted from the superstructure has been enhanced, and characteristics of three different types of devices used to isolated the model of highway viaduct are presented.

In addition to common measurement, temperature effect is considered in the present study, to represent the cold region factor.

And finally, in the last part of the chapter, input earthquake wave is introduced.

References

[1] Liu, Q., Kasai, A., and Usami, T.: Two hysteretic models for thin-walled pipe-section steel bridge piers, *Engineering Structures*, Vol. 23, 2001, pp. 186-197.

[2] Hsu, H.-L., and Chang, D.-L.: Upgrading the performance of steel box piers subjected to earthquakes, *Journal of Constructional Steel Research*, Vol. 57, 2001, pp. 945-958.

[3] Japan Road Asociation: Specifications for Highway Bridges, Part V Seismic Design, December 1996.

[4] Ministry of Construction of Japan: Interim report on the damage of highway bridges by the hyogoken-nanbu earthquake, March 1995.

[5] Liu, Q., Kasai, A., and Usami, T.: Two hysteretic models for thin-walled pipe-section steel bridge piers, *Engineering Structures*, Vol. 23, 2001, pp. 186-197.

[6] Hsu, H.-L., and Chang, D.-L.: Upgrading the performance of steel box piers subjected to earthquakes, *Journal of Constructional Steel Research*, Vol. 57, 2001, pp. 945-958.
[7] Usami, T., and Kumar, S.: Inelastic seismic design verification method for steel bridge piers using a damage index based hysteretic model, *Engineering Structures*, Vol. 20, 1998, Nos. 4-6, pp. 472-480.
[8] Japan Road Association: Specifications for Highway Bridges. Part. II Steel Bridges, December 1996.
[9] Japan Road Association: Specifications for Seismic Design, February 1990.
[10] Rubber Foundation Information Center for Natural Rubber: Is it possible to re-use old bridge bearings, *Natural Rubber*, Vol. 27, 3rd quarter, 2002.
[11] Kelly, J.M.: Seismic base isolation: review and bibliography, *Soil Dynamics and Earthquake Engineering*, Vol. 5, No. 4, pp. 202-216, 1986.
[12] Robinson, W. H.: Lead rubber hysteretic bearings suitable for protecting structures during earthquakes, *Earthquake Engineering,and Structure Dynamics*, Vol. 10, No. 4, pp. 593-604, 1982.
[13] Tanimura, S., Mimura, K., Nonaka, T. and Zhu, W.: Dynamic failure of structures due to the great Hanshin-Awaji earthquake, *International Journal of Impact Engineering*, Vol. 24, No. 6-7, pp. 583-596, 2000.
[14] Bruneau, M.: Performance of steel bridges during the 1995 Hyogoken-Nanbu (Kobe, Japan) earthquake-a North American perspective, *Engineering Structures*, Vol. 20, No. 12, pp. 1063-1078,1998.
[15] Japan Society of Civil Engineers: Proposal on earthquake resistance for civil engineering structures (Special Task Committee of Earthquake Resistance of Civil Engineering Structures), *The 1995 Hyogoken-Nambu earthquake investigation into damage of civil engineering. Earthquake Engineering Committee*, Japan Society of Civil Engineers, 1996.
[16] Japan Road Association (JRA), Specification for Highway Bridges - Part V Seismic Design, Tokyo (Japan), Maruzen, 2002.
[17] Toda, S., Hataya, S., Abe, S. and Miyakoshi, K.: The 1995 Kobe earthquake and problems of evaluation of active faults in Japan, *Engineering Geology*, Vol. 43, No. 2-3, pp. 151-167, 1996.

CHAPTER 3

CHAPTER 3 NONLINEAR DYNAMIC ANALYSIS

3.1 Introduction

Current seismic design philosophies include the possibility of damage to the structures, considering this damage acceptable, under the condition that it does not cause the collapse of the structure. However, such aspect requires an innovative and more accurate method to control and evaluate the damage, therefore, a post-elastic non-linear analysis is a suitable option. Besides, the constant necessity of assessing the inelastic structural behavior under earthquake loads has allowed the increment on the use of non-linear bridge analysis. [1, 2]. In this context, inelastic dynamic analysis provides a realistic measure of structural response because the inelastic model accounts for the redistribution of internal actions due to the non-linear force displacement behavior of the components. Although a non-linear inelastic dynamic analysis is not difficult in concept, it requires careful structural modeling and intensive computing effort.

During the process to ensure the safeness, inelastic dynamic analysis is commonly used for the safety evaluation of bridges to determine their inelastic response when subjected to strong earthquake ground motions. In fact, the three-dimensional frame modeling is considered advantageous to simulate the seismic behavior of bridge structures. In the analytical model, the M-ϕ relation for non-linearities at the member level is used to define the real material non-linear behavior. However, using the M-ϕ model, shortcomings have been pointed out in the analysis of frame bridges in which a change in an axial force occurs. On the other hand, the fiber model has an advantage in that the effects of a change in the axial force bi-directional bending are automatically considered. Therefore, the use of a fiber model comes across as a remarkable technique for bridge seismic. On the other hand, structural responses and strengths have been underestimated by linear analysis, leading by this to an important exigency of an adequate dynamic analysis that includes geometrical non-linearities. Moreover, a realistic treatment of the behavior of highway viaducts under strong earthquake excitation should consider the material non-linearity together with the geometric non-linearity [3, 4]. The finite element method is recognized as an accurate and versatile powerful numerical tool for bridge analysis; especially regarding the recent progresses in numerical methods related to computing and mathematical aspects of the behavior of complex structural systems. Dynamic analysis of bridges is complex and consequently, time required to obtain the numerical solution is considerable. However, the recent advances in computer and modeling techniques have significantly reduced the amount of computing time, and analysis of complex structural phenomena in bridges can be carried out [5 - 9].

This chapter describes an efficient procedure for the non-linear elastoplastic dynamic analysis under strong seismic excitation, considering both geometric non-linearity and material non-linearity. In the analysis, structural components are modeled by the non-linear space beam elements. The element has two nodes with six degrees of freedom per node, and can transmit an axial force, two shear forces, two bending moments and a torque. The total Lagrangian formulation is adopted in this study considering all coupling between bending, twisting and stretching deformations for beam element by the geometrical non-linear beam theory. The kinematic hardening model, unaxial yield criterion flow relations are used to describe the behavior of steel material non-linearity. For inelastic behavior, the spread of plasticity can be achieved through portions of the member cross section in addition to the

ability to model zones of plasticity along the member length utilizing the member segments. Because the fiber model allows modeling of strain hardening, axial-flexural interaction, residual stresses and gradual spread of yielding within the cross section, it is a more realistic model than the more common plastic hinge beam-column model. The fiber model used in this study is physically motivated from actual uniaxial test data of structural steel bars. Explicit expressions for stress in terms of strain also give the instantaneous stiffness, making the model ideal for iterative non-linear analysis. The stress-strain relation is the same for compression and tension. Residual stresses shift the curve along the strain axis until the residual stress level is located at zero strain. Thus, adjacent fibers can have different levels of residual stress. The stress pattern is defined in such a way that equilibrium is maintained, but the maximum residual stress can be chosen. The effects of both the geometrical variations and material non-linearity are accounted for through the tangent stiffness operator. An incremental-iterative method based on the Newmark direct integration method and the Newton-Raphson iteration scheme is employed for obtaining the solution of the non-linear dynamic equilibrium equations.

3.2 Natural Vibration Analysis Formulation

There are many different seismically active regions all along the world, and it makes crucial the accurate calculation of natural vibration characteristics of viaducts, especially in terms of prediction of their structural performance during strong earthquakes. It is essential to accurately determine the natural frequencies and mode shapes of a bridge structure for the solution of its dynamic responses due to seismic loads. The mathematical idealization for three-dimensional free vibrations is discussed in this section taken into account that the highway viaduct considered in the analysis is composed of thin-walled beam members. Free vibration of three-dimensional framework structures is analyzed by using the consistent mass matrix based on the finite element approach.

For this purpose, two different basic types of coordinate systems of structures are considered: distributed coordinate systems and discrete systems [10]. The first type is the distributed-parameter system, which is applied to structures whose physical properties are continuously distributed in three-dimensional space. In this case, the basic relation between forces and displacements for a beam segment subjected to axial, flexural and torsional vibration is formulated by general solutions of differential equations of motion. The above general solutions lead to a dynamic stiffness matrix, which includes natural circular frequencies of vibrating structures. This approach results in exact solutions of vibration and is called the continuous mass method or the eigen stiffness matrix method. The second type is the lumped-parameter system, which defines forces and displacements at a set of discrete nodal points in terms of components having specified directions. The lumped-mass idealization provides a simple means of limiting the number of degrees of freedom that must be considered in conducting a dynamic analysis of an arbitrary structural system. The lumping procedure is most effective in treating systems in which a large proportion of the total mass actually is concentrated at a few discrete points. The analytical procedure for this type can be greatly simplified as an eigenvalue problem because the inertia forces are developed only at these points. In this case, it is necessary to define the displacements and accelerations only at these discrete locations. In the space framework structures, the lumped mass matrix is derived as a diagonal matrix by applying half the mass and its associated mass-moment of each beam segment to the appropriate nodal point. Moreover, the influence coefficients are evaluated by a procedure similar to that used to determine the static stiffness coefficients. The resulting matrix is called the consistent mass matrix, and it contains many off-diagonal terms due to the effect of mass coupling.

A beam segment of a three-dimensional frame with six degrees of freedom at each node: three translations along the *x-, y-, z*-axes and three rotations about these axes, which are shown in **Fig. 3.1**. The linear stiffness matrix for three-dimensional uniform beam segment is readily obtained by the superposition of the axial, torsional and flexural stiffness matrices. The flexural stiffness matrix is used twice in forming the stiffness matrix of a space beam segment to account for flexural effects in the two principal planes (i.e., the *x-y* in-plane and *x-z* out-plane) of the cross section. The stiffness matrix expresses the relationship between the nodal force and the nodal displacement vectors as follows,

$$\{f\} = [k]\{d\} \tag{3.1}$$

where the element nodal force and displacement vectors in local coordinate system are,

$$\{f\} = \{X_i \;\; Y_i \;\; Z_i \;\; M_{xi} \;\; M_{yi} \;\; M_{zi} \;\; X_j \;\; Y_j \;\; Z_j \;\; M_{xj} \;\; M_{yj} \;\; M_{zj}\}^{\mathrm{T}} \tag{3.2}$$

$$\{d\} = \{u_i \;\; v_i \;\; w_i \;\; \theta_{xi} \;\; \theta_{yi} \;\; \theta_{zi} \;\; u_j \;\; v_j \;\; w_j \;\; \theta_{xj} \;\; \theta_{yj} \;\; \theta_{zj}\}^{\mathrm{T}} \tag{3.3}$$

For a three-dimensional frame member the stability function-based stiffness matrix has the following form:

$$[k] = \begin{bmatrix}
EA/l & 0 & 0 & 0 & 0 & 0 & -EA/l & 0 & 0 & 0 & 0 & 0 \\
 & 12EI_z/l^3 & 0 & 0 & 0 & 6EI_z/l^2 & 0 & -12EI_z/l^3 & 0 & 0 & 0 & 6EI_z/l^2 \\
 & & 12EI_y/l^3 & 0 & -6EI_y/l^2 & 0 & 0 & 0 & -12EI_y/l^3 & 0 & -6EI_y/l^2 & 0 \\
 & & & GJ/l & 0 & 0 & 0 & 0 & 0 & -GJ/l & 0 & 0 \\
 & & & & 4EI_y/l & 0 & 0 & 0 & -6EI_y/l^2 & 0 & 2EI_y/l & 0 \\
 & & & & & 4EI_z/l & 0 & 6EI_z/l^2 & 0 & 0 & 0 & 2EI_z/l \\
 & & & & & & EA/l & 0 & 0 & 0 & 0 & 0 \\
 & & & & & & & 12EI_z/l^3 & 0 & 0 & 0 & -6EI_z/l^2 \\
 & & & \textit{Symmetry} & & & & & 12EI_y/l^3 & 0 & 6EI_y/l^2 & 0 \\
 & & & & & & & & & GJ/l & 0 & 0 \\
 & & & & & & & & & & 4EI_y/l & 0 \\
 & & & & & & & & & & & 4EI_z/l
\end{bmatrix} \tag{3.4}$$

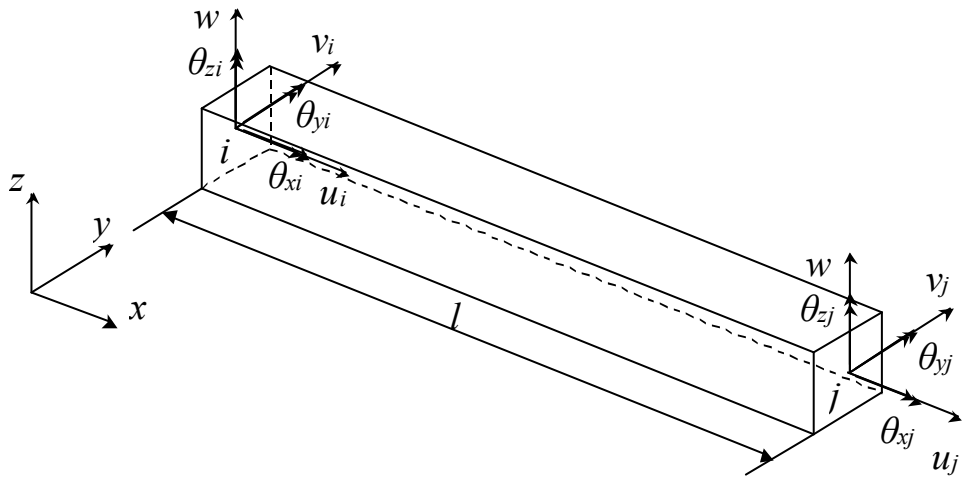


Fig. 3.1 Degrees of freedom and nodal displacements for a three-dimensional beam element

where I_y and I_z are the cross section moments of inertia with respect to the principal axes labeled as y and z, respectively, and l, A and J are the length, cross-sectional area and torsional constant of the beam element, and E is the Young's modulus. In the same manner, the consistent mass matrix type is selected for uniform beam segment of a three dimensional frame, and their components are expressed by combining the consistent mass matrices for axial, torsional and flexural mass effects neglecting the rotary inertia effects as follows:

$$[m]=\frac{\overline{m}l}{420}\begin{bmatrix} 140 & 0 & 0 & 0 & 0 & 0 & 70 & 0 & 0 & 0 & 0 & 0 \\ & 156 & 0 & 0 & 0 & 22l & 0 & 54 & 0 & 0 & 0 & -13l \\ & & 156 & 0 & -22l & 0 & 0 & 0 & 54 & 0 & 13l & 0 \\ & & & 140J/A & 0 & 0 & 0 & 0 & 0 & 70J/A & 0 & 0 \\ & & & & 4l^2 & 0 & 0 & 0 & -13l & 0 & -3l^2 & 0 \\ & & & & & 4l^2 & 0 & 13l & 0 & 0 & 0 & -3l^2 \\ & & & & & & 140 & 0 & 0 & 0 & 0 & 0 \\ & & & & & & & 156 & 0 & 0 & 0 & -22l \\ & & & Symmetry & & & & & 156 & 0 & 22l & 0 \\ & & & & & & & & & 140J/A & 0 & 0 \\ & & & & & & & & & & 4l^2 & 0 \\ & & & & & & & & & & & 4l^2 \end{bmatrix} \tag{3.5}$$

The formulation of the problem implies that the motion of the bridge structure subjected to earthquake loading is assumed to be described by a set of N simultaneous second order linear differential equations in the time domain given by,

$$[M]\{\ddot{d}\} + [C]\{\dot{d}\} + [K]\{d\} = -[M]\{r\}\{\ddot{d}_g\} \tag{3.6}$$

where $[M]$, $[C]$ and $[K]$ are respectively the system mass, damping and stiffness matrices, obtained by assembling the mass, damping and stiffness element matrices presented in Eqs. 3.4 and 3.5. While $\{\ddot{d}\}$, $\{\dot{d}\}$ and $\{d\}$ are the acceleration, velocity and displacement vectors, respectively, $\{r\}$ is a displacement transformation vector that expresses the displacement of each structure degree of freedom due to static application of a unit support displacement, $\{\ddot{d}_g\}$ is the earthquake ground acceleration history applied at the supports. In order to determine the frequencies of the structure, eingenvalue analysis is performed. The free vibrations of an undamped system is described by,

$$[M]\{\ddot{d}\} + [K]\{d\} = \{0\} \tag{3.7}$$

By assuming general solutions in form of harmonic oscillation ($\ddot{\mathbf{d}} = -\omega^2 \mathbf{d}$), where ω is the natural circular frequency. Then, the state of free vibration of a structure is represented by the eigenvalue problem as,

$$\left|\mathbf{K} - \omega^2 \mathbf{M}\right| = 0 \tag{3.8}$$

The computation of eigenvalues in this study is carried out through the Householder's method. For an eigenvalue problem the solution can be expanded in terms of the system eigenfunctions. Indeed, a linear transformation with eigenfunctions as a transformation matrix permits the reduction of system equation to a set of independent equations. The mode shape matrix is n-dimensional vector space, which consists of n linear independent and mutually

orthogonal eigenvectors. The displacement vector can be expressed in terms of any set of *n* independent vectors.

$$\mathbf{d}(t) = \sum_{r=1}^{n} \phi_r \, q_r(t) = \mathbf{\Phi}\, \mathbf{q}(t) \tag{3.9}$$

where $\mathbf{\Phi}$ is $n \times n$ mode shape matrix, $\mathbf{q}(t) = \{q_1(t) \;\; q_2(t) \; \ldots\ldots\ldots\ldots \; q_n(t)\}^{\mathrm{T}}$ is the *n*-dimensional vector of modal coordinates. For the foundation excitation the time variation and spatial distribution is defined by $\{ \ddot{d}_g \}$ and s = **-m r**, respectively. The excitation distribution can be expressed as:

$$\mathrm{s} = -\sum_{r=1}^{n} m\, r = -\sum_{r=1}^{n} \Gamma_r \, m\, \phi_r \tag{3.10}$$

because of the orthogonality relation, premultiplying each term in this equation by ϕ_n^T, gives

$$\Gamma_n = \frac{\phi_n^T \, \mathrm{m}\, \mathbf{r}}{\phi_n^T \, \mathrm{m}\, \phi_n}, \qquad \mathrm{s}_n = \Gamma_n \, \mathrm{m}\, \phi_n \tag{3.11}$$

the s_n denotes the contribution of *n*th mode to the excitation vector **s**, and the Γ_n is defined as modal participation factor, implying that it is a measure of the degree to which the *n*th mode participates in the response. The effective modal mass M_n^* that represent the part of the total mass responding to the earthquake in each mode, can calculated as:

$$\mathrm{M}_n^* = \frac{(\sum_{j=1}^{n} m_j \, \phi_{jn})^2}{\sum_{j=1}^{n} m_j \, \phi_{jn}^2} \tag{3.12}$$

3.3 Three-dimensional Fiber Beam Element Formulation

In order to analyze the elasto-plastic dynamic response of frame structures subjected to strong seismic excitations, a non-linear dynamic finite element technique has been developed. An elastoplastic tangent stiffness matrix of three-dimensional beam element is derived by using the total Lagrangian formulation. This procedure considers both sources of geometric and material non-linearities. An incremental-iterative technique based on the Newmark direct integration method and the Newton-Raphson iteration scheme is employed for obtaining the solutions of the non-linear dynamic equilibrium equations. The finite displacement theory, which reflects the deformed configuration of a body, is composed of a strain-displacement relation, an equilibrium condition and stress-strain relation as well. Since the theory must discern a deformed state from the initial configuration, time- or displacement-dependent variables, necessarily expresses any point of a body. In solid mechanics, an initial configuration of a body is usually given, so it is chosen as a reference state with an affiliated coordinate system. This is called the Lagrangian approach, in which the coordinates of a body at the reference state are chosen as independent variables and solutions such as strains, stresses or displacements are expressed as functions of those variables. If the displacements under consideration are excessively large, the change of the geometrical shape cannot be disregarded in the derivation of the governing equations.

3.3.1 Strain displacement relations

In general, the strain displacement is geometrical relation irrespective of external forces and material used, and there are two methods of describing the deformations of a continuous body. The Lagrangian and the Eulerian, the Lagrangian method employs the coordinates of each particle in the initial position as the independent variables, where as in the Eulerian method the independent variables are the coordinate of each material particle at the time of interest or at the present position. In the Lagrangian method, the initial configuration remains constant. This simplifies the computation. Therefore, the Lagrangian description is selected for the finite element formulation. Recently, a formulation of fiber model has been established. A three-dimensional beam element of six degrees of freedom at each node, in which all coupling among bending; twisting and stretching deformations for beam element is incorporated according to the geometrical non-linear beam theory, has been considered. The deflection of a general point (*x, y* and *z*) inside the beam can be expressed as,

$$\bar{u}(x,y,z) = u(x) - y\frac{dv(x)}{dx} - z\frac{dw(x)}{dx} \tag{3.13a}$$

$$\bar{v}(x,y,z) = v(x) \tag{3.13b}$$

$$\bar{w}(x,y,z) = w(x) \tag{3.13c}$$

where $\bar{u}$, $\bar{v}$ and $\bar{w}$ are the displacements of a point in a beam corresponding to *x-, y-* and *z-* axes, respectively, *u, v* and *w* are the displacements of a point in the centroid axis of a beam corresponding to *x-, y-* and *z-* axes, respectively. The strain in the deformed configuration ε_t can be expressed in terms of the displacement at the equilibrium state at any specified point in the beam cross-section (*x, y* and *z*) that define the state of strain at any arbitrary point. The strain displacement equation (Green-Lagrange representation of axial strain ε_t) is given in the following:

$$\varepsilon_t = \frac{d\,\bar{u}_t}{dx} + \frac{1}{2}\left(\frac{d\,\bar{u}_t}{dx}\right)^2 + \frac{1}{2}\left(\frac{d\,\bar{v}_t}{dx}\right)^2 + \frac{1}{2}\left(\frac{d\,\bar{w}_t}{dx}\right)^2 \tag{3.14}$$

in which it is assumed that $\frac{d\,\bar{u}_t}{dx} << 1$. Thus, $\left(\frac{d\,\bar{u}_t}{dx}\right)^2$ is ignored compared with its linear term. So the normal strain ε_t is calculated using the displacement to give:

$$\varepsilon_t = \frac{d\,\bar{u}_t}{dx} + \frac{1}{2}\left(\frac{d\,\bar{v}_t}{dx}\right)^2 + \frac{1}{2}\left(\frac{d\,\bar{w}_t}{dx}\right)^2 \tag{3.15}$$

where $\bar{u}_t$, $\bar{v}_t$ and $\bar{w}_t$ are the element displacement vector in *x-*, *y-* and *z-*axis directions, respectively. The strain in *t* +1 configuration is unknown, which can be written incrementally from configuration *t* as follows:

$$\varepsilon_{t+1} = \frac{d\,\bar{u}_{t+1}}{dx} + \frac{1}{2}\left(\frac{d\,\bar{v}_{t+1}}{dx}\right)^2 + \frac{1}{2}\left(\frac{d\,\bar{w}_{t+1}}{dx}\right)^2 \tag{3.16a}$$

and its variation is,

$$\delta \varepsilon_{t+1} = \frac{d\delta \bar{u}}{dx} + \frac{d \bar{v}_t}{dx} \cdot \frac{d \delta \bar{v}}{dx} + \frac{d \bar{w}_t}{dx} \cdot \frac{d \delta \bar{w}}{dx} + \frac{1}{2}\delta(\frac{d \bar{v}}{dx})^2 + \frac{1}{2}\delta(\frac{d \bar{w}}{dx})^2 \tag{3.16b}$$

3.3.2 Equilibrium condition

For the principal of energy, that the external work is equivalent to the internal work, the equilibrium equation in the deformed configuration t+1 can be expressed terms of the principle of virtual displacements

$$\delta U - \delta W = 0 \tag{3.17}$$

$$\int_V \sigma_{t+1}\, \delta \varepsilon_{t+1}\, dV + \int_l T_{sv} \frac{d\theta_x}{dx} dx + \frac{1}{2}\int_l GJ(\frac{d\theta_x}{dx})^2 dx - \int_S f_{t+1}^T\, \delta\, d_{t+1}\, dS = 0 \tag{3.18}$$

where U = internal work, W = external virtual work, σ_{t+1} = axial Cauchy stress, V = volume, δ = virtual quantity, f = external applied force and θ_x is the cross-sectional rotation about x axis. Since t+1 configuration is unknown, which can be written incrementally from configuration t consistent with a non-linear Lagrangian scheme as:

$$\int_V (\sigma_t + \sigma)\, \delta \varepsilon_{t+1}\, dV + \int_l T_{sv} \frac{d\theta_x}{dx} dx + \frac{1}{2}\int_l GJ(\frac{d\theta_x}{dx})^2 dx - \int_S (f_t^T + f^T)\ \delta(d_t + d)\, dS = 0 \tag{3.19}$$

where σ = second Piola-Kirchhoff axial stress

$$\int_V (\sigma_t + \sigma)(d\delta u / dx + dv_t / dx \cdot d\delta v / dx + dw_t / dx \cdot d\delta w / dx + \delta(dv / dx)^2 / 2 + \delta(dw / dx)^2 / 2) dV + \int_l T_{sv} \frac{d\theta_x}{dx} dx + \frac{1}{2}\int_l GJ(\frac{d\theta_x}{dx})^2 dx - \int_S (f_t^T + f^T)\, \delta(d_t + d) dS = 0 \tag{3.20}$$

$$\int_V \{\sigma_t (d\delta u / dx + dv_t / dx \cdot d\delta v / dx + dw_t / dx \cdot d\delta w / dx) + \sigma_t \delta(dv / dx)^2 / 2 + \sigma_t \delta(dw / dx)^2 / 2) + \int_l T_{sv} \frac{d\theta_x}{dx} dx + \frac{1}{2}\int_l GJ(\frac{d\theta_x}{dx})^2 dx + \sigma(d\delta u / dx + dv_t / dx \cdot d\delta v / dx + dw_t / dx \cdot d\delta w / dx)\} dV - \int_S (f_t^T + f^T)\delta(d_t + d) dS = 0 \tag{3.21}$$

$$\varepsilon^* = du / dx + dv_t / dx \cdot dv / dx + dw_t / dx \cdot dw / dx \tag{3.22}$$

$$\int_V \{\sigma\, \varepsilon^* + \sigma_t \delta(dv / dx) / 2 + \sigma_t \delta(dw / dx) / 2\} dV + \frac{1}{2}\int_l GJ(\frac{d\theta_x}{dx})^2 dx - \int_S f^T \delta d\, dS = \int_S f_t^T \delta d\, dS - \int_V \sigma_t \varepsilon^* dV - \int_l T_{sv} \frac{d\theta_x}{dx} dx \tag{3.23}$$

3.3.3 Finite element formulation

The displacement transformation matrix of beam element relates the element internal displacement to the nodal point displacement

$$\mathbf{u}(x,y,z) = \{\bar{u}\} = \begin{Bmatrix} \bar{u}(x,y,z) \\ \bar{v}(x,y,z) \\ \bar{w}(x,y,z) \\ \bar{\theta}_x(x,y,z) \end{Bmatrix} = \begin{Bmatrix} u(x) - y\, dv(x)/dx - z\, dw(x)/dx \\ v(x) \\ w(x) \\ \theta_x(x) \end{Bmatrix} = \mathbf{H}(x,y,z)\boldsymbol{\alpha} = \mathbf{H}\ (x,y,z)\mathbf{A}^{-1}\mathbf{d} \tag{3.24}$$

where **u**(*x, y, z*) is the displacement at any general point along the beam element, and four nodal point displacements for expressing $\bar{u}(x,y,z)$, $\bar{v}(x,y,z)$, $\bar{w}(x,y,z)$ and $\theta_x(x,y,z)$ are considered. The shape functions are assumed for the local element displacements *u*, *v*, *w* and θ_x in the local coordinate variable *x*:

The nodal displacement vector is composed of six components, two displacements and a rotational deformation for each nodal point, and they can be expressed with the transformation matrix ***A***, which can be a function of the generalized displacements if geometrical non-linear effects are taken into account. The local-global transformation is expressed

$$\begin{aligned} u &= \alpha_1 + \alpha_2 x \\ v &= \alpha_3 + \alpha_4 x + \alpha_5 x^2 + \alpha_6 x^3 \\ w &= \alpha_7 + \alpha_8 x + \alpha_9 x^2 + \alpha_{10} x^3 \\ \theta_x &= \alpha_{11} + \alpha_{12} x \end{aligned} \tag{3.25}$$

The unknown coefficients $\alpha_1, \alpha_2, \ldots\ldots\ldots\ldots \alpha_{12}$, which are also called the generalized coordinates, will be expressed in terms of the unknown element nodal displacements **d**, defining

To satisfy continuity requirements, the interpolation functions must be assumed continuous in displacement and slope on the element boundaries. Thus appropriate nodal quantities are displacements and rotations at each end of the element. Therefore, the ***H*** matrix is

$$\mathbf{H}(x,y,z) = \begin{Bmatrix} 1 & x & 0 & -y & -2xy & -3x^2y & 0 & -z & -2xz & -3x^2z & 0 & 0 \\ 0 & 0 & 1 & x & x^2 & x^3 & 0 & 0 & 0 & 0 & 0 & 0 \\ 0 & 0 & 0 & 0 & 0 & 0 & 1 & x & x^2 & x^3 & 0 & 0 \\ 0 & 0 & 0 & 0 & 0 & 0 & 0 & 0 & 0 & 0 & 1 & x \end{Bmatrix} \tag{3.26}$$

$$\boldsymbol{\alpha} = \{\alpha_1 \;\; \alpha_2 \;\; \alpha_3 \;\; \alpha_4 \;\; \alpha_5 \;\; \alpha_6 \;\; \alpha_7 \;\; \alpha_8 \;\; \alpha_9 \;\; \alpha_1 \;\; \alpha_{11} \;\; \alpha_{12}\}^T \tag{3.27}$$

$$\{d\} = [A]\{\alpha\} \tag{3.28}$$

in which

$$\mathbf{A} = \begin{vmatrix} 1 & 0 & 0 & 0 & 0 & 0 & 0 & 0 & 0 & 0 & 0 & 0 \\ 0 & 0 & 1 & 0 & 0 & 0 & 0 & 0 & 0 & 0 & 0 & 0 \\ 0 & 0 & 0 & 0 & 0 & 0 & 1 & 0 & 0 & 0 & 0 & 0 \\ 0 & 0 & 0 & 0 & 0 & 0 & 0 & 0 & 0 & 0 & 1 & 0 \\ 0 & 0 & 0 & 0 & 0 & 0 & 0 & 1 & 0 & 0 & 0 & 0 \\ 0 & 0 & 0 & 1 & 0 & 0 & 0 & 0 & 0 & 0 & 0 & 0 \\ 1 & l & 0 & 0 & 0 & 0 & 0 & 0 & 0 & 0 & 0 & 0 \\ 0 & 0 & 1 & l & l^2 & l^3 & 0 & 0 & 0 & 0 & 0 & 0 \\ 0 & 0 & 0 & 0 & 0 & 0 & 1 & l & l^2 & l^3 & 0 & 0 \\ 0 & 0 & 0 & 0 & 0 & 0 & 0 & 0 & 0 & 0 & 1 & l \\ 0 & 0 & 0 & 0 & 0 & 0 & 0 & 1 & 2l & 3l^2 & 0 & 0 \\ 0 & 0 & 0 & 1 & 2l & 3l^2 & 0 & 0 & 0 & 0 & 0 & 0 \end{vmatrix} \tag{3.29}$$

$$\mathbf{u}(x,y,z) = \mathbf{H}(x,y,z)\mathbf{A}^{-1}\mathbf{d} \tag{3.30}$$

Continuing with expression of Eq. 3.22, strains are rewritten in terms of the derivatives of the shape functions through the matrix $\boldsymbol{B}$

$$\varepsilon^* = du/dx + dv_t/dx \cdot dv/dx + dw_t/dx \cdot dw/dx = \mathbf{B}_1\boldsymbol{\alpha} - y\mathbf{B}_2\boldsymbol{\alpha} - z\mathbf{B}_3\boldsymbol{\alpha} = (\mathbf{B}_1 - y\mathbf{B}_2 - z\mathbf{B}_3)\,\boldsymbol{\alpha} \tag{3.31a}$$

$$(dv/dx)^2/2 = (\boldsymbol{\alpha}^T\mathbf{B}_4^T\mathbf{B}_4\,\boldsymbol{\alpha})/2$$
$$(dw/dx)^2/2 = (\boldsymbol{\alpha}^T\mathbf{B}_5^T\mathbf{B}_5\,\boldsymbol{\alpha})/2$$
$$(d\theta_x/dx)^2/2 = (\boldsymbol{\alpha}^T\mathbf{B}_6^T\mathbf{B}_6\,\boldsymbol{\alpha})/2 \tag{3.31b}$$

where

$$\begin{array}{lllllllllll}
\mathbf{B}_1 = \{0 & 1 & 0 & dv_t/dx & 2x\,dv_t/dx & 3x^2\,dv_t/dx & 0 & dw_t/dx & 2x\,dw_t/dx & 3x^2\,dw_t/dx & 0\ \ 0\} \\
\mathbf{B}_2 = \{0 & 0 & 0 & 0 & 2 & 6x & 0 & 0 & 0 & 0 & 0\ \ 0\} \\
\mathbf{B}_3 = \{0 & 0 & 0 & 0 & 0 & 0 & 0 & 0 & 2 & 6x & 0\ \ 0\} \\
\mathbf{B}_4 = \{0 & 0 & 0 & 1 & 2x & 3x^2 & 0 & 0 & 0 & 0 & 0\ \ 0\} \\
\mathbf{B}_5 = \{0 & 0 & 0 & 0 & 0 & 0 & 0 & 1 & 2x & 3x^2 & 0\ \ 0\} \\
\mathbf{B}_6 = \{0 & 0 & 0 & 0 & 0 & 0 & 0 & 0 & 0 & 0 & 0\ \ 1\}
\end{array} \tag{3.32}$$

Due to the considered non-linearities, the expression of the incremental virtual work is fully non-linear, and it is obtained by substituting in Eq. 3.23. Variation of the internal energy is given as,

$$\begin{aligned}
&\int_V \{\sigma\,\varepsilon^* + \sigma_t\delta(dv/dx)/2 + \sigma_t\delta(dw/dx)/2\}dV + \frac{1}{2}\int_l GJ\left(\frac{d\theta_x}{dx}\right)^2 dx \\
&\quad = \int_V \{E_T\,\varepsilon^*\delta\,\varepsilon^* + \sigma_t\delta(dv/dx)/2 + \sigma_t\delta(dw/dx)/2\}dV + \frac{1}{2}\int_l G.\left(\frac{d\theta_x}{dx}\right)^2 dx \\
&\quad = \int_V E_T\,\delta\,\boldsymbol{\alpha}^T(\mathbf{B}_1^T - y\mathbf{B}_2^T - z\mathbf{B}_3^T)(\mathbf{B}_1 - y\mathbf{B}_2 - z\mathbf{B}_3)\boldsymbol{\alpha}\,dV + \int_V \sigma_t\delta\,\boldsymbol{\alpha}^T(\mathbf{B}_4^T\mathbf{B}_4 + \mathbf{B}_5^T\mathbf{B}_5)\boldsymbol{\alpha}\,dV + \int_l GJ\delta\,\boldsymbol{\alpha}^T(\mathbf{B}_6^T\mathbf{B}_6)\boldsymbol{\alpha}\,dx \\
&\quad = \delta\,\boldsymbol{\alpha}^T\int_V E_T\{\mathbf{B}_1^T\mathbf{B}_1 - y(\mathbf{B}_2^T\mathbf{B}_1 + \mathbf{B}_1^T\mathbf{B}_2) + y^2\mathbf{B}_2^T\mathbf{B}_2 - z(\mathbf{B}_3^T\mathbf{B}_1 + \mathbf{B}_1^T\mathbf{B}_3) + z^2\mathbf{B}_3^T\mathbf{B}_3 + zy(\mathbf{B}_2^T\mathbf{B}_3 + \mathbf{B}_3^T\mathbf{B}_2)\}dV\,\boldsymbol{\alpha} \\
&\qquad\qquad + \delta\,\boldsymbol{\alpha}^T\int_V \sigma_t(\mathbf{B}_4^T\mathbf{B}_4 + \mathbf{B}_5^T\mathbf{B}_5)dV\,\boldsymbol{\alpha} + \int_l GJ\delta\,\boldsymbol{\alpha}^T(\mathbf{B}_6^T\mathbf{B}_6)\boldsymbol{\alpha}\,dx \\
&\quad = \delta\,\boldsymbol{\alpha}^T\int\{E_1\mathbf{B}_1^T\mathbf{B}_1 - E_2(\mathbf{B}_2^T\mathbf{B}_1 + \mathbf{B}_1^T\mathbf{B}_2) + E_3\mathbf{B}_2^T\mathbf{B}_2 - E_4(\mathbf{B}_3^T\mathbf{B}_1 + \mathbf{B}_1^T\mathbf{B}_3) + E_5\mathbf{B}_3^T\mathbf{B}_3 + E_6(\mathbf{B}_2^T\mathbf{B}_3 + \mathbf{B}_3^T\mathbf{B}_2)\}\boldsymbol{\alpha}\,dx \\
&\qquad\qquad + \delta\,\boldsymbol{\alpha}^T\int_l F_x(\mathbf{B}_4^T\mathbf{B}_4 + \mathbf{B}_5^T\mathbf{B}_5)dx\,\boldsymbol{\alpha} + \delta\,\boldsymbol{\alpha}^T\int_l GJ(\mathbf{B}_6^T\mathbf{B}_6)\boldsymbol{\alpha}\,dx
\end{aligned} \tag{3.33}$$

whereas the work done by the external forces results in

$$\begin{aligned}
\int_V \sigma_t\,\varepsilon^*\,dV + \int_l T_{sv}\frac{d\theta_x}{dx}dx &= \int_V \sigma_t(\mathbf{B}_1 - y\mathbf{B}_2 - z\mathbf{B}_3)\delta\,\boldsymbol{\alpha}\,dV + \int_l T_{sv}\mathbf{B}_6\delta\,\boldsymbol{\alpha}\,dx \\
&= \delta\,\boldsymbol{\alpha}^T\int_V \sigma_t(\mathbf{B}_1^T - y\mathbf{B}_2^T - z\mathbf{B}_3^T)dV + \delta\,\boldsymbol{\alpha}^T\int_l T_{sv}\mathbf{B}_6^T\,dx = \delta\,\boldsymbol{\alpha}^T\int_l (F_x\mathbf{B}_1^T - M_z\mathbf{B}_2^T - M_y\mathbf{B}_3^T + T_{sv}\mathbf{B}_6^T)dx
\end{aligned} \tag{3.34}$$

in which,

$$\begin{aligned}
&E_1 = E_T\int dydz, \quad E_2 = E_T\int ydydz, \quad E_3 = E_T\int y^2dydz\ , \quad E_4 = E_T\int zdydz, \quad E_5 = E_T\int z^2ydydz, \quad E_6 = E_T\int zydydz \\
&F_x = \int\sigma_t dydz, \qquad M_z = \int\sigma_t ydydz, \qquad M_y = \int\sigma_t zdydz
\end{aligned} \tag{3.35a}$$

That can be determined through numerical integration over the cross section fiber segments as follow

$$\int \sigma_t yzdydz = \int_A \sigma_t yzdA = \sum_{k=1}^{n} \sigma_{tk} y_k z_k A_k \tag{3.35b}$$

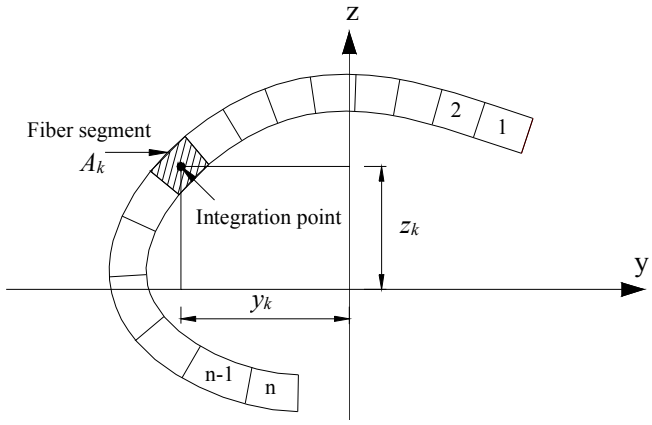


Fig. 3.2 Fiber model of arbitrary cross section

Substitution Eqs. 3.28, 3.33 and 3.34 into Eq. 3.23, the equation of motion can be expressed as

$$\delta \mathbf{d}^T (\mathbf{k}_t \mathbf{d} - \mathbf{f}_t) = \delta \mathbf{d}^T (\mathbf{f} - \mathbf{r}_t) \tag{3.36}$$

from which the tangent stiffness matrix can be obtained as follows,

$$\begin{aligned} \mathbf{k}_t = (\mathbf{A}^{-1})^T \int \{ & E_1 \mathbf{B}_1^T \mathbf{B}_1 - E_2 (\mathbf{B}_2^T \mathbf{B}_1 + \mathbf{B}_1^T \mathbf{B}_2) + E_3 \mathbf{B}_2^T \mathbf{B}_2 - E_4 (\mathbf{B}_3^T \mathbf{B}_1 + \mathbf{B}_1^T \mathbf{B}_3) + E_5 \mathbf{B}_3^T \mathbf{B}_3 \\ & + E_6 (\mathbf{B}_2^T \mathbf{B}_3 + \mathbf{B}_3^T \mathbf{B}_2) + F_x (\mathbf{B}_4^T \mathbf{B}_4 + \mathbf{B}_5^T \mathbf{B}_5) + GJ (\mathbf{B}_6^T \mathbf{B}_6) \} dx \mathbf{A}^{-1} \end{aligned} \tag{3.37}$$

In order to capture the spread of plastic zone in individual element, the beam element is divided along its length and cross section directions, and based on the stress states of integration points in the section, the stiffness quantities of the section are calculated along the cross section as shown in **Fig. 3.2**, then the stiffness quantities of the element are obtained by integrating along the length of the beam, in which the plastic development of the material is automatically considered. The stiffness matrix calculations of the elements are completed by numerical integration procedure. After obtaining the stiffness matrix of the elements with respect to the local coordinate system, transforming them from the element local coordinate system to global coordinate system, then assembling the stiffness matrix of the elements using standard procedures and getting the globe stiffness matrix. During the incremental process, the effects of both the geometrical variations and material non-linearity are accounted for through the tangent stiffness operator.

3.3.4 Solution technique of non-linear equilibrium equation

In using the Newton-Raphson method to the equilibrium iteration, the stiffness matrix **K** and equivalent residual force vector have to be updated for each iteration step. The equivalent stiffness matrix can thus be constructed. The non-linear problem is solved by taking a series of linear steps. In structural terms this process is explained by writing equilibrium equations in the incremental form

$$\mathbf{K}_t \, \mathbf{d} = \mathbf{f}_{t+1} - \mathbf{r}_t \tag{3.38}$$

The non-linear equilibrium equation is solved using the Newton-Raphson method, as shown in **Fig. 3.3**. The equilibrium point is approached by successive approximations to reduce the unbalanced load in iteration. The stiffness or slope of the force-displacement curve is updated at each iteration. The stiffness matrix $\mathbf{k_n}$ is a function of displacements **d** because the problem is non-linear. The current tangent stiffness, $\mathbf{k_n}$, is used to compute the next step, **d**. Then both displacement and stiffness are updated for the next iteration, at the equilibrium state *t,* supposing that the displacement $\mathbf{d}_t$ that correspond to load $\mathbf{r}_t$ is known. In this way, a load versus displacement curve is approximated by a series of straight line segments.

Considering the load versus displacement function,

$$\mathbf{r}_{t+1} = \mathbf{f}_{t+1} \tag{3.39}$$

and supposing that the displacement $\mathbf{d_n}$ that correspond to the load $\mathbf{r_n}$ is known. The load is now increased to $\mathbf{r}_{t+1}$ and the corresponding displacement $\mathbf{d}_{t+1}$ is sought. A Taylor series expansion of $\mathbf{r}_{t+1}$ about $\mathbf{d}_t$ truncated after the first derivative is

$$\mathbf{r}_{t+1} = \mathbf{r}_t + \frac{\delta \mathbf{r}_t}{\delta \mathbf{d}_t}\mathbf{d} \tag{3.40}$$

where the tangent stiffness could be expressed as

$$\mathbf{K}_t = \frac{\delta \mathbf{r}_t}{\delta \mathbf{d}_t} \tag{3.41}$$

A new displacement **d** is seek such that

$$\mathbf{K}_t\,\mathbf{d} = \mathbf{r}_{t+1} - \mathbf{r}_t \tag{3.42}$$

where $\mathbf{r}_{t+1} - \mathbf{r}_t$ can be interpreted as the difference between the applied load and the resisting force of the structure. Recurrence relations of the form characterize the Newton-Raphson method could be written as follows:

$$\begin{aligned} &\mathbf{K}_t^{(i-1)}\mathbf{d}^{(i)} = \Gamma^{(i-1)} \\ &\mathbf{K}_t^{(i)} = \frac{\delta \mathbf{r}_{t+1}^{(i)}}{\delta \mathbf{d}_{t+1}^{(i)}}; \qquad \Gamma^{(i)} = \mathbf{f}_{t+1} - \mathbf{r}_{t+1}^{(i)}; \quad \mathbf{r}_{t+1}^{(0)} = \mathbf{r}_t; \quad \mathbf{f}_{t+1}^{(0)} = \mathbf{f}_t; \quad \mathbf{d}_{t+1}^{(i)} = \mathbf{d}_{t+1}^{(i-1)} + \mathbf{d}^{(i)} \end{aligned} \tag{3.43}$$

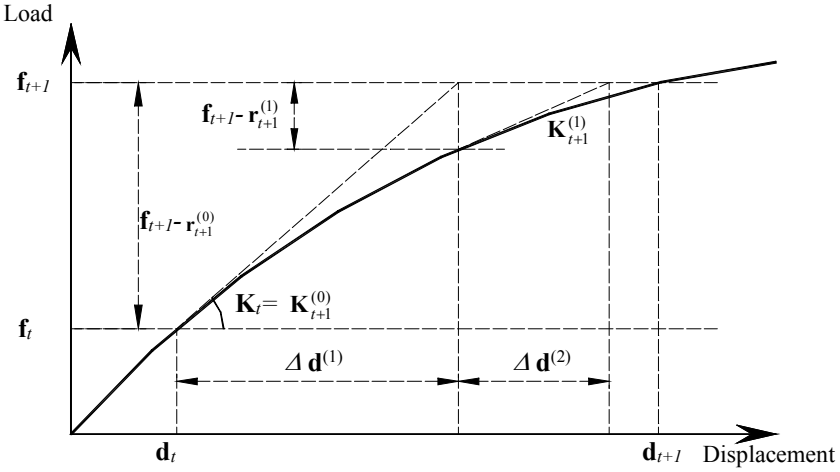


Fig. 3.3 Newton-Raphson integration method

3.4 Non-linear Dynamic Equilibrium Equation of Motion

3.4.1 Dynamic equilibrium equation

The governing non-linear dynamic equation of the viaduct response can be derived by the principle of energy that the external work is absorbed by the work of internal, inertial and damping for any small admissible motion that satisfies compatibility and boundary condition. By assembling the element dynamic equilibrium equation for the time t+1 over all the elements, the incremental FEM dynamic equilibrium equation can be obtained as:

$$[M]\{\ddot{d}\}_{t+1} + [C]\{\dot{d}\}_{t+1} + [K]_{t+1}\{\Delta d\}_{t+1} = \{F\}_{t+1} - \{F\}_{t} \tag{3.44}$$

where $[M]$, $[C]$ and $[K]_{t+1}$ are the system mass, damping and tangent stiffness matrices at time t+1. The tangent stiffness matrix takes into consideration the material non-linearities through bilinear stress strain relation for the beam column element, and the geometrical non-linearities for the case of in-plane, out-plane bending deformations and linear torsional deformations. $\{\ddot{d}\}$, $\{\dot{d}\}$ and $\{\Delta d\}$ are the accelerations, velocities and incremental displacements vectors at time t+1, respectively, $\{F\}_{t+1} - \{F\}_{t}$ is the unbalanced force vector. It can be noticed that the dynamic equilibrium equation of motion takes into consideration the different sources of non-linearities both geometrical and material non-linearities, which affect the calculation of the tangent stiffness and internal forces.

3.4.2 Consistent mass matrix

A mass matrix is evaluated with the same shape functions used for the derivation of the stiffness coefficient is called a consistent mass matrix, cubic Hermitian polynomials can be used as the shape functions for evaluating the mass coefficients for the flexural inertial forces, while a linear polynomial may be used for modeling the axial and torsional inertia forces. The mass coefficient m_{ij} as the force at nodal coordinate i due to a unit acceleration at nodal coordinate j while all other coordinate are maintained at zero acceleration. To calculate the coefficient for the consistent mass matrix, it is necessary first to determine the displacement function by solving the governing equation of response motion to a unit displacement at one of the model coordinates. The shape function of axial or torsional deformations is defined to be linear functions as follows:

$$\psi_1(x) = 1 - \xi, \qquad \psi_2(x) = \xi \qquad \xi = x / l \tag{3.45a}$$

and that of flexural deformations is defined to be cubic Hermitian functions as follows:

$$\begin{aligned} &\psi_3(x) = 1 - 3\xi^2 + 2\xi^3, && \psi_4(x) = \xi\, l\, (1 - \xi)^2 \\ &\psi_5(x) = 3\xi^2 - 2\xi^3, && \psi_6(x) = \xi\, l\, (\xi - 1) \end{aligned} \tag{3.45b}$$

The consistent mass coefficient m_{ij} related to axial and torsional inertial forces of prismatic beam segment, which has distributed mass $\overline{m}$ per unit of length l, could be calculated from

$$m_{ij} = \int_0^l \overline{m}\, \psi_i(x)\, \psi_j(x)\, dx \qquad (i, j = 1, 2) \tag{3.46}$$

while the consistent mass coefficient m_{ij} related to flexural deformations includes translational and rotary inertia forces of beam segment, which has mass moment inertia ($\bar{I}_c = \bar{m} I_c / A$, $c = y$ or z axis) per unit of length, and could be calculated from

$$m_{ij} = \int_0^l \bar{m}\, \psi_i(x)\, \psi_j(x)\, dx + \int_0^l \bar{I}_c\, \psi_i'(x)\, \psi_j'(x)\, dx \qquad (i, j = 3 - 6) \qquad (3.47)$$

3.4.3 Damping mechanism

A correct representation of structural damping cannot be formulated from a practical standpoint. Accordingly, simplified assumptions have to be used. The physical causes of damping in dynamic analysis are any processes, which dissipate energy or reduce the structural response through internal friction. Plastic yield in the non-linear materials automatically absorbs energy when the structure follows a loading and unloading cycle. This is an actual hysteresis effect that produces an accurate form of damping. In this analysis, damping is treated in two categories. First, a phenomenological damping approach is used by considering physical elastic-plastic hysteresis loss in energy dissipation devices. This damping includes the internal hysteresis that occurs in materials such as rubber, friction in bearings, and other non-linear effects such as plastic strain in metals. In the second category, an equivalent viscous damping is introduced, as constant matrix terms, in the system in the form of damping matrix [C]. In this study, different spectral damping schemes are used. A simplified damping assumption is used only to clarify vertical ground motion and damping scheme effects on the bridge dynamic response, where the attenuation of tower structure is adopted the viscous damping of mass proportional type with damping coefficient to the first fundamental natural vibration. Rayleigh's damping scheme is used to form damping matrix [C] as a linear combination of mass and stiffness matrices, which effectively captures the tower structures damping and is also computationally efficient.

$$[C] = a_m [M] + a_k [K] \qquad (3.48)$$

where

$$a_m = \frac{2\omega_i \omega_j (\eta_i \omega_j - \eta_j \omega_i)}{\omega_j^2 - \omega_i^2}, \quad a_k = \frac{2(\eta_i \omega_j - \eta_j \omega_i)}{\omega_j^2 - \omega_i^2} \qquad (3.49)$$

The stiffness and mass proportional damping constants (a_m, a_k) are given in terms of two different natural circular frequencies (ω_i, ω_j) and the corresponding critical damping ratio (η_i, η_j). Damping ratios for other modes can be found as

$$\eta = \frac{1}{2}(a_k \omega + a_m / \omega) \qquad (3.50)$$

The use of more than two proportional damping constants is expensive. In order to prepare for situation where is possible to have more than two damping ratios incorporated in the analysis, a generalized damping matrix could be introduced.

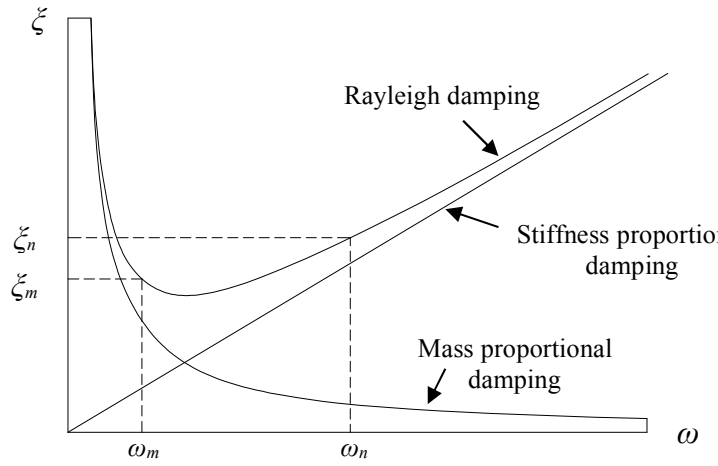


Fig. 3.4 Relationship between damping ratio and frequency for Rayleigh damping type

$$[\Phi]^T[C][\Phi]=\begin{bmatrix} 2\omega_1\eta_1 & \mathbf{0} & \cdots & \mathbf{0} \\ \mathbf{0} & 2\omega_2\eta_2 & & \mathbf{0} \\ & & \ddots & \vdots \\ \mathbf{0} & \mathbf{0} & \cdots & 2\omega_n\eta_n \end{bmatrix} \tag{3.51}$$

where $[\Phi]$ is the modal matrix. The damping matrix can then be determined

$$[C]=[M](\sum_{j=1}^{j=n}\frac{2\eta_j\omega_j}{\overline{M}_j}\{\phi_j\}\{\phi_j\}^T)[M] \tag{3.52}$$

where n is the number of modes considered for damping and $\overline{M}_j$ is the jth modal mass. One disadvantage of this approach is that a full damping matrix $[C]$ is obtained regardless of whether the stiffness and mass matrices are banded or not. An approximation has to be introduced in this regard by discarding elements of damping matrix off the stiffness matrix bandwidth. The relationships between damping ratio and frequency are shown graphically in **Fig. 3.4**.

3.4.4 Integration of dynamic equilibrium equation

Considering the direct integration method, the following three equations represent an implicit scheme:

$$(1-\alpha_M)[M]\{\ddot{d}\}_{t+1}+\alpha_M[M]\{\ddot{d}\}_{t+1}+(1-\alpha_C)[C]\{\dot{d}\}_{t+1}+\alpha_C[C]\{\dot{d}\}_t+(1-\alpha_K)[K]_{t+1}\{\Delta d\}_{t+1} = \{F\}_{t+1}-\{F\}_t \tag{3.53}$$

$$\{\dot{d}\}_{t+1}=\{\dot{d}\}_t+(1-\gamma)\Delta t\{\ddot{d}\}_t+\gamma\Delta t\{\ddot{d}\}_{t+1} \tag{3.54a}$$

$$\{d\}_{t+1}=\{d\}_t+\Delta t\{\dot{d}\}_t+(0.5-\beta)\Delta t^2\{\ddot{d}\}_t+\beta\Delta t^2\{\ddot{d}\}_{t+1} \tag{3.54b}$$

where α_M, α_C, α_K, β and γ are five constants and Δt is the time increment from time step t to time step $t+1$; the above two equations give

$$\{\ddot{d}\}_{t+1}=(1/\beta\Delta t^2)(\{\Delta d\}_{t+1}-\Delta t\{\dot{d}\}_t-(0.5-\beta)\Delta t^2\{\ddot{d}\}_t) \tag{3.55}$$

$$\{\dot{d}\}_{t+1} = (\gamma/\beta\,\Delta t)(\{\Delta d\}_{t+1} - (1-\beta/\gamma)\Delta t\{\dot{d}\}_t - (0.5-\beta/\gamma)\Delta t^2\{\ddot{d}\}_t) \tag{3.56}$$

The substitution of Eqs. 3.55 and 3.56 into Eq. 3.53 leads to the following incremental equivalent stiffness equation for determining the incremental displacement vector:

$$[K]\{\Delta d\}_{t+1} = \{F\} \tag{3.57}$$

in which effective stiffness matrix and the equivalent incremental load vector can be written as:

$$[K] = (1-\alpha_M)(1/\beta\,\Delta t^2)[M] + (1-\alpha_C)(\gamma/\beta\,\Delta t)[C] + (1-\alpha_K)[K]_{t+1} \tag{3.58}$$

$$\begin{aligned}\{F\} = \{F\}_{t+1} - \{F\}_t + (1/\beta\,\Delta t)((1-\alpha_M)[M] + \Delta t(\gamma-\beta-\alpha_C\gamma)[C])\{\dot{d}\}_t \\ + (1/2\beta)((1-2\beta-\alpha_M)[M] + \Delta t(\gamma-2\beta)(1-\alpha_C)[C])\{\ddot{d}\}_t\end{aligned} \tag{3.59}$$

if $\alpha_C = \alpha_K$, then it represents the generalized-α trapezoidal scheme. If $\alpha_M = 0$ and $\alpha_K \neq 0$, then it results in the Hilber-Hughes-Taylor scheme. If $\alpha_K = 0$ and $\alpha_M \neq 0$, then it leads to the Wood-Bossak-Zienkiewicz scheme. If $\alpha_K = 0$ and $\alpha_M = 0$, then it reduce to the Newmark's β scheme. For the Newmark's β scheme, if $\beta = 1/4$ and $\gamma = 1/2$ then it results in the constant acceleration scheme, while $\beta = 1/6$ and $\gamma = 1/2$ leads in the linear acceleration scheme. An alternative efficient time integration scheme is the generalized-θ mid-point scheme.

In this study, the incremental equation of motion, Eq. 3.44 that is derived from consideration of static equilibrium at time t and t+1 can be written as follows:

$$I + H + R = F \tag{3.60}$$

where *I, H, R* and *F* are the incremental inertia, damping, elastic and unbalanced forces, respectively. To solve the equation of motion, the Newmark's step-by-step integration method is used for the integration of equation of motion, since it has been experienced that the Newmark's β method is the most suitable for non-linear analysis; it has the lowest period elongation and has no amplitude decay or amplifications. In addition, the stability concern is not a problem with the variable ratio of time increment to natural period. Using the Newmark's integration method, the equation 3.60 terms can be expressed as

$$\begin{aligned} I &= \mathbf{M}\,\ddot{\mathbf{d}} = \mathbf{M}\left[\frac{1}{\beta\Delta t^2}\mathbf{d} - \frac{1}{\beta\Delta t}\dot{\mathbf{d}}_t - \frac{1}{\beta}\ddot{\mathbf{d}}_t\right],\quad R = \mathbf{K}_t\mathbf{d} \\ H &= \mathbf{C}\,\dot{\mathbf{d}} = \mathbf{C}\left[\frac{\gamma}{\beta\Delta t}\mathbf{d} - \frac{\gamma}{\beta}\dot{\mathbf{d}}_t - (\frac{\gamma}{2\beta}-1)\,\Delta t\,\ddot{\mathbf{d}}_t\right] \end{aligned} \tag{3.61}$$

where γ and β are Newmark's integration parameters that can be chosen according to the accuracy and stability concerns. The algorithm is unconditionally stable if $\beta \geq (\gamma + 0.5)^2/4$. In this study the Newmark's β of constant acceleration scheme is considered for which γ and β are equal to 0.5 and 0.25 respectively.

The equation of motion is solved for the incremental displacement $\{\Delta d\}_{t+1}$using the Newton Raphson iteration method where the stiffness matrix is updated at each increment to consider the geometrical and material nonlinearities and to speed the convergence rate. As the

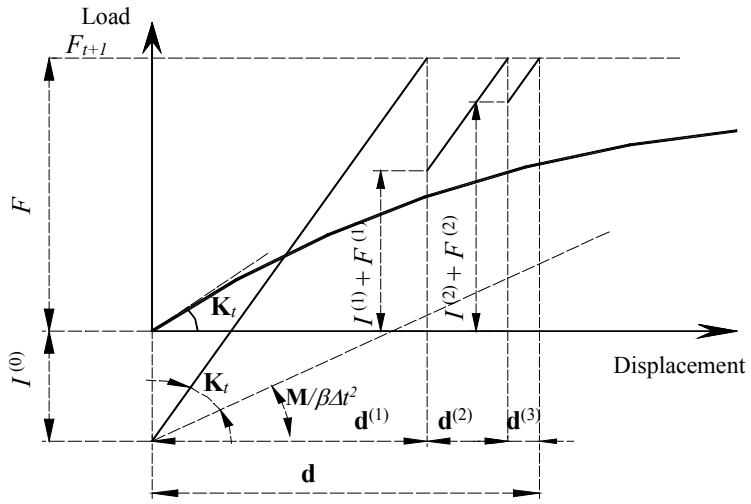


Fig. 3.5 Newmark's β method and Newton-Raphson iteration technique

incremental displacement is determined by the solution of Eq. 3.57, the response displacement at the end of the time step and the incremental displacement, velocity and acceleration components increment measured from the previous convergence configuration at time t can be expressed as

$$\begin{aligned}
\mathbf{d} &= \mathbf{d}_{t+1} - \mathbf{d}_t = \Delta t\, \dot{\mathbf{d}}_t + (0.5-\beta)\,\Delta t^2 \ddot{\mathbf{d}}_t + \beta\,\Delta t^2 \ddot{\mathbf{d}}_{t+1} \\
\dot{\mathbf{d}} &= \dot{\mathbf{d}}_{t+1} - \dot{\mathbf{d}}_t = \frac{\gamma}{\beta\,\Delta t}\mathbf{d} - \frac{\gamma}{\beta}\dot{\mathbf{d}}_t - (\frac{\gamma}{2\beta}-1)\Delta t\, \ddot{\mathbf{d}}_t \\
\ddot{\mathbf{d}} &= \ddot{\mathbf{d}}_{t+1} - \ddot{\mathbf{d}}_t = \frac{1}{\beta\,\Delta t^2}\mathbf{d} - \frac{1}{\beta\,\Delta t}\dot{\mathbf{d}}_t - \frac{1}{\beta}\ddot{\mathbf{d}}_t
\end{aligned} \tag{3.62}$$

The equation of equilibrium, using Eq. 3.61, can be expressed as

$$(\mathbf{K}_t + \frac{\gamma}{\beta\,\Delta t}\mathbf{C} + \frac{\gamma}{\beta\,\Delta t^2}\mathbf{M})\mathbf{d} = F - H^{(0)} - I^{(0)} \tag{3.63}$$

in which $H^{(0)}$ and $I^{(0)}$ are directly obtained by substitution for the incremental displacement value $\mathbf{d} = \mathbf{0}$ in Eq. 3.61. A schema of Newmark's β method and Newton Raphson iteration technique is illustrated in **Fig 3.5**. Recurrence relations of the form characterize the Newmark's β method and Newton-Raphson iteration technique in the form of a pseudo static equation for the displacements at the end of the time step could be written as follows

$$(\mathbf{K}_{t+1}^{(i)} + \frac{\gamma}{\beta\,\Delta t}\mathbf{C} + \frac{\gamma}{\beta\,\Delta t^2}\mathbf{M})\mathbf{d}^{(i+1)} = F - R^{(i)} - H^{(i)} - I^{(i)} = \Gamma^{(i)} \tag{3.64}$$

$$\begin{aligned}
\mathbf{d}^{i+1} &= \mathbf{d}_{t+1}^{i+1} - \mathbf{d}_{t+1}^{i} \\
\dot{\mathbf{d}}^{i+1} &= \dot{\mathbf{d}}_{t+1}^{i+1} - \dot{\mathbf{d}}_{t+1}^{i} \\
\ddot{\mathbf{d}}^{i+1} &= \ddot{\mathbf{d}}_{t+1}^{i+1} - \ddot{\mathbf{d}}_{t+1}^{i}
\end{aligned} \tag{3.65}$$

The pseudo stiffness matrix and the total displacement for each time step are defined as

$$\hat{\mathbf{K}}_{t+1}^{(i+1)} = \mathbf{K}_{t+1}^{(i)} + \frac{\gamma}{\beta\,\Delta t}\mathbf{C} + \frac{\gamma}{\beta\,\Delta t^2}\mathbf{M}\,,\ \mathbf{d} = \sum_{1}^{i} d^{(i)} \tag{3.66}$$

The iterative process is terminated when $\mathbf{F}^{(i+1)}$ and $\mathbf{d}^{(i+1)}$ fall with prescribed tolerance. In this study, the convergence is fixed for

$$\frac{\mathbf{d}^{(i)}}{\mathbf{d}} \le 0.001 \tag{3.67}$$

3.5 Energetic Analysis

In nature, the process for an earthquake to damage a structure can be viewed as an energy transferring process. Energy is produced by the collision of underground plates, and the movement of the ground transfers part of the energy to structures to induce structural vibration. Although the motion of the ground at a specific site is independent of the structure built at this site, the response of the structure and the amount of energy inputted to the structure depend highly on the structural characteristics such as the periods of vibration and damping. This input energy is then transferred to different energy forms such as strain energy, kinetic energy, and damping energy. Therefore, studying the energy characteristics and energy transfer in structures during earthquakes will provide a good basis for protecting structures.

An energy method to quantify seismic structural response was apparently first proposed by Housner [11]. He pointed out that a ground motion effectively feeds energy into a given structure, some of this energy being dissipated through damping and the remainder stored in the structure in the forms of kinetic energy or motion of the mass, and strain energy or deformation of the structural members. Housner formulated the fundamental concept that at any instant the sum of the kinetic energy, strain energy, energy dissipated through normal damping, and energy dissipated through permanent deformation, must be equal to the total input. This provided the initial impetus to the later developments of energy methods in earthquake engineering. However, this proposal has remained an isolated episode until the last decade, when the availability of a great quantity of records from severe earthquakes had determined a decisive impulse to researches on energy criteria. During the last two decades many researchers have considered the energy concepts applied to the non-linear seismic analysis of structures. Uang and Bertero [12] provided mathematically consistent definitions of energy methods, Zahrah and Hall [13] studied seismic energy absorption in SDOF systems, and Akiyama [14] used an energy method based on the equation of Housner for the design of steel buildings. In the last few years, the seismic design methodology based on energy criteria has been introduced in the Japanese Seismic Code as an effective tool in the earthquake-resistance design of new structures and in the seismic assessment of the existing structures [4].

In this study, the non-linear seismic response of the bridge is also calculated on the basis of the equilibrium of energy, observing that energy methods produce goods indicators of the non-linear inelastic seismic structural performance.

The equation of motion of a multi-degree-of-freedom system subjected to ground motion can be written as follows

$$[M]\{\ddot{d}\} + [C]\{\dot{d}\} + [K]\{d\} = -[M]\{\ddot{d}_g\} \tag{3.68}$$

where [*M*], [*C*] and [*K*] are the mass, damping, and stiffness matrices, respectively, $\{\ddot{d}\}$, $\{\dot{d}\}$ and $\{d\}$ are the relative displacement, velocity, and acceleration vectors, respectively, and $\{\ddot{d}_g\}$ is the earthquake ground acceleration vector. By multiplying both sides of Eq. 3.68 by $\{\dot{d}^T\}$ and by integrating the product over the entire duration of the earthquake, i.e. from $t = 0$ to t_0, where t_0 refers to the instant when the earthquake fades away, the energy balance equation becomes

$$\int_0^t \{\dot{d}^T\}[M]\{\ddot{d}\}dt + \int_0^t \{\dot{d}^T\}[C]\{\dot{d}\}dt + \int_0^t \{\dot{d}^T\}[K]\{d\}dt = -\int_0^t \{\dot{d}^T\}[M]\{\ddot{d}_g\}dt \tag{3.69}$$

where

$$E_I = E_K + E_D + E_S \tag{3.70}$$

E_I is the absolute input energy where the inertia force applied to the structure is expressed in terms of the total acceleration relative to a fixed reference axis. E_K represents the absolute kinetic energy that includes the effects of the rigid body translation of the structure. E_D is the consumed energy due to damping mechanism of the system, and E_S corresponds to the absorbed energy, which is composed of recoverable elastic strain energy and irrecoverable hysteretic energy.

Then, at the end of the motion, Eq. 3.70 becomes

$$E_I = E_D + E_S \tag{3.71}$$

i.e. the total energy imparted to the structure by the earthquake must be dissipated by damping and inelastic deformations. Evaluating Eq. 3.69 over the entire duration of an earthquake motion, the cumulative energy balance is obtained.

3.6 Conclusions

The highway viaduct object of this study is expected to experience complex behavior during an earthquake. This structural system cannot be fully represented by static analysis, and, therefore, is seismically evaluated based on the results of dynamic analysis to verify the safety of the bridge under seismic loading. A non-linear finite element formulation for the non-linear dynamic analysis of bridge structures is developed to have a through understanding and a realistic prediction of the structural response, hence to improve design procedures and seismic performance precisely. This formulation includes the best features of several previous studies, where a fiber flexural element is developed for tower characterization; the element incorporates both geometric and material non-linearities, which are vital to understanding the complex structural mechanical behavior. The fiber flexural element modeling is adopted to capture the spread of plastic zone in individual element, the beam element is divided along its length and cross section directions, and based on the stress states of integration points in the section, the stiffness quantities of the section are calculated along the cross section, then the stiffness quantities of the element are obtained by integrating along the length of the beam, in which the plastic development of the material is automatically considered. The stiffness matrix calculations of the elements are completed by numerical integration procedure. After obtaining the stiffness matrix of the elements with respect to the local coordinate system,

transforming them from the element local coordinate system to global coordinate system, then assembling the stiffness matrix of the elements using standard procedures and getting the globe stiffness matrix.

The fiber model used in this study is physically motivated from actual unaxial test data of structural steel bars. Explicit expressions for stress in terms of strain also give the instantaneous stiffness, making the model ideal for iterative non-linear analysis. The stress-strain relation is the same for compression and tension. Residual stresses shift the curve along the strain axis until the residual stress level is located at zero strain. Thus, adjacent fibers can have different levels of residual stress. The stress pattern is defined in such a way that equilibrium is maintained, but the maximum residual stress can be chosen. The differential equations of motion are solved in incremental form by employing the Newmark method. In convergent process, the Newton-Raphson method is used for the solution of the nonlinear problem, and the iteration continues until the tolerance reaches an acceptable specified value. During the incremental process, the effects of both the geometrical variations and material non-linearity are accounted for through the tangent stiffness operator.

Additionally, in this study, the nonlinear seismic response of the bridge is calculated on the basis of the equilibrium of energy. Energetic analysis is formulated under the principle that at any instant the sum of the kinetic energy, strain energy, energy dissipated through normal damping, and energy dissipated through permanent deformation, must be equal to the total input.

References

[1] Committee of Earthquake Engineering: *The 1995 Hyogoken-Nanbu Earthquake, Investigation into Damage to Civil Engineering Structures,* Japan Society of Civil Engineers, June, 1996.

[2] Moehle, J. P.: Northridge earthquake of January 17, 1994: reconnaissance report, volume 1 - highway bridges and traffic management, *Earthquake Spectra*, Vol.11, pp. 287-372, 1995.

[3] Ali, H. M. and Abdel-Ghaffar, A. M.: Modeling the nonlinear seismic behavior of cable-stayed bridges with passive control bearings*, Computers and Structures,* Vol. 54, No. 3, pp. 461-492, 1995.

[4] Japan Road Association, *Specification for Highway Bridges - Part V Seismic Design*, Chapter 1-8, 1996.

[5] Bathe, K. J., Ramm, E. and Wilson E. L.: Finite element formulations for large deformation dynamics, *International Journal for Numerical Methods in Engineering,* Vol. 9, pp. 353-386, 1975.

[6] Bathe, K. J. and Bolourchi S.: Large displacement analysis of three-dimensional beam structures, *International Journal for Numerical Methods in Engineering,* Vol. 14, pp. 961-986, 1979.

[7] Yang, T. Y. and Saigal S.: A simple element for static and dynamic response of beams with material and geometric nonlinearities, *International Journal for Numerical Methods in Engineering,* Vol. 20, pp. 851-867, 1984.

[8] Shi, G. and Atluri, S. N.: Elasto-plastic large deformation analysis of space frames, *International Journal for Numerical Methods in Engineering,* Vol. 26, pp. 589-615, 1988.

[9] Bathe, K. J.: *Finite element procedures in engineering analysis,* Englewood Cliffs, New Jersey, Prentice-Hill, 1982.

[10] Clough, W. R. and Penzien, J.: *Dynamic of structures,* 2nd ed., New York, McGraw-Hill, 1993.
[11] Housner G. W.: Behavior of structures during earthquakes, *Journal of Engineering Mechanics* ASCE*,* Vol. 25, pp. 85-109, 1959.
[12] Uang, C. M. and Bertero V. V.: Evaluation of seismic energy in structures, *Earthquake Engineering and Structural Dynamics,* Vol. 19, pp. 77-90, 1990.
[13] Zahrah, T. and Hall J.: Earthquake energy absorption in SDOF structures, *Journal of Structural Engineering* ASCE*,* Vol. 110, No. 8, pp. 1757-1772, 1984.
[14] Akiyama H.: Earthquake resistant limit state design for buildings, *University of Tokyo Press,* Tokyo, 1985.

CHAPTER 4

SEISMIC RESPONSE OF HIGHWAY VIDADUCTS EQUIPPED WITH LRB UNDER LOW TEMPERATURE

4.1 Introduction

The increasing need for safer bridges has stimulated the adoption of a common earthquake protection strategy consisting in the replacement of the vulnerable steel bearing supports with seismic isolation devices. An isolation system placed between the bridge superstructure and its supporting substructure is generally capable of increasing both flexibility and energy dissipation. Flexibility in the horizontal plane will lower the fundamental frequency of the bridge below the range of the most-damaging frequencies, which dominate general earthquake input so that the earthquake-induced acceleration will be decreased. The energy-dissipating capacity of isolation bearings is used to considerably reduce the damaging energy exerted to the bridge piers. Moreover, when isolation bearings are installed at the top of the piers, the lateral force of a superstructure can be distributed to each substructure, and thus the concentration of lateral force to several specific substructures can be avoided.

Bridge bearings have historically been one of the most vulnerable components in resisting earthquakes. Steel bearings in particular have performed poorly and have been damaged by relatively minor seismic shaking [1, 2]. Among the great variety of seismic isolation systems, lead-rubber bearings (LRB) have found wide application in bridge structures [3]. This is due to their simplicity and the combined isolation-energy dissipation function in a single compact unit. LRB bearings are steel reinforced elastomeric bearings in which a lead plug is inserted to provide hysteretic damping as well as rigidity against minor earthquakes, wind and service loads. The lead plug yields at relatively low shearing stress resulting in significant dissipation of seismic energy and reduction of earthquake response [4]. By using hydraulic jacks, the superstructure of the bridge can be lifted to remove the original bearings, easily replacing them with suitable LRB bearings. In practice, isolated bridges with LRB bearings have been proven to perform effectively reducing the bridge seismic response during earthquake shaking. The Thjorsa River Bridge in Iceland survived two major earthquakes of moment magnitudes (M_w) 6.6 and 6.5 without serious damage and was open for traffic immediately after the earthquakes as reported by Bessason and Haflidason [5].

LRB bearings of isolated highway viaducts, due to their inherent flexibility, can be subjected to large shear deformations in the event of great earthquake ground motions. According to experimental test results, LRB bearings experience significant hardening behavior beyond certain high shear strain levels due to geometric effect

[6-8]. Therefore, the effects of hardening of LRB bearings, induced by strong near-fault earthquakes, on the overall non-linear seismic response of highway viaducts have been included in this study.

This chapter presents the three-dimensional effects of seismic isolation with LRB bearings on the Level II earthquake behavior of curved viaducts separated by expansion joints. In order to quantify the benefits in seismic performance, non-linear responses of the non-isolated bridge are compared with those obtained for the isolated configuration. The non-linear response comparison has been accomplished by extensive parametric studies conducted by varying those isolation bearing design parameters, which have major influence on the overall bridge response. Moreover, the temperature effect on lead rubber bearings especially under extreme low temperature condition have been introduced, as additional cold region factor, to evaluate its influence on the behavior of seismically isolated viaducts subjected to great earthquake ground motions.

4.2 Lead-rubber Bearing Isolation System

Many innovative devices and systems are being developed for the purpose of seismic isolation of bridges [9]. One of the most widely adopted isolation system is the lead-rubber bearing (LRB) shown in **Fig. 4.1**. This type of elastomeric bearing protects the bridge from the destructive effects of earthquake ground motions increasing the structure fundamental period beyond the energy-containing periods of earthquakes and also by dissipation of seismic energy through the additional hysteretic damping due to yielding of the lead plug [10]. Under normal conditions, LRB bearings behave like regular bearings. The isolation device is characterized by a high initial stiffness provided by the lead plug inserted in the bearing to avoid undesirable displacements under service requirements, wind action and minor earthquakes. However, the shear stiffness decreases favorably for moderate levels of deformation, allowing the isolator to uncouple the bridge from the damaging action of earthquake ground motions. Therefore, the seismic damage the structure acquires is drastically minimized through the reduction of the seismic inertial loads [11].

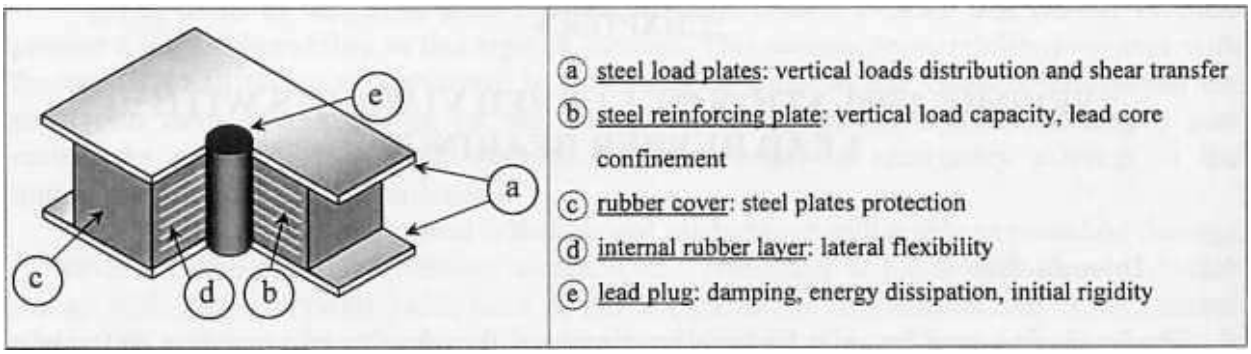


Fig. 4.1 Components of LRB Bearing Supports

Bridges are ideal candidates for the adoption of base isolation technology due to the facility of installation, inspection and maintenance of isolation devices. Although seismic isolation is an effective technology for improving the seismic performance of a bridge, there are certain limitations on its usage. Seismic isolation improves the performance of a bridge under earthquake loading partially by increasing the fundamental vibration period. Thus the vibration period of a bridge is moved away from the high-energy seismic ground period and seismic energy transfer to the structure is minimized. Therefore usage of seismic isolation on soft or weak soil conditions, where high period ground motion is dominant, reduces the benefits offered by the technology [12]. The seismic isolation system has a relatively high vibration period compared to a conventional structure. Due to the principle of dynamic resonance, a larger difference between the dynamic vibration frequencies of the isolation system and the superstructure results in a minimized seismic energy transfer to the superstructure. Therefore, seismic isolation is most effective in relatively rigid structural systems and will provide limited benefits for highly flexible bridges. Another consideration is related to the large deformations that may occur in the seismic base-isolation bearings during a major seismic event, which causes large displacements in a deck [13]. This may result in an increased possibility of collision between deck and abutments, and in the adoption of large expansion joints for the bridge with cause noise, vibration and maintenance problems. Damping is crucial to minimize the seismic energy flow to the superstructure and to limit the horizontal displacements of the bearings [14]. The lead plug deforms plastically at a predetermined flow stress and thus dissipates energy through hysteretic damping.

4.2.1 LRB analytical model

LRB bearings have been represented using a number of analytical models, from the simplicity of the equivalent linear model composed of the effective stiffness and equivalent damping ratio formulated by Hwang et al. [15] to the sophisticated finite element formulation developed by Salomon et al. [16]. However, the most extensively adopted model for dynamic analysis of seismic isolated structures is the trilinear idealization for the force-displacement hysteretic loop (Ali et al. [17]). Due to its simplicity and accuracy to identify the force-displacement relationship of the isolation devices, LRB bearing supports can be represented by the trilinear force-displacement hysteresis loop given in **Fig. 4.2**. The principal parameters that characterize the model are the pre-yield stiffness K_1, corresponding to the combined stiffness of the rubber bearing and the lead plug, the stiffness of the rubber K_2 and the yield force of the lead plug F_1. The value of F_1 is influenced primarily by the characteristics of the lead plug, but it is important to take into account that in areas of cold temperatures, natural rubber will cause significant increment of F_1 values. Two additional parameters have been adopted for characterizing the hardening effect: K_3 and F_2 representing respectively the stiffness of rubber at high strain level, and the hardening force level. The hardening parameters are fitted to the test data carried out using shaking tables in the typical range reported for elastomeric bearing characteristically in litterateur.

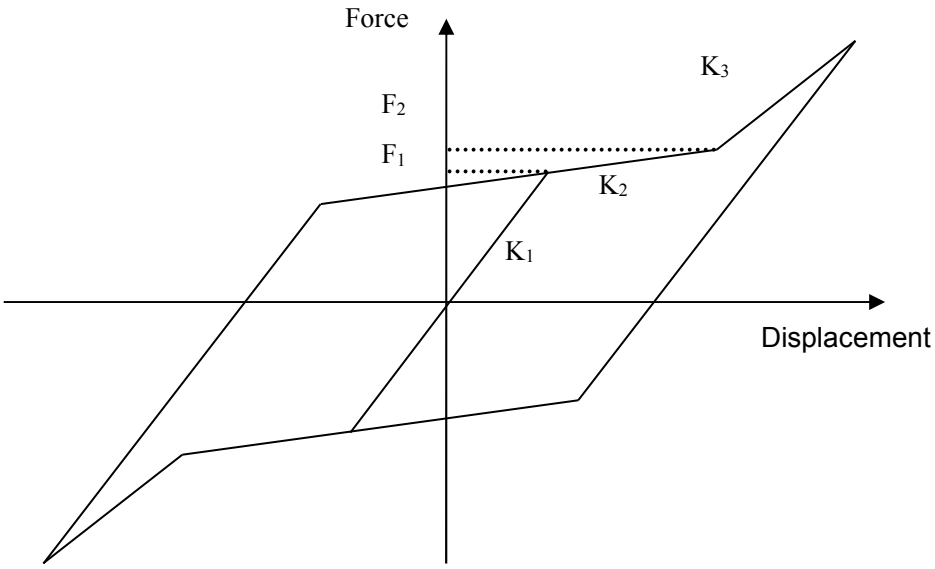


Fig. 4.2: Analytical Model of LRB

Three LRB systems with various properties are discussed in the present study, all fix support cases are added as comparison to evaluate the base isolation performance of LRB bearings in addition. The structural characteristics of isolation bearings are summarized in **Table 4.1**. It is also noted that properties of LRB bearings have been selected depending on the differences in dead load supported from the superstructure. The aim is to attract the appropriate proportion of non-seismic and seismic loads according to the resistance capacity of each substructure ensuring a near equal distribution of ductility demands over all piers.

Table 4.1 Structural Properties of Bearings (*K*(MN/m) *F*(MN))

LRB Product	Side Length (mm)	K_1	K_2	K_3	F_1	F_2
LRB-S-200	200	1.489	0.212	0.549	0.063	0.125
LRB-S-350	350	2.662	0.380	0.984	0.096	0.191
LRB-S-500	500	3.850	0.550	1.425	0.138	0.275

4.2.2 Radial restraint configurations of LRB isolation system

Bridges are designed to accommodate movement exclusively in the longitudinal direction. Undesirable lateral deck displacements may have negative consequences in the seismic bridge performance. In the particular case of isolated structures, the flexibility introduced by LRB bearings may induce excessive lateral displacements to the superstructure when the structure is subjected to strong earthquake ground motions. For this reason, adding steel stoppers can provide displacement constraint of the bridge superstructure. The stopper is usually made with two stiffened angles or welded plates placed on each side of the bearings.

It have been examined in the previous study[18] that one particular configuration of stoppers has the best seismic performance. Displacements of LRB bearings have been partially limited through the installation of lateral side stoppers on P1 and P4

(the outer piers), as shown graphically in **Fig. 4.3**. Out-plane radial displacements are restricted in for all isolation units of P1 and P4, which are not restricted in for those of P2 and P3, representing the most effective used method of bearing restraint.

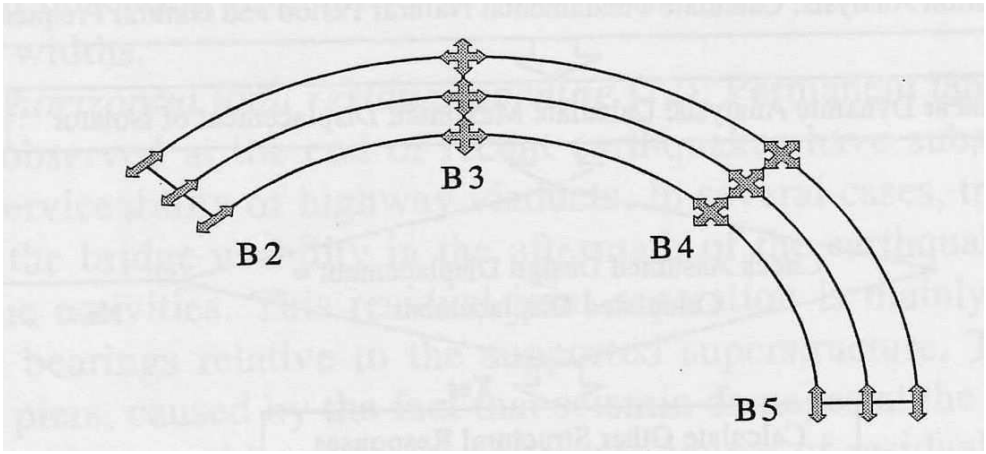


Fig. 4.3 Restraint Configurations of LRB Bearings Supporting Superstructure

4.2.3 Low temperature effect on LRB

For engineering purposes, cold regions are defined as any region where cold temperatures [19], unique terrain, and snowfall significantly affect engineering structures for one month or more each year. About one quarter of the earth's land mass may be termed severely cold. In **Fig. 4.4**, this area is indicated by the area above line A in the Northern Hemisphere and below line A in the Southern Hemisphere. In these areas, mean annual air temperatures stay below freezing, maximum snow depths exceed 60 centimeters, and ice covers lakes and rivers for more than 180 days each year. Another quarter of the earth is termed moderately cold. In **Fig. 4.4**, this area fits between lines A and B (including most of the United States and Eurasia). Its mean temperatures during the coldest month are below freezing.

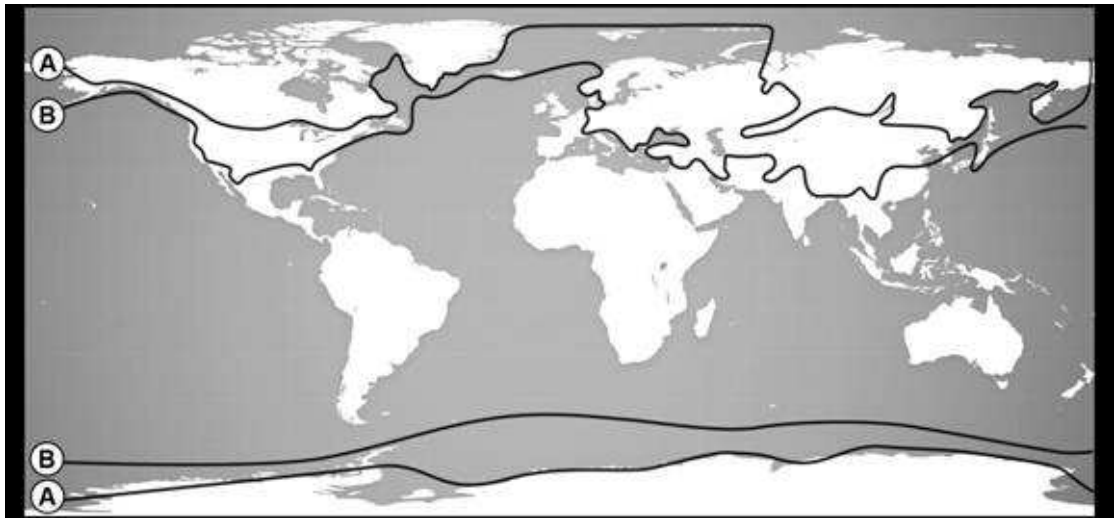


Fig. 4.4 Cold regions of the world

At low temperature, stiffness of the rubber-based bearings increases as a function of temperature and time, which presents the normalized shear modulus, G_{cold} /G_{room}, as a function of time at low temperature [20]. Increase of stiffness associated with a

change in temperature is called instantaneous thermal stiffening. Instantaneous stiffness of an elastomeric bearing is measured after the bearing temperature reaches ambient temperature. Change of stiffness with respect to time is referred to as crystallization.

Thus, a lot of experimental investigations have been done to ensure that an base isolation bearing would perform satisfactorily under low-temperature exposure during its service life. The experimental observations have shown the temperature dependence mechanical behavior of lead-rubber bearings, as shown in **Fig. 4.5**.

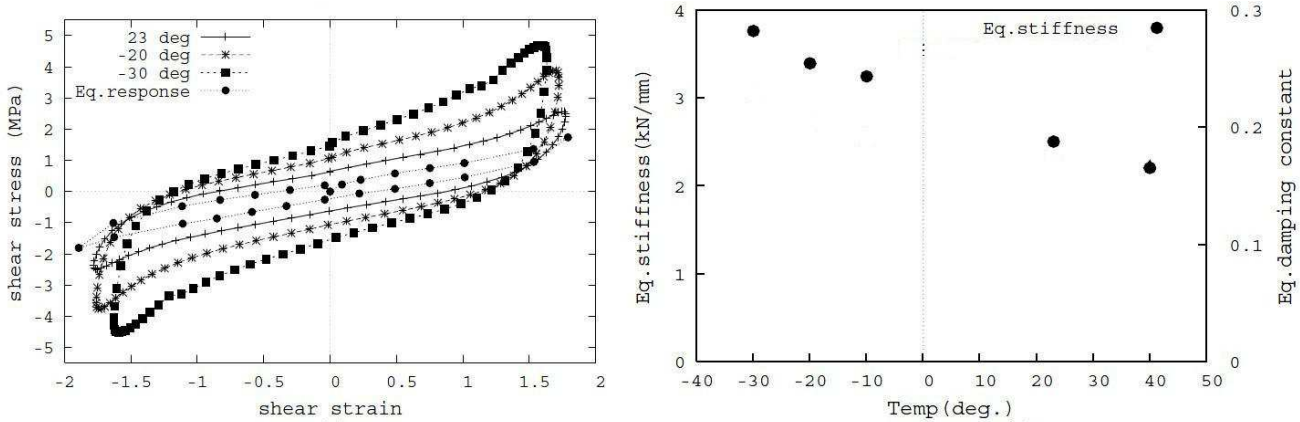


Fig. 4.5 Shear Stress-strain Response of LRB under Various Temperature

Base on the experiment results, for the case of a long-term low temperature accumulation, the equivalent stiffness of LRB increases about 30%. Since the area of cold regions unavoidably overlap with seismic zone, i.e. Hokkaido Island of Japan. It is necessary to take account of the low temperature effect on LRB in seismic response analysis.

4.2.4 Heat production and temperature variation analysis

Base isolation devices, which are mainly made of material rubber, have temperature dependence behavior due to its material characteristics as an elastomer type of polymer. The thermal effect, when applied to polymers, induce a transition from an elastomeric, rubbery phase to a brittle, glassy solid amorphous phase on cooling. Consequently, the stiffness of polymer trends to increase with the decreasing temperature. With the increment of stiffness of rubber material, the flexibility of base isolation devices is deteriorated and therefore its seismic protection capability will be weakened.

However, in an earthquake event, base isolation bearings absorb earthquake energy and release it as heat. The heat conduction will raise the temperature of LRB. Thus, as the main objective of the current study is to have deep understanding of the thermo-mechanical behavior of LRB, an dynamic stiffness definition comprised of temperature variation of time and stiffness variation of temperature is proposed in this study.

The numerical studies conducted mainly focus on the sensitivity of time variations of temperature of base isolation devices. In order to assess the temperature rise with

respect to time as well as the temperature distribution at the transient state, the thermal characteristics of the bearing system was analyzed using ANSYS, which is a commercial finite element analysis software package. The lead rubber bearing which has overall dimensions commonly used in practice was chosen for modeling [21]. All specified bearing properties applied in thermal analysis are supplied by base isolation devices manufacturer, as shown in **Table.4.2**. Low-temperature thermal analysis is conducted under the initial temperature of -30℃. And convection of heat from all the surfaces of the bearing model are also set to -30℃, which represents the low temperature environment. The heat generation of bearings is assessed by adopting the values of earthquake strain energy time history, assuming the bearings absorb earthquake energy and release it as heat during earthquake.

Table 4.2 Geometry and Material Properties of LRB

Geometry parameter				(Rubber layer thickness t_r = 8 mm)
L (mm)	200	350	500	Rubber square side length
T_e (mm)	112	136	160	Total rubber height
H_b (mm)	234	280	326	Total isolator's height
Rubber material property				(Rubber code: G4)
G (N/mm2)		0.385		Shear modulus
E_B (N/mm2)		1176		Bulk modulus of elasticity
E_0 (N/mm2)		2.20		Young's modulus of rubber
κ		0.85		Young's modulus correction factor according to hardness
Steel and lead plug				
Reinforced steel plate				SS400（JIS G 3101）
Flange plate				SS400（JIS G 3101）
Connecting plate				SS400（JIS G 3101）
Lead plug				Pb（JIS H 2105 special）

During an earthquake event, the complete earthquake energy balance is given by

$$E_I = E_S + E_K + E_D + E_H \quad (1)$$

where, at a given instant in time, t, E_I = cumulative input energy; E_S = instantaneous strain energy stored by the structure; E_K = instantaneous kinetic energy of the moving mass; E_D = cumulative damping energy; and E_H = cumulative hysteretic energy.

At the end of the earthquake $t = t_f$, the kinetic energy is zero, the strain energy is decided by the inelastic deformation for an inelastic system, the cumulative damping energy is dissipated by damping system and the cumulative hysteretic energy is all converted to the heat. Since the all the values of this equation could be obtained by numerical analysis, the internal heat generation is consequently obtained, as shown in **Fig.4.6**.

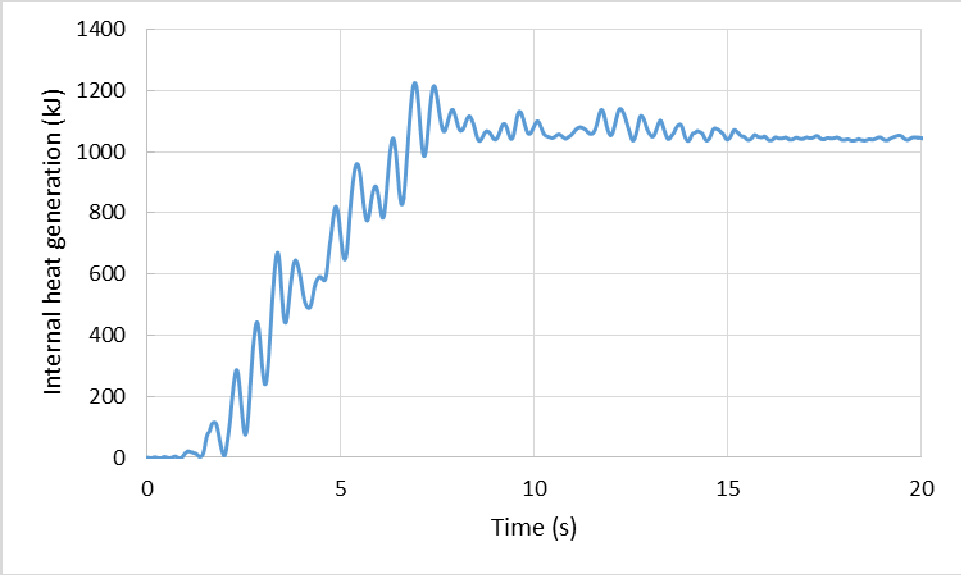


Fig. 4.6 Internal Heat Generation

In the present study, two functions are introduced to simulate this temperature / bearing property variation process: the time variation of temperature which is concluded by vibration tests of LRB, and the temperature variation of performance which is concluded by bearing performance test under different temperature conditions. The 1995 Kobe earthquake ground motion which is obtained from JR Takatori Station is adopted, not only because it is a typical near-fault great earthquake, but also its duration (20 seconds) is a suitable time for this study.

By carrying out numerical results on this thermal analysis which has been particularly described above, and adopting the temperature increment condition, the relationship between time and temperature of LRB can be obtained, as shown in **Table.4.3**. It can be summarized that, for a earthquake with a duration of 20 seconds, the temperature increment is only approximately 10℃, i.e. LRB devices are still influenced by low temperature effect to a certain extent. Therefore detailed quantitative analysis on temperature dependent performance of LRB is necessary.

Table 4.3 Time Sample Points List

Time (s)	Temperature (℃)	Stiffness Scale Factor	Yield Force Scale Factor
0	-30	1.38	1.62
2	-28.93	1.36	1.58
4	-27.87	1.34	1.55
6	-26.80	1.32	1.52
8	-25.74	1.31	1.50
10	-24.67	1.29	1.47
12	-23.61	1.28	1.45
14	-22.54	1.26	1.43
16	-21.48	1.25	1.41
18	-20.41	1.24	1.39
20	-19.35	1.23	1.37

4.2.5 Application of dynamic bearing property definition

In order to have deep understanding of the thermo-mechanical behavior of rubber made bearings, experimental schemes comprised of multiple test methods were proposed in past studies, among which a cooperative research by Rubber Bearing Association and Civil Engineering Research Institute for Cold Region carried out an integrated and practical conclusion [22].

Based on their experiment results, for the case of a long-term low temperature accumulation, the equivalent stiffness of LRB increases about 30%. And with the heat conduction during earthquake event, the temperature of LRB gradually increases while the stiffness of LRB accordingly decreases. The detailed bearing property values could be calculated by following equations.

Equations about Bearing property variation

$$y_1 = -0.206 \times \mathrm{Ln}(x + 40) + 1.855 \quad (2)$$

$$y_2 = -0.335 \times \mathrm{Ln}(x + 40) + 2.388 \quad (3)$$

Where, y_1 is stiffness ratio; y_2 is yield force ratio;
x is temperature.

By adding a matrix substitution statement at the begging of calculation loop in FEM analysis program, these equation could be adopted to build a dynamic bearing property definition, as shown in **Table 4.3**. This could contribute to obtaining a accurate and practical numerical result in seismic response analysis.

Cooperating the temperature conditions with the equations about the temperature variation of performance listed above, a dynamic bearing property definition is formed. Considering this dynamic bearing property definition, the bridge seismic performance has been evaluated on three different LRB bearing systems with low, medium and large initial stiffness, respectively. All three systems satisfy the requirement of vertical load as a prerequisite. Dimension and property of these three bearing systems are selected properly to ensure the seismic performance. Room temperature(20℃) condition and low temperature(-30℃) condition are discussed and compared. As to the low temperature condition, both fixed and dynamic stiffness cases are considered in this study. Although fixed conditions have no reality, they still represent the cases that maximum stiffness value are applied and therefore could contribute to understanding the low temperature effect on seismic performance. The temperature configurations and corresponding performance of bearings is summarized in **Table.4.4**, it should be mentioned, for the low temperature condition cases, only initial values are listed in this Table.

Table 4.4 Bearing Configuration (K(MN/m) F(MN))

	Case	K_1	K_2	K_3	F_1	F_2	Temperature
1	s200	1.489	0.212	0.549	0.063	0.125	+20℃, fixed
2	s200l-d	2.055	0.293	0.758	0.102	0.203	-30℃, increasing
3	s200l-f	2.055	0.293	0.758	0.102	0.203	-30℃, fixed
4	s350	2.662	0.380	0.984	0.096	0.191	+20℃, fixed
5	s350l-d	3.674	0.524	1.358	0.155	0.309	-30℃, increasing
6	s350l-f	3.674	0.524	1.358	0.155	0.309	-30℃, fixed
7	s500	3.850	0.550	1.425	0.138	0.275	+20℃, fixed
8	s500l-d	5.313	0.759	1.966	0.224	0.446	-30℃, increasing
9	s500l-f	5.313	0.759	1.966	0.224	0.446	-30℃, fixed

4.3 Numerical Results Considering Low Temperature Effect

The analysis on the highway viaduct model is conducted using an analytical method based on the elasto-plastic finite displacement dynamic response analysis. Structural responses are examined for all selected types of bearings under the action of earthquake wave. Dynamic response analysis of substructure has been focused on two central piers (P3) because central piers support double weight and consequently, the most severe seismic response is found in this structural member . The extreme low temperature effect on LRB which cause the increment of stiffness is considered in the present study.

4.3.1 Natural vibration analysis

The limited increase of natural period is called Menshin design in Japan. Instead of elongating the period to high values, emphasis in the Menshin design is given on increasing energy dissipation capability and distribution of lateral forces to as many substructures as possible in order to decrease the lateral forces for design of substructures.

The accuracy of the fundamental natural period of an isolator plays a crucial role in predicting the seismic responses of seismic isolated bridges. Therefore, the fundamental natural period of the viaduct is calculated by the method which is introduced in the **Section 3.4**. According to recommendations of Specifications for Highway Bridges in Japan [23], the pre-yield to post-yield stiffness ratio (K_1/K_2) of the LRB bearings is preselected to ensure a moderate period shift. Characteristics of isolation bearings are selected to obtain periods about twice the fundamental period of the bridge when no isolation is applied. Natural vibration analysis of the model of viaduct supported on six different cases is carried out, as shown in **Table 4.5**.

Table 4.5 Fundamental Natural Frequencies and Periods

Case	ω [rad/sec]	T[sec]	ratio to T of fix	Bearing Condition
1	3.53	1.78	2.07	LRB-s200, +20℃, fixed
2	3.72	1.70	1.97	LRB-s200, -30℃, increasing
3	3.91	1.61	1.87	LRB-s200, -30℃, fixed
4	4.38	1.44	1.67	LRB-s350, +20℃, fixed
5	4.58	1.38	1.60	LRB-s350, -30℃, increasing
6	4.77	1.32	1.53	LRB-s350, -30℃, fixed
7	4.94	1.27	1.48	LRB-s500, +20℃, fixed
8	5.13	1.23	1.42	LRB-s500, -30℃, increasing
9	5.32	1.18	1.37	LRB-s500, -30℃, fixed
all-fix	7.340	0.856	1	Fixed Support, +20℃, fixed

The results of natural vibration analysis, calculated in this section, provides valuable information about the bridge characteristics and its structural behaviour during earthquakes, and they are used for the solution of dynamic response of the bridge, and also to evaluate the constants defining the Rayleigh damping matrix.

The natural period of a bridge depends on the stiffness and heights of its piers, the foundation ground type, and the characteristics of its superstructure and bearing supports. In this study, the influence of bearing support on natural vibration response of the model of viaduct is analyzed. This influence is mainly reflected in the equivalent horizontal stiffness value of the bearings.

This fundamental natural period corresponds to the modal shape in the longitudinal direction of the bridge. Low values of period indicate that the viaduct is not able to shift its fundamental natural period into ranges that exceed those of the input ground motions. On the other hand, the moderate period shift obtained for the other values allows for reflecting a major portion of the earthquake energy, limiting the increased displacements experienced by the bridge deck during strong earthquake ground motions.

It is clearly showed that with the utilization of LRB bearings, the viaduct shifts its fundamental natural period away from the fixed support bridges to avoid the dominant period range of earthquakes, thus reducing the probable damage level of the structure. In the present study, particular attention has been given to the decrement of natural period under low temperature by comparison of case 1 and case 2, case 4 and case 5 as well as case 7 and case 8. This is, obviously, an unfavorable phenomenon. It weakens the base isolation function.

4.3.2 Shear force-displacement response at bearing

Shear Force-Displacement relationship at bearing is an important response parameter for seismic analysis, because both variables control overall behaviors of the whole bridge system. It is fundamental to limit peak shear force transmitted from superstructure to pier tops, in such a way that bending moment transferred to the base of piers is controlled. On the other hand, it is essential to obtain moderate maximum bearing shear displacements to avoid large peak deck displacements which may result in collisions between span and abutments, and also to improve the serviceability of the bridge which is seriously affected if the clearance between decks and abutments at an expansion joint exceeds the standard design values.

Fig. 4.7 show the shear force-displacement response of bearing supports P3. In case of bridge equipped with LRB-S-200 under room temperature (case 1), the maximum inertial force transmitted to LRB bearing support is 174 kN, whereas the maximum displacement of LRB bearings is 0.42 m. When the bridge equipped with the same base isolation system under low temperature (case 2), force values are increased while displacement values are decreased due to the increment of stiffness, being obtained maximum values for reaction forces of 198 kN and reaction displacement 0.35 m, respectively. The same results occur in the comparison of case 4 and case 5, as well as the comparison of case 7 and case 8 (same bearing support under room temperature and low temperature).

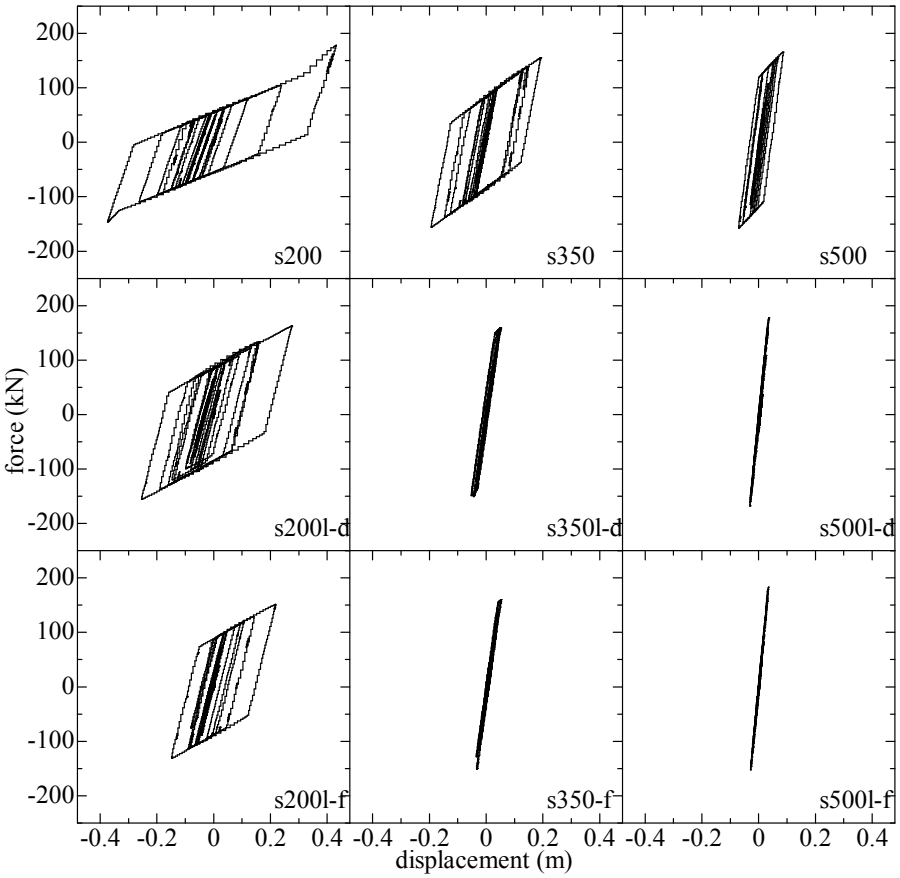


Fig. 4.7 Shear Force-Displacement Response at Bearing
(P3 X-Direction)

It can be observed, from these results, that piers under low temperature sustains between 5-13% more of the total inertial force than piers under room temperature. Meanwhile, the deformation of LRB bearings under low temperature is between 11-20% less than deformation of the same devices under room temperature. This is attributable to the stiffness variation caused by the temperature dependence of material rubber. It should be emphasized that, deformation of the LRB bearing is main seismic protection mechanism of the base isolation system. LRB bearings deform in order to dissipation the earthquake energy transmitted to the superstructure. The basic idea of seismic design is to make maximum use of the deformation of base isolation system in the safety range, i.e. controlling the maximum displacement to avoid collision between deck and abutment. Therefore, the decrement of bearing displacement under low temperature should be considered as a negative effect as well as the increment of shear force.

Comparing LRB cases with fix support cases, it is clear that LRB evidently reduce inertial forces acting on bridge piers and this is just the function of the base isolation system. The low temperature effect in this section is clear as well, with the increment of stiffness, peak shear force increases and maximum bearing displacement decreases significantly, which are definitely unfavorable. And it should be particularly mentioned, by the comparison of case 1 (room temperature) and case 2 (low temperature), hardening effect of LRB is also enlarged under low temperature. As a very serious problem, this combination harm of low temperature and hardening effect will be discussed separately later.

4.3.3 Bending moment-curvature response

In most cases, structural damage due to earthquakes can be attributed to the plastic hinges formed at the piers of the bridge [24]. The bottoms of bridge piers subjected to earthquakes sustain maximum loading, therefore, the failure mechanisms usually start with formation of plastic hinges, attributable to local earthquake-induced plate buckling in those regions. For this reason, the bending moment at the base of the piers is considered to be a good measure in order to quantify and express the damage level induced into the bridge system by the seismic input.

Moment-curvature loops at pier base (P3) are plotted in **Fig. 4.8** for the model of viaduct supported on the different types of bearing supports considered in the study.

The yield moment of the pier is 84.8MN, and therefore inelastic deformation occurs in all the cases. When it is under room temperature, the yield moment of piers with LRB bearings is exceeded by 4% - 5%, and consequently piers behave almost in the elastic range. And under low temperature, large inelastic deformation occurs for all the piers. Structural damage on this substructure element is confirmed by the significantly large moment-curvature loop at base of the pier.

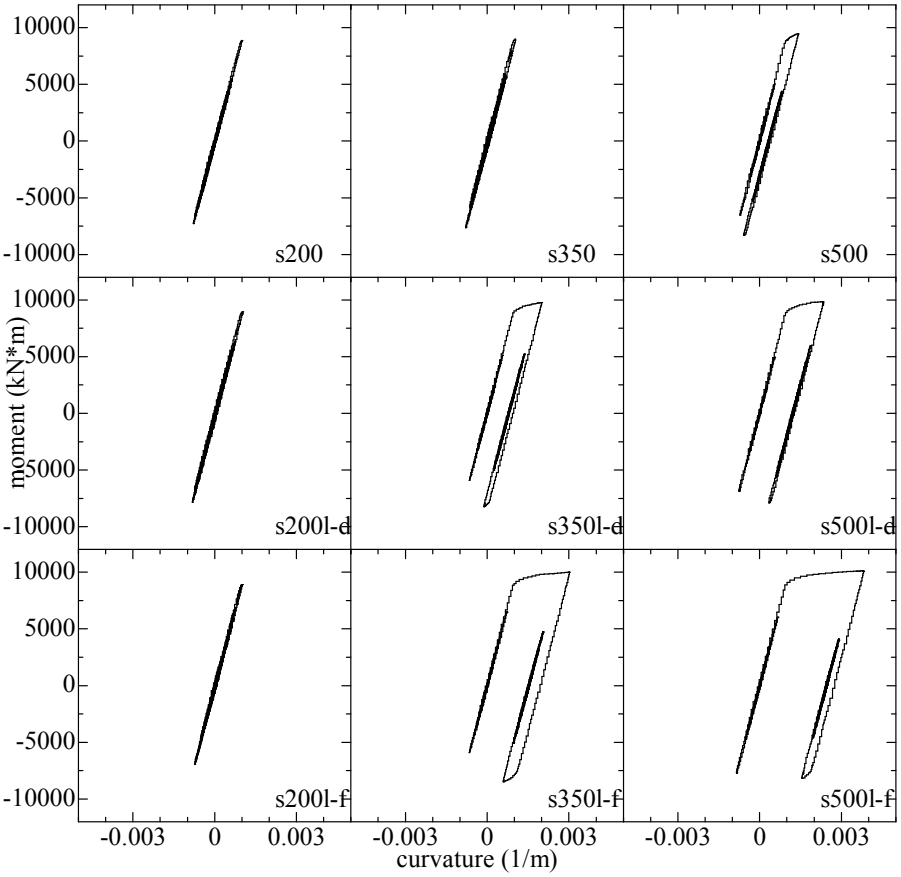


Fig. 4.8 Bending Moment-Curvature Response
(P3 X-Direction)

Consistent results are obtained because the envelope curve for viaducts isolated with LRB systems under room temperature, presents a linear behavior which indicates that pier remains under elastic range from the top to the bottom, at every nodal point. In contrast, for low temperature, the maximum moment distribution envelope intersects the the yield moment limit line for all the piers. This characteristic indicates that the pier is severely damaged and has yielded.

LRB bearings can substantially reduce the seismic forces on piers by comparison of LRB cases and fix support case. And again, low temperature obviously increase the damage level in all the cases. But it should be mentioned specifically, a proper designed base isolation system (case 1), could be affected slightly under low temperature (case 2).

4.3.4 Energy-time history

Several studies [25, 26] have advised the use of energy concepts as an alternative way to the traditional design strategies for the identification of the seismic demands imposed by the earthquakes to the structures. Recently, Bertero,R. D. and Bertero, V. V. [27] presented a conceptual methodology for earthquake resistant design, in which total input energy and energy dissipation obtained through damping energy and plastic hysteretic energy are considered simultaneously, to discuss the damage potential of ground motions and the damage index of structures.

During earthquakes input energy flows from the ground to structures and should be dissipated by damping mechanisms and by plastic deformation which is responsible in part for structural damage [28]. The basic concept is that the energy balance equation, presented in **Section 3.5** and obtained by integrating the equation of motion of a MDOF system subjected to ground excitation, implies that the seismic input energy imparted to a structure, at the end of the earthquake record, is equal to the sum of the kinetic and strain energies plus the energy dissipated by damping.

Kinetic energy includes the effects of the rigid body translation of the structure. However, the effect of this type of energy is likely to be ignored, because an examination of analysis results indicates that values of kinetic energy can be expected to be smaller compared to the other types of energies at the conclusion of the earthquake. Damping energy is the consumed energy due to damping mechanism of the system, and strain energy corresponds to the absorbed energy by the hysteresis loops of steel bridge piers and the hysteretic energy dissipated by the bearings.

In this section, energy is used as an alternative response factor to response quantities like force or displacement to examine the seismic damage effect on bridge structures. The performance of the bearing systems is analyzed by comparing the energy-time histories for the structural system.

Depending on the temperature conditions, the seismic energy transmitted into a bridge structure varies sensibly, as it is confirmed in **Fig. 4.9**.

In case of room temperature, the total input energy is 3952.1 kNm for the model supported on LRB-S-200 bearings (case 1), 3252.5 kNm for the LRB-S-350 bearings (case 4) supported viaduct, and 1932. 6 kNm for viaduct with LRB-S-500 bearings (case 7). And for low temperature, values of input energy are 3839.6, 2745.8,and 1897.9 kNm for model with LRB-S-200 (case 2), LRB-S-350 (case 5), and LRB-S-500 (case 8) bearing systems, respectively.

The obtained results show that the amount of seismic energy inputted to the viaduct depends highly on the structural characteristics such as the fundamental period of vibration and damping properties. In comparing the energy-time histories for the two temperature conditions, it is remarked that the seismic energy dissipated by the same base isolation system under room temperature is always larger than that of low temperature.

LRB system with lower stiffness has more isolation function, therefore could dissipate more strain energy. And under low temperature, energy dissipation decreases significantly, which is just simply because the stiffness of LRB increases. And this is, definitely, an unfavorable phenomena caused by low temperature.

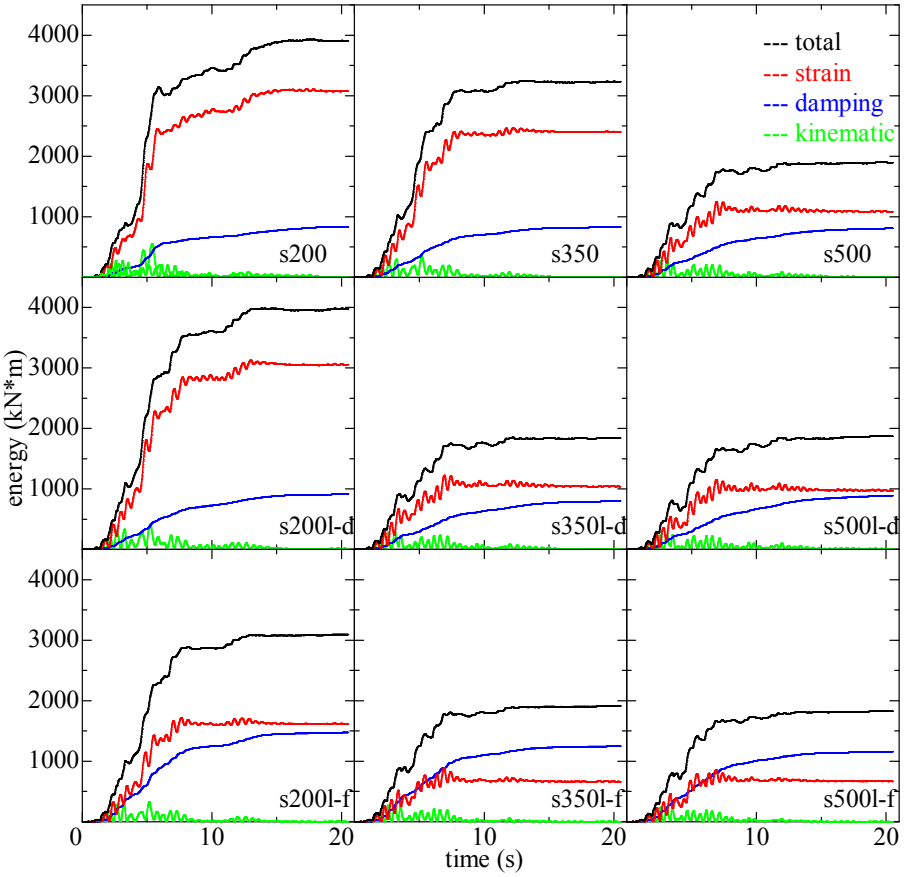


Fig. 4.9 Energy Time History

4.3.5 Displacement-time history at top of pier

Bridge structures should not only remain standing but should also be usable after a very large earthquake because, during the time which they cannot be used, society may suffer a tremendous cost and inconvenience. Based on the experiences after the 1995 Hyogoken-Nanbu earthquake, a large number of bridge piers that suffered flexural failure at their base did not collapse, but large residual displacements at the top made the structures unusable, unsafe, and in some cases irreparable. The check of residual displacement of bridge piers after the Hyogoken-Nanbu earthquake concluded that about 100 piers with a tilt angle of 1 degree had to be demolished, and new piers were built due to the difficulty involved in setting the superstructures back to the original alignments and levels[29].

In this study, residual displacement of pier top is considered a good indicator of the structural damage sustained after an earthquake. For this reason, displacement-time histories at top of bridge piers are shown in **Fig. 4.10** to evaluate the final position of the piers respect to the original.

According to the Specifications for Highway Bridges in Japan [23], residual displacements of steel bridge piers are examined by using the results of the dynamic made of the input seismic vibration waves. When a large residual displacement is generate in the substructure body after an earthquake, restoration work may be difficult to perform. The allowed residual displacement is generally 1/100 of the height from the bottom edge of the bridge pier to the point where the inertial force

acts on the superstructure, or in the other words, it is 1/100 (rad) of the angle of rotation of the bridge pier.

Moderate peak responses results from the application of room temperature to the model with different bearing support conditions. The residual displacement for the fixed support is unacceptable in this case, and much smaller values are obtained for the base isolation bearing support conditions: only 0.1 cm for LRB-S-200 (case 1), 0.2 cm for LRB-S-350 (case 4) and 0.2 cm for LRB-S-500 (case 7). Scarcely residual deck displacement is observed in LRB cases indicates that almost all structural elements are functioning well under room temperature.

But In case of low temperature, displacement responses at top of piers are sensibly increased. In terms of the residual plastic deformation after the earthquake, even the pier equipped with LRB bearings also shows considerable residual displacement of 1.2 cm for LRB-S-200 (case 2), 2.4 cm for LRB-S-350(case 5) and 3.9 cm for LRB-S-500 (case 8), due to the curvature originated at its pier base.

Under room temperature, residual displacement which is caused by the residual curvature generated by inelastic deformation at the pier base and deformation of base isolator, could only be observed in the worst case (case 5). This result means a proper designed base isolation system works well under room temperature. But, under low temperature, residual displacement is observed in all the cases. And the maximum displacement increases meanwhile. This is one more unfavorable effect of low temperature.

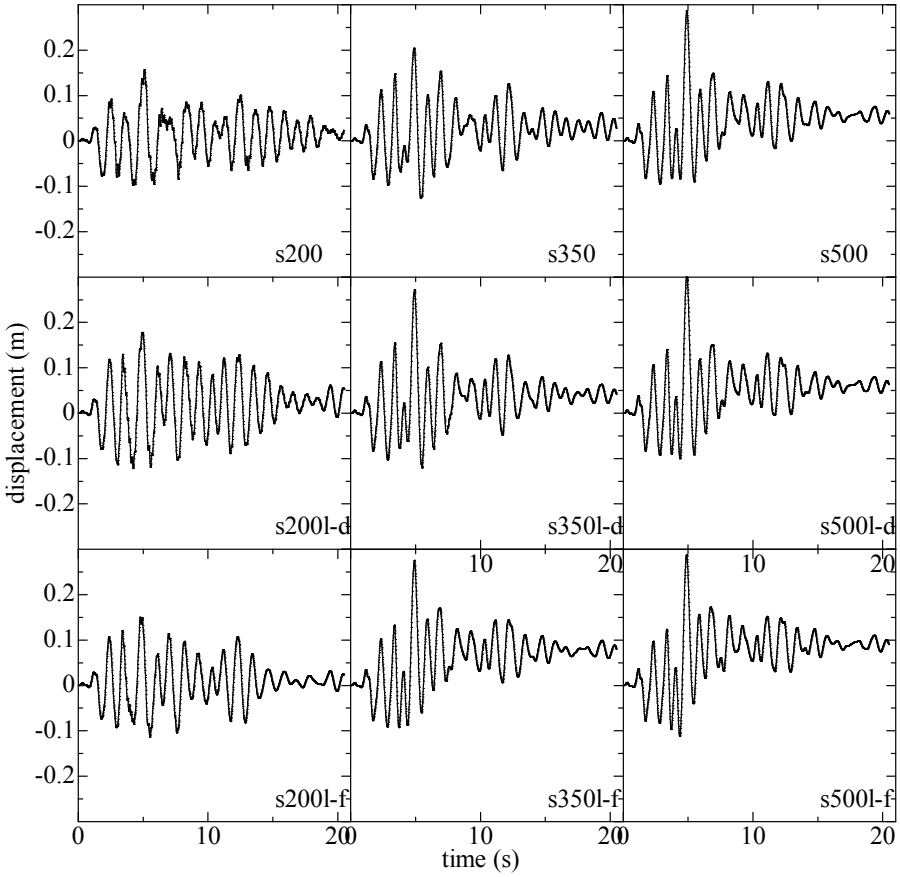


Fig. 4.10 Displacement-Time History at Top of Piers
(P3 X-Direction)

4.4 Conclusions

In this chapter, nonlinear dynamic analysis of a finite element model of highway viaduct with various support configurations under two temperature conditions is carried out. Seismic responses are studied and compared to investigate the influence of snow load conditions on the overall behaviour of the bridge. With this intention, the results are presented based on three types of bearings systems: LRB-S-200 (case 1,2,3), LRB-S-350 (case 4,5,6), LRB-S-500 (case 7,8,9), for three different temperature conditions: room temperature which is the standard value (case 1, 4, 7) , dynamic low temperature which is the main focus of this study (case 2, 5, 8) and fixed low temperature which represents the worst situation (case 3,6,9).

Based on the analysis of the seismic response of the bridge to input earthquakes, it is found that:

(1) Based on the analysis of the response of the bridge to input earthquakes, it is found that the demand-reduction features of isolation bearings provide a significant reduction in seismic forces that the bridge structure must resist. Forces acting on LRB bearings are effectively reduced by lengthening the fundamental period of the bridge away from the dominant period of ground motions, and by increased energy dissipation capacity through hysterctic behaviour of LRB bearings. Seismic forces acting on piers of a bridge with isolation bearings are distributed uniformly between all piers and consequently, the resulting force which corresponds to an individual pier is sensibly reduced, as compared to this value for the viaduct with fixed support bearing. Therefore, piers with LRB isolation systems are seismically protected, remaining under elastic range during the earthquakes, because these bearings do not transmit a level of shear force sufficient to damage them. Another positive effect of base-isolation systems is related to the primary difference in deck displacement response. In a viaduct supported on fixed support bearings the deck displacement occurs in the pier, whereas in an isolated bridge most of the deck displacement is concentrated in deformation across the isolator devices. The input seismic energy to the bridge isolated with LRB bearings is predominately dissipated by hysteretic behaviour due to inelastic bearing deformation for LRB bearings. Thus a maximization of the energy dissipation at bearing level, reflected by the measured hysteresis curves, is a good indicator to reflect the effectiveness of the base-isolation systems.

(2) The basic concept of the function of LRB bearings could be described following: Bearings deform instead of the whole bridge. And therefore natural frequency of the bridge is shifted away from the dominate frequencies of the input earthquake ground motion, earthquake force transmitted to the superstructure is reduced and earthquake energy is dissipated by bearings. From this basic concept, it is clearly that LRB bearing with less stiffness have better isolation function. It deforms more, vibrates more slowly, dissipate more seismic energy and reduce the seismic damage. In practical seismic design, LRB which is as soft as possible in the safety range should be the primary selection.

(3) By conducting thermal analysis and adopting dynamic bearing property definition method, the necessity of considering low temperature effect, in a short-duration earthquake, has been absolutely proved. More accurate seismic design considering not only performance but also low temperature effect, should be taken into account in cold regions.

(4) Under low temperature, base isolation devices which are mainly made from rubber are hardened because of the material characteristics. A harder state of base isolation device, which means the loss of flexibility, has less base isolation function than its original state. By comparison with fixed room temperature and fixed low temperature cases, it is found that the variation low temperature cases with dynamic bearing property have intermediate base isolation performance. This is just simply because the stiffness values of variation low temperature cases are also between that of other two conditions.

(5) Vibration which is generated by a long-duration earthquake, such as 2011 East Japan earthquake, could finally heat up the temperature of base isolation device to the room temperature. The low temperature effect in this case will be evaluated separately in the **Chapter 5**.

(6) As suggested by specifications, hardening effect, which drastically increase the stiffness of LRB at high shear force level, should be avoided as much as possible. However, it was found that an LRB bearing could hardly avoid both hardening effect and low temperature effect. For example, LRB-S-200 cases which showed hardening effect (case 1) could avoid low temperature effect (case 2), while LRB-S-350 cases which has no hardening effect (case 4) encountered low temperature effect (case 5). This problem will discussed further in **Chapter 6**.

References

[1] Moehle, J. P., and Eberhard, M. O.: Chapter 34: Earthquake damage to bridges. In: Chen, W. F., and Duan, editors.: Bridge Engineering Handbook, Boca Raton, CRC Press, 1999.

[2] DesRoches, R., Choi, E., Leon, R. T., Dyke, S. J., and Aschheim, M.: Seismic response of multiple span steel bridges in central and southeastern United States. I: As built, *Journal of Bridge Engineering ASCE*, Vol. 9, No. 5, pp. 464-472,2004.

[3] Pan, P., Zamfirescu, D., Nakasliima, M., Nakayasu, N., and Kashiwa, H.: Base-isolation design practice in Japan: Introduction to the post-Kobe approach, *Journal of Earthquake Engineering*, Vol. 9, No. 1, pp. 147-171,2005.

[4] Turkington, D. H., Carr, A. J., Cooke, N., and Moss, P.J.: Seismic design of bridges on lead-rubber bearings, *Journal of Structural Engineerings ASCE*, Vol. 115, No. 12, pp. 3000-3016, 1989.

[5] Bessason, B., and Haflidason, E.: Recorded and numerical strong motion response of a base-isolated bridge, *Earthquake Spectra*, Vol. 20, No. 2, pp. 309-332,2004.

[6] Ruiz Julian, F. D., and Hayashikawa, T.: Effect of hardening of lead-rubber bearings on nonlinear behaviour of highway viaducts under great earthquakes, *Proceedings of 13th World Conference on Earthquake Engineering*, CD-ROM, Paper No. 3332, Vancouver, Canada, 1-6 August, 2004.

[7] Sato, N., Kato, A., Fukushima, Y., and Iizuka, M.: Shaking table tests on failure characteristics of base isolation system for a DFBR plant, *Nuclear Engineering and Design*, Vol. 212, pp. 293-305, 2002.

[8] Highway Innovative Technology Evaluation Center (HITEC): Evaluation findings for dynamic isolation systems elastomeric bearings, Technical Evaluation report, CERF Report No. 40376, pp. 25-35, 1998.

[9] Moehle, J. P., and Eberhard, M. O.: Chapter 34: Earthquake damage to bridges. In: Chen, W. F., and Duan, editors. Bridge Engineering Handbook, Boca Raton, CRC Press, 1999.

[10] DesRoches, R., Choi, E., Leon, R. T., Dyke, S. J., and Aschheim, M.: Seismic response of multiple span steel bridges in central and southeastern United States. I: As built, *Journal of Bridge Engineering ASCE*, Vol. 9, No. 5, pp. 464-472,2004.

[11] Bessason, B., and Haflidason, E.: Recorded and numerical strong motion response of a base-isolated bridge, *Earthquake Spectra*, Vol. 20, No. 2, pp. 309-332,2004.

[12] Turkington, D. H.,Carr, A. J., Cooke, N., and Moss, P.J.: Seismic design of bridges on lead-rubber bearings, *Journal of Structural Engineering*, ASCE, Vol. 115, No. 12, pp. 3000-3016, 1989.

[13] Pan, P., Zamfirescu, D., Nakashima, M., Nakayasu, N., and Kashiwa, H.: Base-isolation design practice in Japan: Introduction to the post-Kobe approach, *Journal of Earthquake Engineering*, Vol. 9, No. 1, pp. 147-171,2005.

[14] Ruiz Julian, F. D., and Hayashikawa, T.: Effect of hardening of lead-rubber bearings on nonlinear behaviour of highway viaducts under great earthquakes, *Proceedings of 13th World Conference on Earthquake Engineering*, CD-ROM, Paper No. 3332, Vancouver, Canada, 1-6 August, 2004.

[15] Huang, J. S., and Chiou, J. M.: An equivalent linear model of lead-rubber seismic isolation bearings, *Engineering Structures*, Vol. 18, No. 7, pp. 528-536, 1996.

[16] Salomon, 6., Oiler, S., and Barbat, A.: Finite element analysis of base isolated buildings subjected to earthquake loads, *International Journal for Numerical Methods in Engineering*, Vol. 46, pp. 1741-1761, 1999.

[17] Ali, H. M., and Abdel-Ghaffar, A. M.: Modeling the nonlinear seismic behavior of cable-stayed bridges with passive control bearings, *Computers and Structures*, Vol. 54, No. 3, pp. 461-492, 1995.

[18] Tanaka, R., Galindo, C. M., Hayashikawa, T.: Nonlinear seismic dynamic response of continuous curved highway viaducts with different bearing supports, World Academy of Science, Engineering and Technology, No. 35, pp. 327-333, 2009.

[19] Bates, R.E., and Bilello, M.A.: Defining the cold regions of northern hemisphere. Hanover, NH: CRREL, Technical Report 179.

[20] Oshima, T., Mikami, S., Yamazaki, T., Ikenaga, M., Matsui, Y., and Kubo, K.: Experimental of functional confirmation on lead rubber bearing (LRB) under low temperature, *J. Struct. Eng*, 44A, pp.753-760, 1998.

[21] Product Prospectus of Mageba S.A, 2012.

[22] Imai, T., Satoh, T., Nishimura, T., Tanaka, H., and Mitamura, H.: The performance evaluations of rubber bearings for bridges in cold districts(2), *Proceeding of Hokkaido Chapter of JSCE*, Vol.64, pp.A-18, 2008.2.

[23] Japan Road Association (JRA), Specification for Highway Bridges - Part V Seismic Design, Tokyo (Japan), Maruzen, 2002.

[24] Hsu, H.-L., and Chang, D.-L.: Upgrading the performance of steel box piers subjected to earthquakes, *Journal of Constructional Steel Research*, Vol. 57, 2001, pp. 945-958.

[25] Decanini, L. D., and Mollaioli, F.: An energy-based methodology for the assessment of seismic demand, *Soil Dynamics and Earthquake Engineering*, Vol. 21, 2001, pp. 113-137.

[26] Bruneau, M., and Wang, N.: Some aspects of energy methods for the inelastic seismic response of ductile SDOF structures, *Engineering Structures*, Vol. 18, No. 1, 1996, pp. 1-12.

[27] Bertero, R. D., and Bertero, V. V.: Performance-Based Seismic Engineering: The need for a reliable conceptual comprehensive approach, *Earthquake Engineering and Structural Dynamics*, Vol. 31, 2002, pp. 627-652.

[28] Cruz, M. F.,and Lopez, O. A.: Plastic energy dissipated during an earthquake as a function of structural properties and ground motion characteristics, *Engineering Structures*, Vol. 22,2000,pp. 784-792.

[29] MacRae, G. A., and Kawashima,K.: Post-Earthquake residual displacements of bilinear oscillators, *Earthquake Engineering and Structural Dynamics*, Vol. 26, 1997, pp. 701-716.

CHAPTER 5

EVALUATION AND DISCUSSION OF LONG DURATION EARTHQUAKE CASES

5.1 Introduction

In **Chapter 4** of this thesis, an overall three-dimensional non-linear numerical analysis was conducted, to evaluate the seismic performance of curved grillage girder viaducts equipped with base isolation system under severe cold environment. For this purpose, a finite element model was adopted to examine the seismic response of bridge system in detail under strong earthquake ground motions. Various lead rubber bearing (LRB) isolation cases that represent various temperature conditions are systematically compared and discussed. Low temperature effect and temperature variation of LRB is taken into account particularly. And for practicability and preciseness, a dynamic bearing property definition method was introduced to carry out detailed temperature and performance variation process of base isolation system during the earthquake.

However, the duration of earthquake ground motion applied in **Chapter 4**, which was obtained from JR Takatori Station in 1995 Kobe earthquake, is only about 20 seconds. This well known earthquake is the first one in which earthquake tremors in Japan are officially recorded at the highest seismic intensity of Level 7 on the scale of Japan Meteorological Agency (JMA). And therefore it is widely used in seismic response analysis for ultimate damage evaluation. Nevertheless, its lasting time is too short to ensure enough heat production in bearing support location, for the case of low temperature effect study. According to the calculation of **Chapter 4**, the temperature of base isolation systems was only raised up to -10 ℃, resulting in only a slight variation of bearing properties. Thus, although low temperature effect has been well investigated and discussed, the application range of conclusions of **Chapter 4** is still limited.

In order to extend the application range of low temperature effect investigation, a long duration earthquake lasting about 1 minute is applied in this chapter. Subjected to a longer duration earthquake, temperature rising of base isolation devices is increased, and variation of bearing properties is also enlarged consequently. Combining the results of last chapter, more comprehensive conclusions of low temperature effect of base isolation system by seismic response analysis are drawn in this chapter.

5.2 2003 Tokachi-Oki Earthquake

A severe earthquake struck Hokkaido, Japan, at 4:50 am on September 26, 2003. Epicenter of the earthquake was about 80km east-southeast of Erimo Cape, offshore of Tokachi, as shown in **Fig.5.1**. The depth of the epicenter was 42km, and its magnitude 8.0 (M_{JMA}). This magnitude of the earthquake is 10 times as large as that of Kobe Earthquake [1].

The source of this earthquake was the plate-boundary or subduction zone, and caused by the release of the stress built up between the Pacific Ocean Plate and the North American Plate. Relative to North American Plate, Pacific Ocean Plate moves in northwest direction with an average velocity of 8 cm per year. Since the movement length between these plates is large, a major earthquake is likely to occur when the stress is released, and the return period of M7 to 8 Earthquake is estimated to be several decades to centuries [2]. In the past decades, three major earthquakes had hit this area: 1952 Tokachi-oki Earthquake (M8.2), 1973 Nemuro-oki Earthquake (M7.4), 2003 Tokachi-oki Earthquake (M8.2), as shown in **Fig.5.1**

This kind of earthquake is characterized by accompanying with Tsunami. The Committee of Earthquake Survey said in this March that they expected M8.1 earthquake would occur in this area "with 60% probability in another 30 years". According to the Japan Meteorological Agency (JMA), this earthquake may correspond to the expected earthquake by the committee. The National Research Institute for Earthquake Science and Disaster Prevention estimates that the overall rupture plate of the fault is 100km long and 50km wide, the displacement or slip length of the fault is 4 to 5 meters in the east-west direction, and the moment magnitude (Mw) is estimated to be 7.9. According to the Geographical Survey Institute of Japan, the observation stations in Erimo-cho and Hiroo-cho moved 95cm and 97cm respectively during the earthquake. That is, the Hokkaido Island extended in the south east direction due to the ground movement caused by the stress release at the subduction zone. This indicates that there was crustal change in the large area over Toyokoro-cho to Onbetsu-cho.

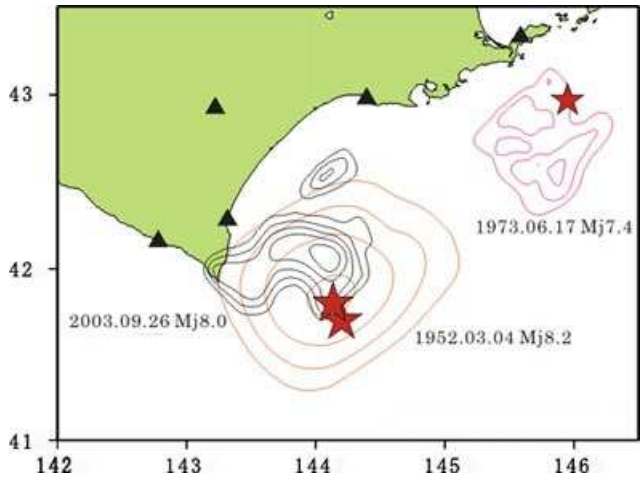


Fig. 5.1 Tokachi-oki Earthquakes in the History

The 2003 Tokachi-oki Earthquake recorded as 8.3 on the moment magnitude scale, and approximate Level 6 as the highest seismic intensity at Hiroo Machi (HKD100). This location and moment tensor solution of this earthquake are consistent with the fact that it is a result of thrust faulting between the North American Plate and the Subducting Pacific Plate. Consequently, Tokachi-Oki Earthquakes unavoidably occurred many times in the history and usually they were named as -Year-Tokachi-Oki Earthquake. Meanwhile, this location is also a typical cold region classified in **Chapter 1**. Therefore, this ground motion is suitable for the present study.

To assess the seismic performance of the viaduct in this study, the nonlinear bridge model is subjected to the longitudinal, transverse and vertical components of a strong ground motion records from the Hiroo Machi (HKD100) during the 2003 Tokachi-Oki Earthquake, as shown in **Fig.5.2**. The longitudinal earthquake component shakes the highway viaduct parallel to the X-axis of the global coordinate, while the transverse and vertical components are acting in the Y- and Z-axes, respectively. The tremors of 2003 Tokachi-Oki Earthquake lasted for approximately 2 minutes, in which a 1 minute cut is adopted, being considered as a proper record for this study. Since the seismic intensity of this earthquake is only Level 6, which may not cause enough damage to evaluate the seismic performance of base-isolated bridge, earthquake ground motions of triple amplification cases are also calculated.

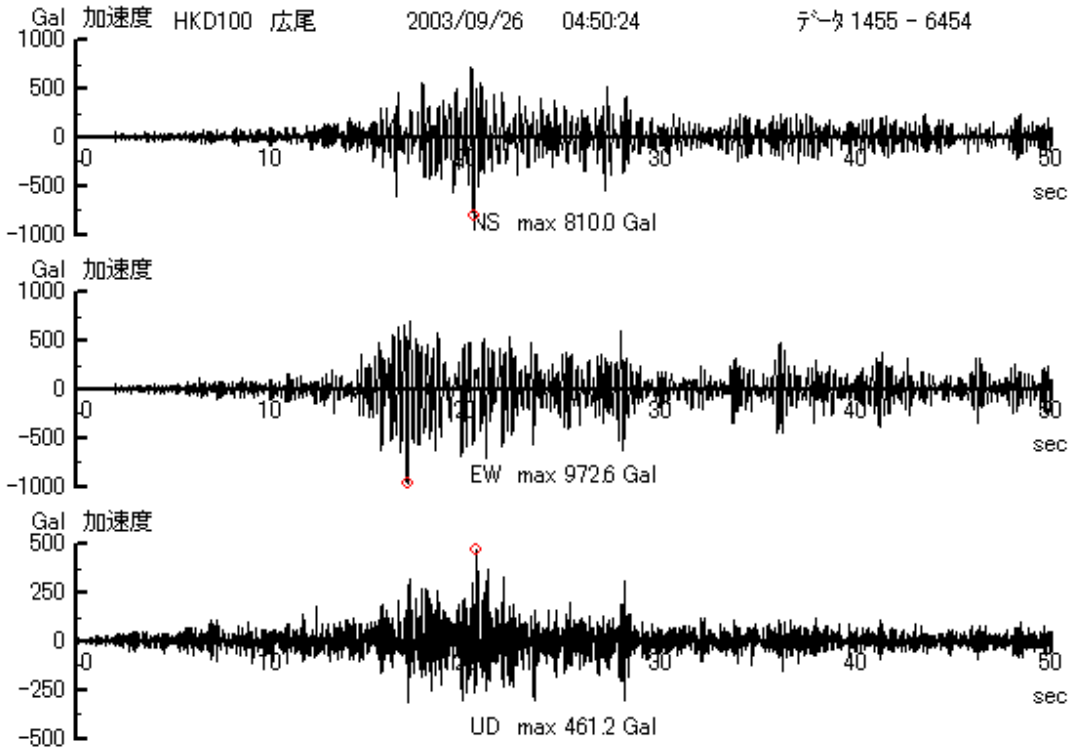


Fig.5.2 Earthquake Ground Motions

5.3 Analytical Cases

Based on the thermal analysis results of **section 4.3.2** of this thesis, for the case of a long-term low temperature environment, the equivalent stiffness of LRB increases about 30%, as listed in **Table.5.1**.

Table 5.1 Time Sample Points List

Time (s)	Temperature (℃)	Stiffness ratio (y_1)	Yield force ratio (y_2)
0	-30.00	1.38	1.62
2	-28.93	1.36	1.58
4	-27.87	1.34	1.55
6	-26.80	1.32	1.52
8	-25.74	1.31	1.50
10	-24.67	1.29	1.47
12	-23.61	1.28	1.45
14	-22.54	1.26	1.43
16	-21.48	1.25	1.41
18	-20.41	1.24	1.39
20	-19.35	1.23	1.37
22	-18.28	1.22	1.36
24	-17.22	1.21	1.34
26	-16.15	1.20	1.33
28	-15.09	1.19	1.31
30	-14.02	1.18	1.30
32	-12.95	1.17	1.28
34	-11.89	1.17	1.27
36	-10.82	1.16	1.26
38	-9.76	1.15	1.25
40	-8.69	1.14	1.23
42	-7.63	1.14	1.22
44	-6.56	1.13	1.21
46	-5.50	1.12	1.20
48	-4.43	1.12	1.19
50	-3.37	1.11	1.18
52	-2.30	1.11	1.17
54	-1.24	1.10	1.16
56	-0.17	1.09	1.15
58	0.89	1.09	1.14
60	1.96	1.08	1.14

In order to gain deep understanding of the thermo-mechanical behavior of rubber made bearings, experimental schemes composed of multiple test methods were proposed in past studies, among which a cooperative research by Rubber Bearing Association and Civil Engineering Research Institute for Cold Region is carried out, and obtained an integrated and practical conclusion [3].

According to their conclusion, with the heat production during earthquake event, the temperature of LRB gradually increases while the stiffness of LRB accordingly decreases. The detailed bearing property can be calculated by the following equations.

$$y_1 = -0.206 \times \mathrm{Ln}(x + 40) + 1.855 \quad (1)$$

$$y_2 = -0.335 \times \mathrm{Ln}(x + 40) + 2.388 \quad (2)$$

Where, y_1 is stiffness ratio; y_2 is yield force ratio; x is temperature.

Combining the temperature conditions with the equations about the temperature variation of performance listed above, a dynamic bearing property definition, which can perform temperature and bearing property modification real-timely, is established. This can contribute to obtain more accurate and practical numerical result in seismic response analysis.

By adding a matrix substitution statement at the beginning of calculation loop in FEM analysis program to apply this dynamic bearing property definition, the bridge seismic performance has been evaluated on a properly designed LRB bearing system. This system firstly satisfies the requirement of vertical load as a prerequisite. Its dimensions and properties are selected properly to ensure the seismic performance, according to the calculation results of **Chapter 4**.

Room temperature (20℃) condition and low temperature (-30℃) condition are discussed and compared. As to the low temperature condition, both fixed and dynamic stiffness cases are considered in this study. Although fixed conditions have no reality, they still represent the cases that maximum stiffness value are applied and therefore can contribute to understanding of the low temperature effect on seismic performance. The input ground motions, temperature schemes and corresponding performance of bearings are summarized in **Table 5.2**. It should be noticed, for the low temperature condition cases, only initial values are listed in this Table.

	Case	K_1	K_2	K_3	F_1	F_2	(K(MN/m) F(MN)) Temperature
1	Tokachi	2.662	0.380	0.984	0.096	0.191	+20℃, fixed
2	Tokachi	3.674	0.524	1.358	0.155	0.309	-30℃, increasing
3	Tokachi	3.674	0.524	1.358	0.155	0.309	-30℃, fixed
4	Tokachi - triple	2.662	0.380	0.984	0.096	0.191	+20℃, fixed
5	Tokachi - triple	3.674	0.524	1.358	0.155	0.309	-30℃, increasing
6	Tokachi - triple	3.674	0.524	1.358	0.155	0.309	-30℃, fixed
7	Kobe	2.662	0.380	0.984	0.096	0.191	+20℃, fixed
8	Kobe	3.674	0.524	1.358	0.155	0.309	-30℃, increasing
9	Kobe	3.674	0.524	1.358	0.155	0.309	-30℃, fixed

5.4 Numerical Results of Long Duration Earthquake Cases

Nonlinear dynamic analysis is performed to obtain structural responses of the viaduct under the input earthquake wave, and the response of pier (P3) is examined in this paper, because it supports the superstructure on both sides and consequently, the severest seismic response is expected at this pier.

The main object of this study is to confirm the necessity of considering low temperature effect of base isolation devices in seismic response analysis. In order to achieve this, calculation results due to a short duration earthquake (JR Takatori records from 1995 Kobe earthquake) are also added for comparison. In **Chapter 4** of this thesis, when a base-isolated bridge system is subjected to a short duration earthquake, the influence of low temperature effect was clearly observed. Therefore, comparing long duration earthquake cases with short duration earthquake cases can be helpful to draw a more comprehensive conclusion.

5.4.1 Natural vibration analysis

A basic problem in the earthquake design of viaducts is that their fundamental frequency is in the range of frequencies that earthquake energy is predominant. One of the objectives of seismic design is to shift the fundamental frequencies of viaducts away from the predominant frequency of earthquake ground motions to reduce the response of superstructure, which needs the structure to be flexible. The necessary flexibility can be achieved at the bearing level by the use of base isolation. Therefore, calculation of natural vibration characteristics of highway viaducts is crucial for prediction of their structural behaviour during strong earthquakes. Natural vibration analyses of the viaduct model supported on aforementioned nine different cases are carried out, and the results are summarized in **Table.5.3**. It should be mentioned, for dynamic stiffness cases, natural frequency also varies during earthquake, and only one intermediate value is listed here due to the limited space. Since stiffness of LRB increases under low temperature, low temperature cases (2, 3, 5, 6, 8, 9) have a shorter natural period than room temperature cases (+20℃, case 1,4,7). This means low temperature weakens the base isolation function by hardening the rubber material. Obviously, this is an unfavorable phenomenon. In addition, it should be emphasized, under low temperature, dynamic stiffness cases (temperature increases during earthquake, which is the main focus of this study) perform better than fixed low temperature cases (which is introduced as a reference value).

Since fundamental natural frequency is a inherent attribute of a bridge system, it is not dependent on the input earthquake ground motions. On the other hand, the response spectrum of earthquake wave, as shown in **Fig.5.3**, can be a convenient reference to get a preliminary identification of earthquake damage. It shows that this base isolation system successfully shifts fundamental natural periods of bridge away from predominant ones of the earthquake wave, resulting in avoiding the peak response zone (from 0.1s to 1.0s of resulting plot) of the response spectrum.

Table 5.3 Fundamental Natural Frequencies

Case	Temperature	ω[rad/sec]	T[sec]	ratio to T of fix
1,4,7	+20℃, fixed	4.38	1.44	1.67
2,5,8	-30℃, increasing	4.58	1.38	1.60
3,6,9	-30℃, fixed	4.77	1.32	1.53
All-Fix	+20℃, fixed	7.34	0.86	1

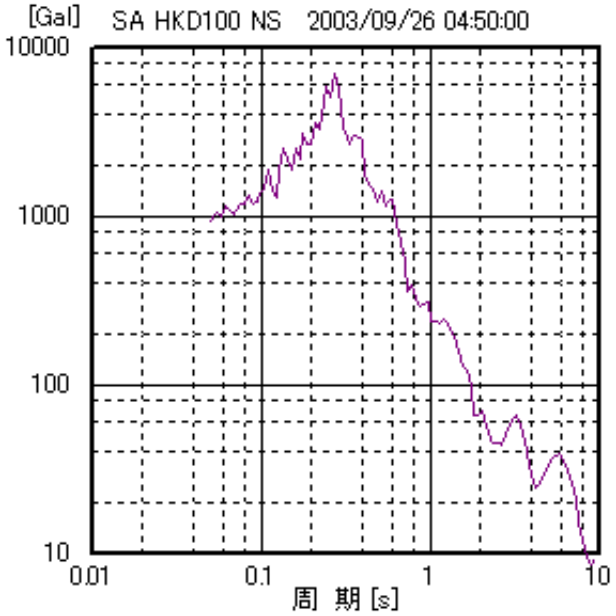


Fig.5.3 Response Spectrum of Tokachi-oki Earthquake

5.4.2 Shear force-displacement response at bearing

The effect of low temperature on LRB bearings is evaluated in detail. The calculation results of shear force-displacement relationship at bearing are shown in **Fig.5.4**. As expected, both the deformation of the bearings and the area of the hysteresis loops decrease under low temperature, especially when the temperature is fixed to -30℃. One of the most effective ways to provide a substantial level of additional damping is through hysteretic energy dissipation. Therefore, the reduce of area of the hysteresis loops results in the deterioration of base isolation function. On the other hand, with the flexibility decreases and natural period shortens, the response force increases as shown in the same figure. And hardening effect that is suggested to avoid by specifications is not observed in all the cases, benefiting from the properly selected base isolation system.

Original Tokachi-Oki earthquake cases (case 1, 2, 3) have slight damage and temperature dependence tendency due to the well designed base isolation system. But this also means the calculation results cannot sufficiently evaluate the influence of low temperature effect since the performance of this base isolation system is good enough to neglect flexibility deterioration under low temperature, when it is subjected to the earthquake of this level. Triple amplification cases (case 4, 5, 6) that undergo 60s vibration show similar results as Kobe earthquake cases (case 7, 8, 9) whose duration is only 20s. While short duration and less heat production show low

temperature effect more in Kobe earthquake cases, this effect is also shown clearly in long duration earthquake cases.

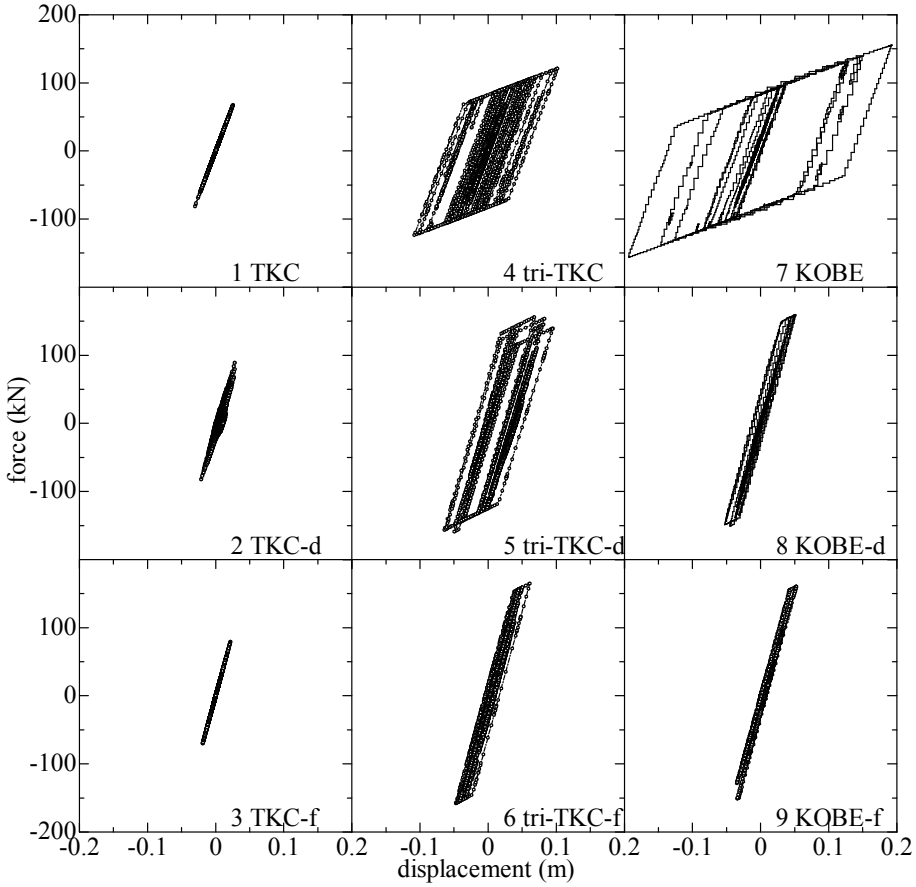


Fig.5.4 Shear Force-displacement Response at Bearing
(P3 X-Direction)

5.4.3 Bending moment-curvature response at pier base

Fig.5.5 shows the bending moment-curvature response at the base of piers, which is considered to be a good indicator to decide the earthquake damage level. It is clearly shown that a proper selection of LRB bearing system can effectively reduce inertial forces acting on bridge piers. The base isolation function should not only ensure the period shift that can protect superstructure but also reduce the inertia force to keep the substructure remain in the elastic range as much as possible. However, in this study, the yield moment of the pier is 84.8MN, and therefore inelastic deformation occurred in all cases. It can be acceptable that, in certain cases, the substructure has a post elastic behavior. The comparison of ending moment and curvature response can still make clear the damage conditions for different cases. It definitely shows us that the bridge system withstands more earthquake damage under low temperature. Base isolation function conspicuously is weakened with stiffness increasing, therefore results in a higher damage level. And more shear force response (being carried out in **Section 5.4.2**), leads to more bending moment at the base of piers, which is also shown in this figure.

In this section, low temperature effect still makes sense in long duration

earthquake cases as well as in short duration earthquake cases. So far, the necessity to consider low temperature effect in cold region seismic design is clearly indicated by the numerical results.

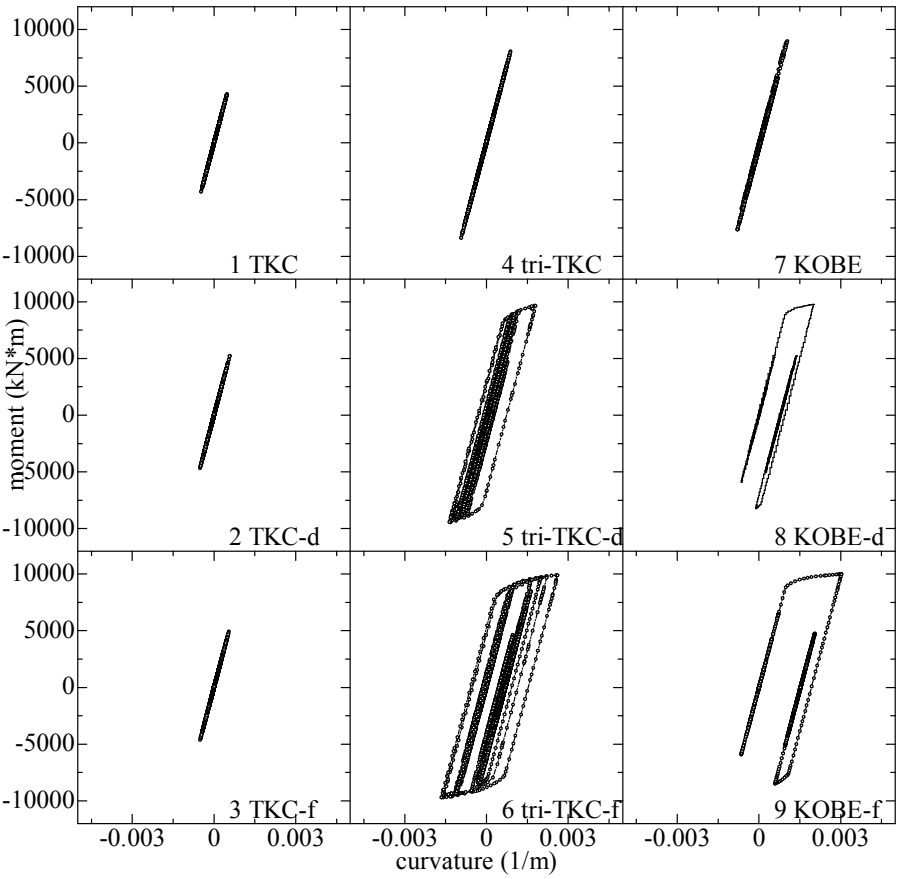


Fig.5.5 Bending moment-curvature response
(P3 X-Direction)

5.4.4 Energy-time history

The energy dissipation performance of the bearing systems is summarized by comparing the energy-time histories, as shown in **Fig.5.6**. By observing the distribution of total energy, it should be noticed that a proper designed base isolation system generally allows for a significant reduction of damage of structural members. While a bridge system is base isolated, the total earthquake energy is increased due to the large seismic energy dissipation at the isolators, i.e., most of the energy is dissipated by the isolators instead of by the structural members, thus resulting in considerable reduction of seismic damage. With the stiffness increasing and base isolation function weakening under low temperature, the energy response tends to be closer to fix support cases, and strain energy that represents the energy dissipation mechanism by hysteresis loops at bearing significantly decreases. Thus, the inelastic behavior at piers absorbs earthquake energy in these cases, and consequently resulting in the structural damage.

Furthermore, the original Tokachi-Oki earthquake cases show small responses under different temperature conditions, while triple amplification cases show large

responses similar to Kobe earthquake cases and the amount of energy dissipation significantly decreases under low temperature. Therefore, when a bridge confronts extreme strong earthquakes, the deterioration of energy dissipation function of base isolation system due to low temperature, may cause serious problem, as discussed in all the numerical results.

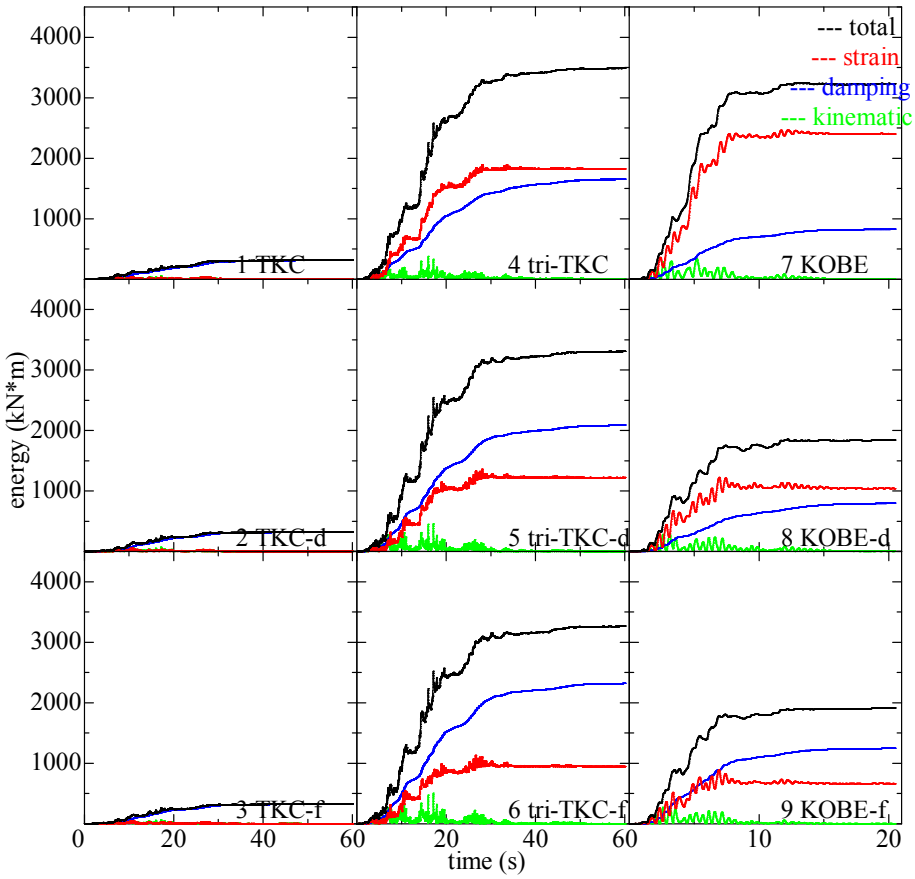


Fig.5.6 Energy-time History

5.4.5 Displacement-time history at top of piers

Finally, the results of residual displacement at the tops of piers are shown is **Fig.5.7**. As a serious problem, permanent tangential deformation of bridge expansion joints observed in recent earthquakes have severely interfered the post-earthquake serviceability of highway viaducts. Bridge structures should not only remain standing but also are expected to be usable after a large earthquake, because during the time they cannot be used society may suffer a tremendous cost and inconvenience. The investigation of residual displacements after 1995 Kobe earthquake concluded that piers with a residual deformation of 1/100 pier height had to be demolished and replaced by new piers. Thus, JRA Specifications prescribed residual displacement limitation. In this study, the calculation results denote that the residual displacement is under 0.2m limitation (1/100 of 20m) for all the cases. However, the low temperature amplifies the residual displacement in this result.

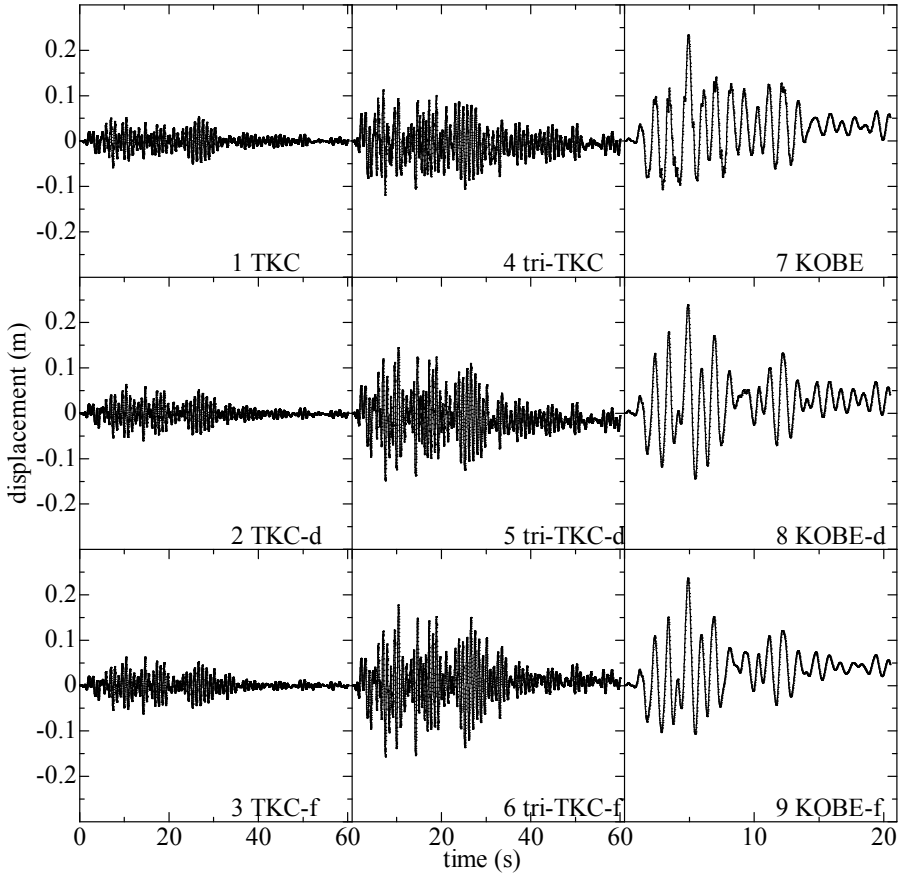


Fig.5.7 Displacement time history at the tops of piers
(P3 X-Direction)

5.5 Conclusions

In this chapter, a dynamic bearing property definition method is introduced in a nonlinear 3-dimensional seismic response analysis of a highway viaduct with proper base isolation system. Numerical results under changeable temperature are carried out. Seismic responses are examined and compared to investigate the influence of bearing conditions on the overall behavior of the bridge, in which low temperature effect is focused on particularly. In order to examine heat production during earthquake thoroughly, both short duration earthquake and long duration earthquake ground motions are adopted and evaluated. And the conclusions are drawn as follows.

(1) In previous studies, whether low temperature effect should be considered in seismic response analysis was doubted, because during an earthquake event, the base isolation devices absorb earthquake energy and release it as heat. By intuition, such a great thermal behavior will raise the initial low temperature condition to room temperature level immediately. In this study, by adopting dynamic bearing property definition method and examining the numerical results, the necessity of considering low temperature effect, not only in a short-duration earthquake, but also in a long-duration earthquake, has been clearly indicated. More accurate seismic design

considering not only performance but also low temperature effect should be taken into account in cold regions.

(2) Under low temperature, base isolation devices that are mainly made from rubber are hardened because of the material characteristics. A harder state of base isolation device, which means the loss of flexibility, has less base isolation function than its original state. By comparison with fixed room temperature and fixed low temperature cases, it is found that the changeable low temperature cases with dynamic bearing property have intermediate base isolation performance. This is just simply because the stiffness values of changeable low temperature cases are also between those of other two conditions.

(3) Short duration strong earthquake is more dangerous when considering low temperature effect, because inadequate heat conduction keeps base isolation devices cool and hard. Although long time vibration raises the temperature over freezing value, low temperature effect still has a significant influence on seismic response behavior of a base-isolated bridge.

References

[1] Ministry of Land, Infrastructure, Transport and Touris: About 2003 Tokachi-oki earthquake, 2003.

[2] Hirata, K., Y. Tanioka, K. Satake, S. Yamaki and E. L. Geist： The tsunami source area of the 2003 Tokachi-oki earthquake estimated from tsunami travel timees and its relationship to the 1952 Tokachi-oki earthquake, *Earth Planets Space*, 56, 367-372, 2004.

[3] Imai, T., Satoh, T., Nishimura, T., Tanaka, H., and Mitamura, H., The performance evaluations of rubber bearings for bridges in cold districts(2), *Proceeding of Hokkaido Chapter of JSCE*, Vol.64, pp.A-18, 2008.

CHAPTER 6

TEMPERATURE-DEPENDENT BEHAVIOR OF HIGH DAMPING RUBBER BEARING

6.1 Introduction

In **Chapter 5** of this thesis, a dynamic bearing property definition method is introduced in a nonlinear 3-dimensional seismic response analysis of a highway viaduct with proper base isolation system. Numerical results under changeable temperature are carried out. Seismic responses are examined and compared to investigate the influence of bearing conditions on the overall behavior of the bridge, in which low temperature effect is focused on particularly. In order to examine heat production during earthquake thoroughly, both short duration earthquake and long duration earthquake ground motions are adopted and evaluated.

However, the conclusion of last chapter clearly shows that even long time vibration raises the temperature over freezing value, low temperature effect still has a significant influence on seismic response behavior of a base-isolated bridge equipping with lead rubber bearing (LRB) system, i.e. base isolation strategy should be reconsidered when it is applied under low temperature environment.

Application of laminated rubber bearings as base isolation devices [1,2] got wider acceptance in Japan after promising field level performances in 1995 Kobe Earthquake. To introduce energy dissipation properties within the bearing device, lead rubber bearing (LRB) was developed in New Zealand [3,4] with lead plugs installed inside laminated natural rubber bearings (RB). High damping rubber (HDR) later emerged as a novel material for such bearing devices not only to eliminate the necessity of installing lead plugs inside RB but also to enhance energy dissipation properties compared to LRB. A more recent concern over the reduction of energy dissipation property per cycle in LRB due to self-heating of lead plug upon cyclic loading [5,6] is also questioning the capability of LRB in long duration earthquakes, for example 2011 Tohoku earthquake. The innovation of HDR led to a wide adoption of high damping rubber bearings (**Fig.6.1**) as visco-elasto-plastic dampers in next generation base isolated structures all over the world. In contrast to LRB, where rate dependence effect is much less significant even for low temperature cases [3,7], however, even after years of practice, some of the very important mechanical behaviors of HDR, such as the rate or temperature dependent behaviors are still difficult and less under-stood issues in engineering practice [8]. Yet, evaluation of seismic response of bridge equipping with HDR bearing for designing base isolated structures in cold weather conditions and more general dynamic loading cases is much warranted.

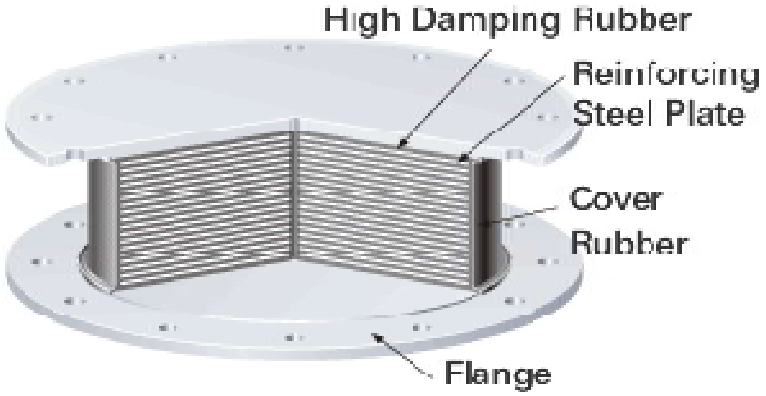


Fig.6.1 High Damping Rubber Bearing

6.2 High-Damping Rubber Bearing Isolation System

HDR can provide at the same time period shift and energy dissipation. They consist of alternate layers of rubber and steel plates bonded by vulcanisation and are for some aspects similar to standard elastomeric bearings, being able to support vertical loads with limited or negligible deflection and horizontal loads with large deflections. Since HDR bearings are mainly made from rubber, some characteristics of rubber material conspicuously influence the performance of HDR. Such as strain hardening effect and the stiffness increment under low temperature. According to the basic conception of base isolation system, high stiffness that means less flexibility basically is not a favorable property of HDR, because it may cause intensive response of the superstructure and less energy dissipation. Therefore, stiffness increment as well as strain hardening under low temperature may lead to problems.

6.2.1 Thermal analysis

In an earthquake event, base isolation bearings absorb earthquake energy and release it as heat. The heat production will raise the temperature of HDR. Thus, as the main objective of this study is to seek deep understanding of the themo-mechanical behavior of HDR, and a dynamic stiffness definition composed of temperature variation of time and stiffness variation of temperature is proposed. Therefore, a thermal analysis is additionally conducted in the present study.

The numerical studies conducted mainly focus on the sensitivity of time variations of temperature of base isolation devices. In order to assess the temperature rise with respect to time as well as the temperature distribution at the transient state, the thermal characteristics of the bearing system was analyzed using ANSYS, which is a commercial finite element analysis software package. The circular steel-laminated bearing was chosen for modeling. This bearing has overall dimensions commonly used in practice. All specified bearing properties are supplied by base isolation devices manufacturer. Low-temperature thermal analysis is conducted under the initial temperature of -30℃. And convection of heat from all the surfaces of the bearing model are also set to -30℃, which represents the low temperature environment. The

heat generation of bearings is assessed by adopting the values of earthquake strain energy time history, assuming the bearings absorb earthquake energy and release it as heat during earthquake.

During an earthquake event, the complete earthquake energy balance is given by:

$$E_I = E_S + E_K + E_D + E_H \quad (1)$$

where, at a given instant in time, t, E_I = cumulative input energy; E_S = instantaneous strain energy stored by the structure; E_K = instantaneous kinetic energy of the moving mass; E_D = cumulative damping energy; and E_H = cumulative hysteretic energy.

At the end of the earthquake $t = t_f$, the kinetic energy is zero, the strain energy is decided by the inelastic deformation for an inelastic system, the cumulative damping energy is dissipated by damping system and the cumulative hysteretic energy is all converted to the heat. Since the all the values of this equation could be obtained by numerical analysis, the internal heat generation is consequently obtained.

6.2.2 Time-varying temperature of HDR

In this study, two functions are introduced to simulate the temperature and bearing property variation process: the time variation of temperature which is concluded by thermal analysis of HDR, and performance variation due to temperature that is obtained by performance test under different temperature conditions. The 2003 Tokachi-Oki earthquake ground motion obtained from Hiroo Machi (observation site code HKD100) is adopted, not only because it is a periodic great earthquake in Hokkaido Island, but also its duration (60 seconds) is a suitable time for this study.

By carrying out numerical results on this thermal analysis which has been particularly described in **Section 6.2.2**, and adopting the temperature increment condition, the relationship between time and temperature of HDR can be obtained, as shown in **Fig.2**. It can be summarized that, for a earthquake with a duration of 60 seconds, the temperature increment is approximately 30℃, i.e. HDR devices are still influenced by low temperature effect to a certain extent. Therefore detailed quantitative analysis on temperature dependent performance of HDR is necessary.

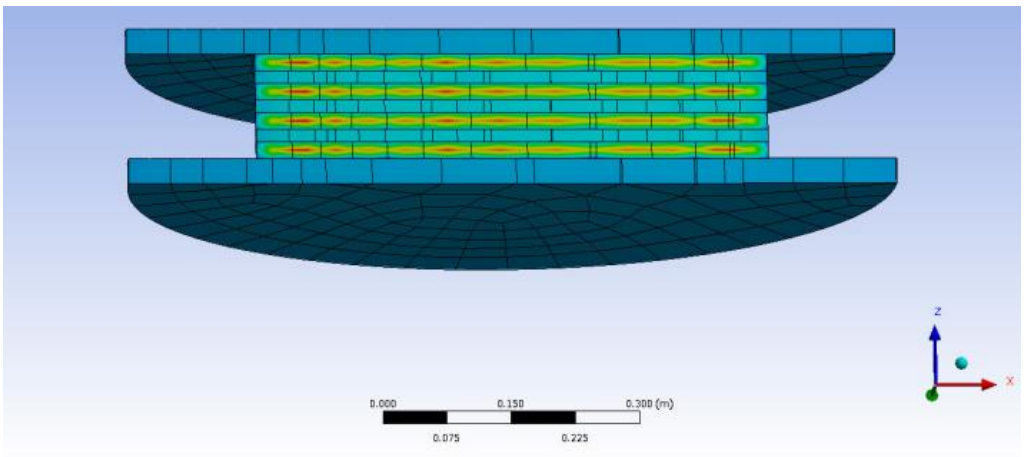


Fig.6.2(a) Thermal Analysis of HDR (Temperature Distribution)

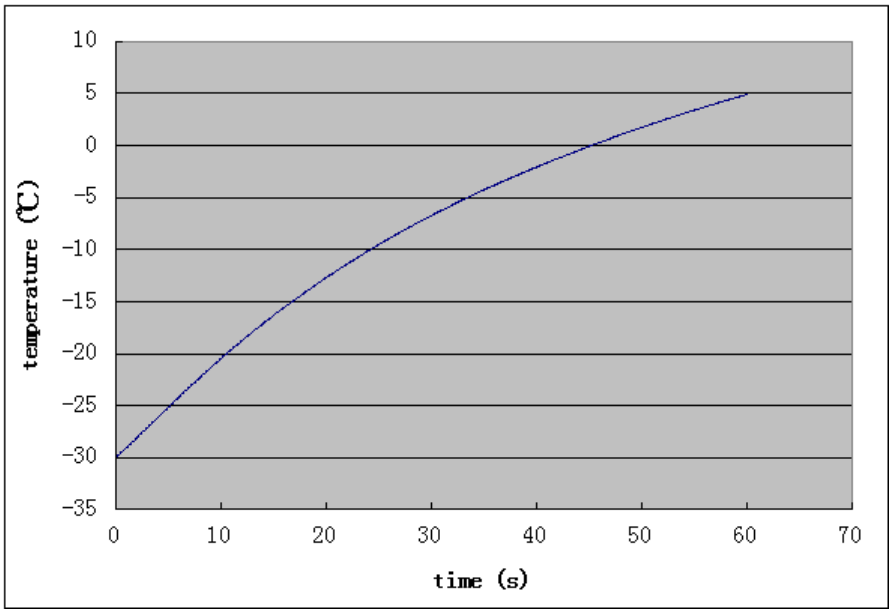


Fig.6.2(b) Thermal Analysis of HDR (Temperature Variation)

6.2.3 Behavior variation with temperature

In order to gain deep understanding of the thermo-mechanical behavior of rubber made bearings, experimental schemes composed of multiple test methods were proposed in past studies, among which a cooperative research by Rubber Bearing Association and Civil Engineering Research Institute for Cold Region is carried out, and obtained an integrated and practical conclusion[5].

Based on the experiment results, for the case of a long-term low temperature environment, the equivalent stiffness of LRB increases about 30%. And with the heat production during earthquake event, the temperature of HDR gradually increases while the stiffness of HDR accordingly decreases. The detailed bearing property can be calculated by the following equations:

$$y_1 = -0.510 \times \mathrm{Ln}(x + 40) + 3.116 \quad (2)$$

$$y_2 = -0.588 \times \mathrm{Ln}(x + 40) + 3.435 \quad (3)$$

Where, x is temperature, y_1 is stiffness scale factor; y_2 is yield force scale factor.

It should be made clear here, y_1 represents the ratio of stiffness in current temperature to stiffness in room temperature, while y_2 represents the ratio of yield force in current temperature to yield force in room temperature. Since these two values will be increased under low temperature, naming them as “scale factor” will be easy to understand.

By adding a matrix substitution statement at the beginning of calculation loop in FEM analysis program, these equation can be used to build a dynamic bearing property definition, as shown in **Table 6.1**.

Table 6.1 Time Sample Points List

Time (s)	Temperature (℃)	Stiffness scale factor (y_1)	Yield force scale factor (y_2)
0	-30.00	1.93	2.08
10	-20.488	1.72	1.83
20	-12.709	1.57	1.66
30	-6.7334	1.45	1.52
40	-2.0665	1.35	1.41
50	1.7532	1.28	1.32
60	4.9113	1.21	1.24

2.4 HDR modeling

Combining the temperature conditions acquired in **Section 6.2.2** with the equations about the temperature variation of performance listed in **Section 6.2.3**, a dynamic bearing property definition, which can perform temperature and bearing property modification real-timely, is established. This can contribute to obtain more accurate and practical numerical result in seismic response analysis. By applying this dynamic bearing property definition, the bridge seismic performance has been evaluated on a properly designed HDR bearing system. This system firstly satisfies the requirement of vertical load as a prerequisite. Its dimensions and properties are selected properly to ensure the seismic performance.

As shown in **Fig.6.1**, the rubber-based bearing isolation system consists of layers of rubber and steel, with the rubber being arranged with steel plates one by one for horizontal flexibility and vertical stiffness. In the manufacture of HDR, natural rubber is vulcanized together with carbon black, plasticizer, oil, and so on, and, consequently, the rubber possesses specific characteristics such as maximum strain dependency of stress evolution, energy absorbing properties and hardening properties.

Under normal conditions, HDR bearings behave like regular bearings. However, in the event of a strong earthquake, with the utilization of this base-isolation system, the superstructure of a bridge is decoupled from its substructure, and the response of the superstructure to the dynamic seismic loading is altered favorably and the seismic dynamic energy transferred to the superstructure is reduced. Thus seismic inertial loads are reduced and the seismic damage the structure acquires is drastically reduced. The force-displacement relationship of HDR is trilinear hysteretic, as shown in **Fig.6.3**. The parameters of the trilinear model are five: the elastic stiffness of the lead core K_1, the post-yield stiffness of the rubber material K_2, the yield force of the lead core F_1, the stiffness of rubber at high strain levels K_3,and the second yield displacements, F_2, in which the last two parameters are for characterizing the hardening behaviour of the bearing.

Room temperature condition (being denoted as +20℃, fixed) and low temperature condition (being denoted as -30℃, increasing) are discussed and compared. As to the low temperature condition, both fixed and dynamic stiffness cases are considered in this study. Although fixed conditions (being denoted as -30℃,

fixed) have no reality, they still represent the cases that maximum stiffness value are applied and therefore can contribute to understanding of the low temperature effect on seismic performance. And LRB cases are also added. The input ground motions, temperature schemes and corresponding performance of bearings are summarized in **Table.6.2**. It should be noticed, for the low temperature condition cases, only initial values are listed in this Table.

Table 6.2 Anylytical Cases (K(MN/m) F(MN))

	Case	K_1	K_2	K_3	F_1	F_2	Temperature
1	HDR	3.203	0.320	0.830	0.044	0.088	+20℃, fixed
2	HDR-d	6.213	0.621	1.610	0.092	0.183	-30℃, increasing
3	HDR-f	6.213	0.621	1.610	0.092	0.183	-30℃, fixed
4	LRB	2.662	0.380	0.984	0.096	0.191	+20℃, fixed
5	LRB-d	3.674	0.524	1.358	0.155	0.309	-30℃, increasing
6	LRB-f	3.674	0.524	1.358	0.155	0.309	-30℃, fixed

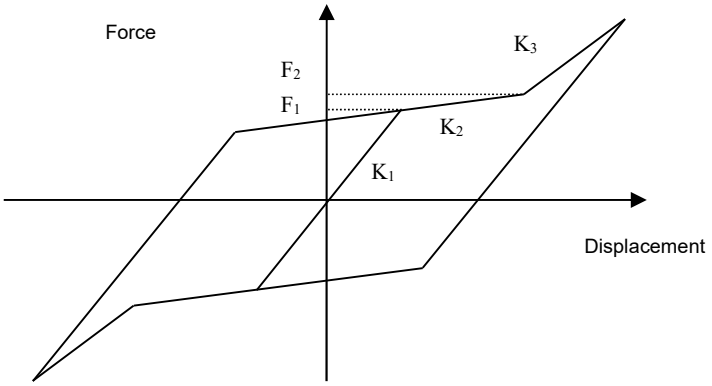


Fig.6.3 Analytical Model of HDR

6.3 Numerical Results of HDR Cases

Nonlinear dynamic analysis is performed to obtain structural responses of the viaduct under the input earthquake wave, and the response of pier (P3) is examined in this paper, because it supports the superstructure on both sides and consequently, the severest seismic response is expected at this pier. The main object of this study is to confirm the necessity of considering low temperature effect of HDR devices in seismic response analysis. In order to achieve this, calculation results of LRB are also added for comparison, since LRB is more widely applied in cold region than HDR.

6.3.1 Natural vibration analysis

A basic problem in the earthquake design of viaducts is that their fundamental frequency is in the range of frequencies that earthquake energy is predominant. One of the objectives of seismic design is to shift the fundamental frequencies of viaducts

away from the predominant frequency of earthquake ground motions to reduce the response of superstructure, which needs the structure to be flexible. The necessary flexibility can be achieved at the bearing level by the use of base isolation. Therefore, calculation of natural vibration characteristics of highway viaducts is crucial for prediction of their structural behaviour during strong earthquakes. By applying the post-yield stiffness of the rubber material K_2, natural vibration analyses of the viaduct model supported on aforementioned nine different cases are carried out, and the results are summarized in **Table.6.3**. It should be mentioned, for dynamic stiffness cases, natural frequency also varies during earthquake, and only one value on 30 seconds is listed here due to the limited space. Since stiffness of HDR increases under low temperature, low temperature cases (2, 3, 5, 6) have a shorter natural period than room temperature cases (+20℃, case 1,4). This means low temperature weakens the base isolation function by hardening the rubber material. Obviously, this is an unfavorable phenomenon. In addition, it should be emphasized, under low temperature, dynamic stiffness cases (temperature increases during earthquake, which is the main focus of this study) perform better than fixed low temperature cases (which is introduced as a reference value).

One important conclusion of this section is, low temperature obviously influence HDR more than LRB. Under low temperature, the nature period shortens from 1.52s to 1.34s in HDR cases, while only from 1.44s to 1.38s in LRB cases. This is a simple but critical reason why LRB is more widely applied in cold regions.

Since fundamental natural frequency is a inherent attribute of a bridge system, it is not dependent on the input earthquake ground motions. On the other hand, the response spectrum of earthquake wave, as shown in **Fig.6.4**, can be a convenient reference to get a preliminary identification of earthquake damage. It shows that this base isolation system successfully shifts fundamental natural periods of bridge away from predominant ones of the earthquake wave, resulting in avoiding the peak response zone (from 0.1s to 1.0s of resulting plot) of the response spectrum.

Table 5 Fundamental Natural Frequencies

Case	ω[rad/sec]	T[sec]	ratio to T of fix
1	4.13	1.52	1.77
2	4.69	1.34	1.56
3	5.07	1.24	1.44
4	4.38	1.44	1.67
5	4.58	1.38	1.60
6	4.77	1.32	1.53
All-Fix	7.34	0.86	1

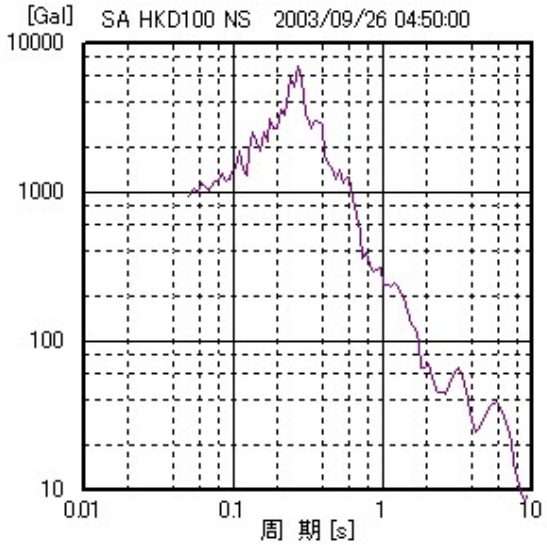


Fig.6.4 Response Spectrum of Tokachi-Oki Earthquake

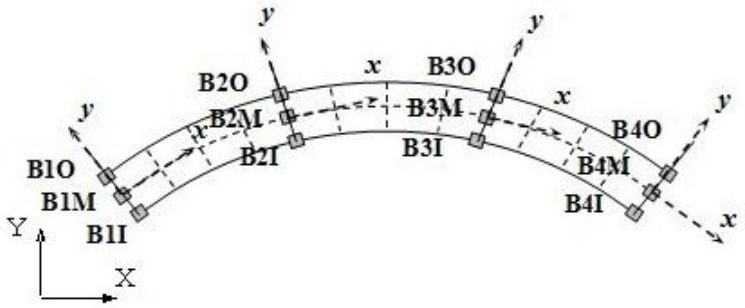
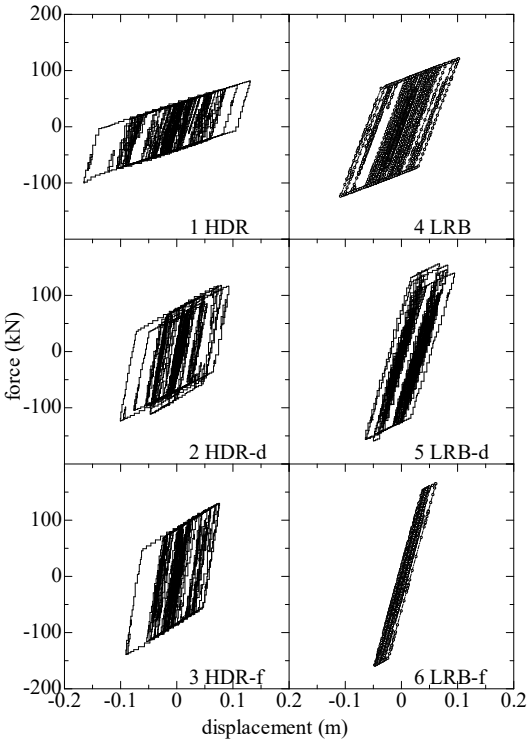


Fig.6.5 Plan View of Curved Grillage Viaduct Model

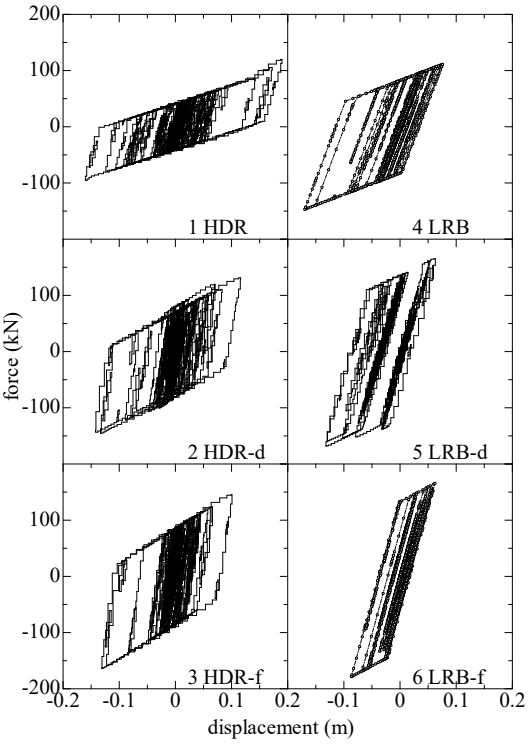
6.3.2 Shear force-displacement response at bearing

The effect of low temperature on base isolation bearings (both inner bearings B3I and outer bearings B3O, as shown in **Fig.6.5**) is evaluated in detail. The calculation results of shear force-displacement relationship at bearing are shown in **Fig.6.6**. As expected, both the deformation of the bearings and the area of the hysteresis loops decrease under low temperature. One of the most effective ways to provide a substantial level of additional damping is through hysteretic energy dissipation. Therefore, the reduce of area of the hysteresis loops results in the deterioration of base isolation function. On the other hand, with the flexibility decreases and natural period shortens, the response force increases as shown in the same figure. And hardening effect that is suggested to avoid by specifications is not observed in all the cases, benefiting from the properly selected base isolation system.

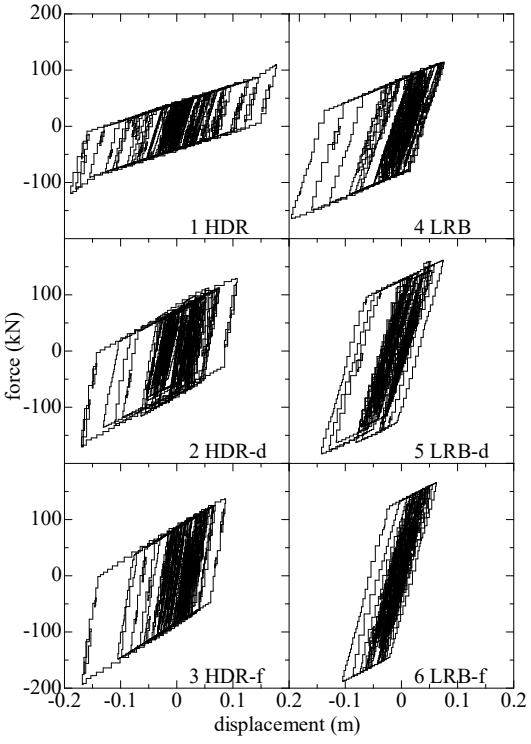
On the other hand, HDR cases, which is expected to be worse, still keep relatively large area of hysteresis loops under low temperature. This is because the yield force of HDR is much lower than LRB with a lead plug inside. Then HDR could take more advantage of stiffness after yield stage, achieving an overall low stiffness.



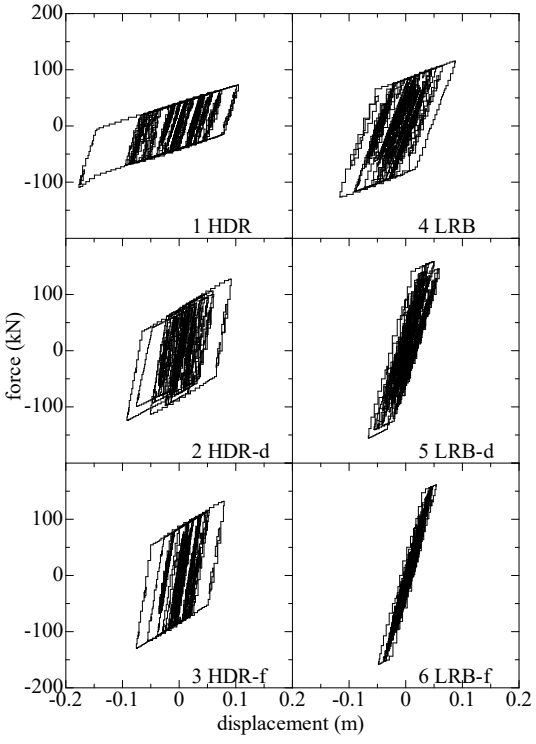
(B3I X-Direction)



(B3I Y-Direction)



(B3O X-Direction)



(B3O Y-Direction)

Fig.6.6 Shear Force-displacement Response at Bearing

6.3.3 Bending moment-curvature response at pier base

Fig.6.7 shows the bending moment-curvature response at the base of piers, which is considered to be a good indicator to decide the earthquake damage level. It is clearly shown that a proper selection of base isolation system can effectively reduce inertial forces acting on bridge piers. The base isolation function should not only ensure the period shift that can protect superstructure but also reduce the inertia force to keep the substructure remain in the elastic range as much as possible. However, in this study, the yield moment of the pier is 84.8MN, and therefore inelastic deformation occured in all cases. It can be acceptable that, in certain cases, the substructure has a post elastic behavior. The comparison of ending moment and curvature response can still make clear the damage conditions for different cases. It definitely shows us that the bridge system withstands more earthquake damage under low temperature. Base isolation function conspicuously is weakened with stiffness increasing, therefore results in a higher damage level. And more shear force response (being carried out in **Section 6.3.2**), leads to more bending moment at the base of piers, which is also shown in this figure.

And again, low temperature effect obviously raises the damage level in LRB cases, Base isolation function conspicuously weakens with stiffness increasing. More shear force response leads to more bend moment at the base of piers, which is also shown in this figure. One the contrary, HDR cases are affected much slightly. A proper designed base isolation system (case 1), could survive well in low temperature condition (case 2). This result also agrees well with the last section.

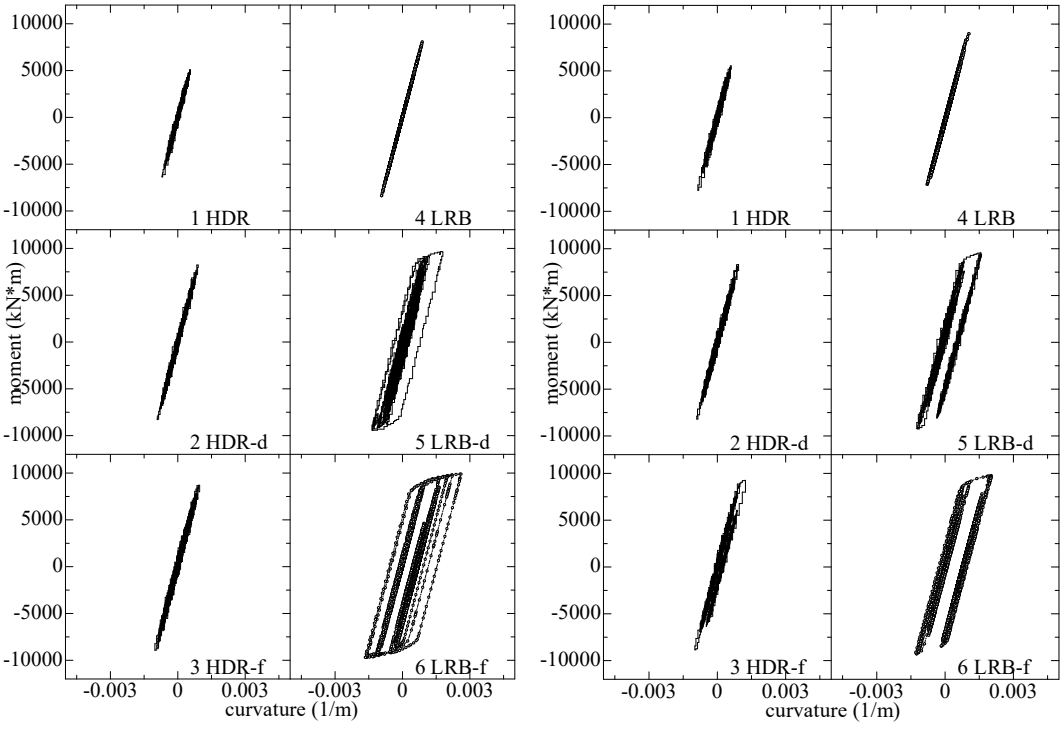


Fig.6.7 Bending Moment-curvature Response

4.4 Energy-time history

In this section, energy is used as an alternative response factor to response quantities like force or displacement to examine the seismic damage effect on bridge structures. The performance of the bearings are analyzed by comparing the energy-time histories for the structural system. The energy dissipation performance of the bearing systems is summarized by comparing the energy-time histories, as shown in **Fig.6.8**. By observing the distribution of total energy, it should be noticed that a proper designed base isolation system generally allows for a significant reduction of damage of structural members.

While a bridge system is base isolated, the total earthquake energy is increased due to the large seismic energy dissipation at the isolators, i.e., most of the energy is dissipated by the isolators instead of by the structural members, thus resulting in considerable reduction of seismic damage.

With the stiffness increases and base isolation function weakens under low temperature, the strain energy of LRB cases which represents the energy dissipation mechanism by hysteresis loops at bearing, significantly decreases. Thus, the inelastic behavior at piers absorbs earthquake energy in these cases, and consequently resulting the structural damage.

Whereas, it should be appreciated that a proper designed HDR base isolation system generally allows for a significant reduction of damage of structural elements. Even under low temperature, benefiting from its large deformation, the strain energy holds a steady level.

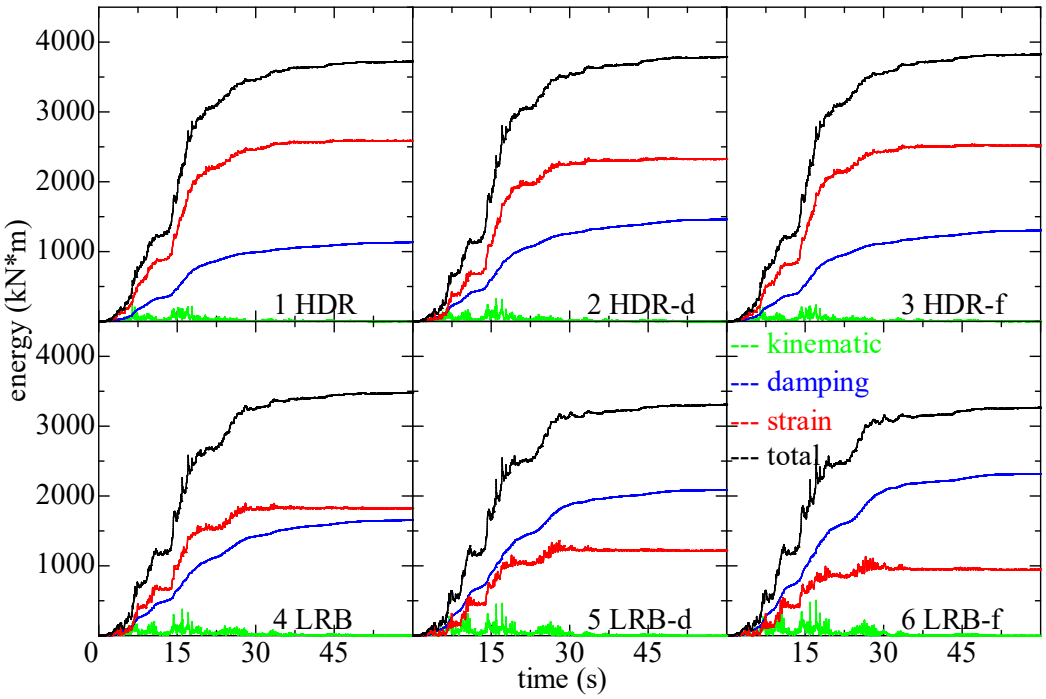


Fig.6.8 Energy-time History

4.5 Displacement-time history at top of piers

Finally, the results of displacement time history at the tops of piers are shown is **Fig.6.9**. As a serious problem, permanent tangential deformation of bridge expansion joints observed in recent earthquakes have severely interfered the post-earthquake serviceability of highway viaducts. Bridge structures should not only remain standing but also are expected to be usable after a large earthquake, because during the time they cannot be used society may suffer a tremendous cost and inconvenience.

The investigation of residual displacements after 1995 Kobe earthquake concluded that piers with a residual deformation of 1/100 pier height had to be demolished and replaced by new piers. Thus, JRA Specifications prescribed residual displacement limitation. In this study, the calculation results denote that the residual displacement is under 0.2m limitation (1/100 of 20m) for all the cases. However, the low temperature amplifies the residual displacement in this result.

The numerical results of this section shows one more advantage of HDR over LRB. Although bearings themselves have more deformation during hysteresis loops, the displacement at pier tops of bridge equipped with HDR bearings is still less than that of LRB cases, on account of less curvature and deformation of piers.

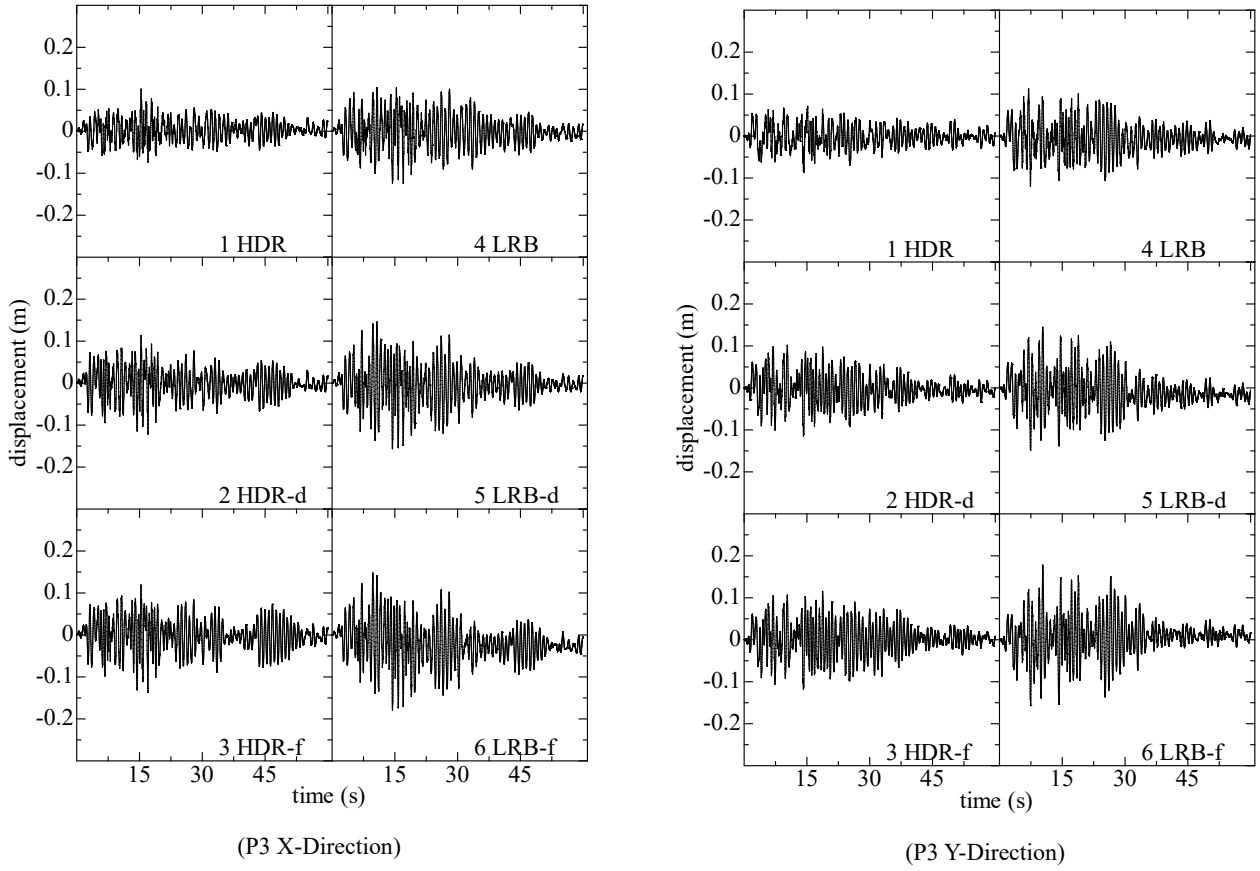


Fig.6.9 Displacement Time History at the Tops of Piers

6.4 Conclusions

In this chapter, a dynamic bearing property definition method is introduced in a nonlinear 3-dimensional seismic response analysis of a highway viaduct with proper base isolation system. Numerical results under changeable temperature are carried out. Seismic responses are examined and compared to investigate the influence of bearing conditions on the overall behavior of the bridge, in which low temperature effect is focused on particularly. In order to examine heat production during earthquake thoroughly, long duration earthquake ground motions is adopted and thermal analysis is conducted. And the conclusions are drawn as follows.

(1) Contrary to the expectation, HDR has better performance better than LRB under low temperature. With lower yield force and more yield stiffness usage, HDR could keep its flexibility. High damping rubber(HDR) material applies for such bearing devices not only to eliminate the necessity of installing lead plugs inside laminated rubber bearing but also to enhance seismic protection properties compared to LRB.

(2) Lower yield force and larger deformation could also cause problem such as hardening effect. Therefore further study of low temperature effect on HDR devices is still required.

References

[1] Kelly, J.M.: Earthquake-resistant design with rubber 2nd edition, London:Springer-Verlag, 1997.

[2] Kumar, M., Whittaker, A.S.and Constantinou M.C.: An advanced numerical model of elastomeric seismic isolation bearings, *Earthquake Eng Struct Dyn*, 43(13), 1955-1974, 2014.

[3] Robinson, W.H.: Lead rubber hysteretic bearings suitable for protecting structures during earthquakes, *Earthquake Eng Struct Dyn*, 10(4), 593–604, 1982.

[4] Skinner, R.I., Robinson, W.H. and McVerry, G.H.: An introduction to seismic isolation, England: John Wiley and Sons, 1993.

[5] Kalpakidis, I. and Constantinou, M.: Effects of heating on the behavior of lead-rubber bearings. I: Theory, *JStruct Eng ASCE*, 135(12), 1440-1449, 2009.

[6] Kalpakidis, I. and Constantinou, M., Effects of heating on the behavior of lead-rubber bearings. II:Verification of theory, *JStruct Eng ASCE*, 135(12), 1450-1461, 2009.

[7] Razzaq, M.K., Okui,Y., Bhuiyan A.R., Amin, A., Mitamura, H. and Imai, T.:Application of rheology modeling to natural rubber and lead rubber bearings:a simplified model and low temperature behavior, *Struct Eng/Earthquake Eng JSCE*, 29(2), 40-55, 2012.

[8] Cardone, D., Gesualdi, G. and Nigro,D.: Effects of air temperature on the cyclic behavior of elastomeric seismic isolators, *Bull Earthquake Eng*, 9 (4), 1227-1255, 2011.

CHAPTER 7

CONCLUSIONS

7.1 Summary of the Present Study

This thesis set out to investigate the possible problems that various types of base-isolation bearings have on the seismic performance of highway viaducts when applied in the cold region. The main focus of the thesis has been to evaluate the capacity of base-isolation systems to protect bridge structures from the destructive power of great earthquake ground motions which are also affected by the low temperature environment. This task is seriously influence by the trade off between two opposite tendencies that take place in base-isolation applications: the extent of force isolation and acceptable relative displacements across the isolation system during the earthquake motion. The large deformations that may occur in the seismic base-isolation bearings during a major seismic event may cause extremely large displacements in a deck, thus probability of collisions between deck and abutments is increased, as well as large expansion joints for the bridge needs to be adopted to accommodate these displacements, causing noise, vibration and maintenance problems for the bridge.

Base-isolation bearings with energy dissipation capacity, demonstrate to be very effective in suppressing excessive force responses acting on bridge piers when subjected to strong earthquakes. Based on the dynamic analysis results, it is found that these types of bearing systems may prevent structural damage during a seismic event, because their demand-reduction features provide a significant reduction in the seismic forces that the bridge structure must resist. Moreover, due to an appropriate selection of the design parameters of these bearing systems, moderate deformations of isolator devices are observed. This result is significant in that it indicates that base-isolation systems are capable of controlling peak deck displacement response. Whereas cold region factors conspicuously weaken this base isolation function, which is the main conclusion of this study.

The following is a summary of the most significant observations and conclusions based on the results discussed in each chapter:

Chapter 1 illustrates the catastrophic consequences of damage to bridge structures in the event of a strong earthquake, emphasizing the good performance of LRB bearing supports in the event of an earthquake. Reviews about researches carried out to investigate the effect of cold region factors are also included in this chapter. And finally, the basement of the need for this research is summarized.

In **Chapter 2** the analytical model of the highway viaduct object of this study is presented. Bridge members are modeled using analytical models which plenty represents their mechanical and structural characteristics, and are shown to be adequate for their implementation in the finite element analysis. The seismic response of the viaduct is investigated under the action of Level II earthquake ground motions. In this chapter, the role of bridge bearings as one of the most important structural elements of the bridge is emphasized, and seismic base-isolation features are explained according to the properties of each type of isolation system considered in this study.

Chapter 3 heightens the necessity of nonlinear dynamic analysis for the model of viaduct, due to the complexity degree of the bridge behaviour under seismic loading. This chapter discusses the analytical method for determining nonlinear dynamic response, based on the elasto-plastic finite displacement dynamic response analysis composed by finite element, Newmark β and Newton-Raphson methods. The tangent stiffness matrix, including geometrical and material nonlinearities is adopted in this study because bridge structures in regions of high seismic risk are not expected to respond elastically to the design earthquakes specified for the site. The damping of the structure is supposed as Rayleigh type which is considered advantageous with respect to the mass and stiffness proportional types, in order to obtain accurate results for numerically sensitive analysis. On the other hand, formulation of the dynamic problem, based on the equilibrium of energy, is presented as an alternative method to response quantities like force or displacement to examine the seismic damage effect on bridge structures. And finally, in the last part of the chapter, characteristics of the input earthquake waves used in dynamic analysis are analyzed, according to different parameters to represent a measure of the earthquake risk. It is concluded that the peak ground acceleration alone does not express the actual damage to structures, being necessary the analysis of other parameters related to the seismic energy content for a reliable evaluation of the real destructive power of earthquake ground motions.

Chapter 4 presents the three-dimensional effects of seismic isolation with LRB bearings on the Level II earthquake behaviour of curved viaducts. In order to quantify the benefits in seismic performance, non-linear responses of the non-isolated bridge are compared with those obtained for the isolated configuration. Furthermore, the nonlinear response comparison has been accomplished by extensive parametric studies conducted by varying those bearing design parameters, which represents the low temperature effect on LRB bearings and have a major influence on the overall bridge response. Finally, a trilinear analytical model of LRB bearings is introduced to accurately evaluate the influence of hardening of isolators at the high strains induced by near-fault earthquake ground motions.

A dynamic bearing property definition is introduced in this chapter, by cooperating the temperature conditions with the equations about the temperature

variation of performance, which practically simulates the temperature variation and temperature dependence performance of base isolation system applied in cold region.

Based on the dynamic analysis results, the essential facts emerging from this study indicates that base-isolation bearing systems provide a significant reduction in the seismic forces that the bridge structure must resist. The design philosophy applied to a non-isolated bearing supported viaduct focuses on the idea of concentrating most of the seismic forces on the pier with fixed support. However, seismic forces acting on piers of a bridge with isolation bearings are distributed uniformly between all piers and consequently, the resulting force which corresponds to an individual pier is sensibly reduced, as compared to this value for the viaduct with non-isolated bearings. This point makes an isolated bridge more effective since it is fundamental to limit peak shear forces transmitted from the superstructure to the top of piers, in such a way that bending moment transferred to the base of piers is limited.

The results indicate that LRB bearings effectively reduce the forces acting on bearings by lengthening the period of the bridge away from the dominant period of the ground motion, and by the energy dissipation through hysteretic behaviour of the lead core inserted in the isolation bearings. Piers with LRB isolation systems are protected, remaining under elastic range during the earthquakes, because these bearings do not transmit a level of shear force sufficient to damage them.

The analysis of energy-time variation has been proven to be very effective as an alternative method to examine the seismic damage effect on bridge structures. It is pointed out that depending on the type of bearing supports, the seismic energy transmitted into a bridge structure varies sensibly. The amount of energy inputted to the structure depends highly on the structural characteristics modified by bearings, such as the fundamental period of vibration and damping properties. In case of the viaduct with non-isolated bearings, a large amount of input energy is dissipated through strain energy, which indicates that almost the entire energy of the earthquake is transmitted into the structural elements of the bridge to be dissipated by inelastic deformation of the member which implies structural damage. For the model supported on LRB bearings, the amount of seismic energy input is predominately dissipated by hysteretic behaviour due to inelastic bearing deformation for LRB bearings. Thus a maximization of the energy dissipation at bearing level, reflected by the measured hysteresis curves, is a good indicator to reflect the effectiveness of the base-isolation systems.

However, The numerical results also clearly demonstrate that unsuitable bearing characteristics which in the present study is caused by the low temperature effect on LRB bearings, may considerably increase all bridge seismic responses. Therefore, the advantage of seismic isolation of substantially reducing the damage of bridges during earthquakes needs to be accomplished with a complete understanding of the isolation device design parameters, especially for a designer of cold regions.

Furthermore, hardening effect of LRB bearings tends to simultaneously increase the maximum forces acting on the bearing, reducing the maximum deformation. It is shown in this chapter, a proper designed base isolation system with slight hardening effect could drastically deteriorate under low temperature. The drastic increment of

stiffness definitely weakens the isolation function. Therefore the combination of low temperature effect and hardening effect may absolutely subvert the regular rule of performance of LRB, additional attention should be paid seriously.

In **Chapter 5** several parametrical studies have been carried out to evaluate the effect of long duration earthquake on the seismic response of the highway viaduct. In order to extend the application range of low temperature effect investigation, a long duration earthquake lasting about 1 minute is applied in this chapter. Subjected to a longer duration earthquake, temperature rising of base isolation devices is increased, and variation of bearing properties is also enlarged consequently. Combining the results of last chapter, more comprehensive conclusions of low temperature effect of base isolation system by seismic response analysis are drawn in this chapter.

Usually, whether low temperature effect should be considered in seismic response analysis was doubted, because during an earthquake event, the base isolation devices absorb earthquake energy and release it as heat. By intuition, such a great thermal behavior will raise the initial low temperature condition to room temperature level immediately. In this chapter, by adopting dynamic bearing property definition method and examining the numerical results, the necessity of considering low temperature effect, not only in a short-duration earthquake, but also in a long-duration earthquake, has been clearly indicated. More accurate seismic design considering not only performance but also low temperature effect should be taken into account in cold regions.

Chapter 6 deals with the overall three-dimensional seismic response of the viaduct equipped with HDR bearing system is investigated in detail through non-linear dynamic response analysis. The effect of the installation of high damping rubber bearings has been evaluated and compared with LRB system.

The numerical results show that HDR has better performance better than LRB under low temperature. With lower yield force and more yield stiffness usage, HDR could keep its flexibility. High damping rubber(HDR) material applies for such bearing devices not only to eliminate the necessity of installing lead plugs inside laminated rubber bearing but also to enhance seismic protection properties compared to LRB.

7.2 Recommendations for Further Research

Temperature dependence performance of base-isolation systems of highway viaducts offers many possibilities for further research. It is understood that the results obtained in previous studies are strictly dependent on the fixed performance configuration examined, i.e. the properties of base isolation bearings are constant in the earthquake event. But actually, earthquake energy is dissipated as heat by base isolation systems during hysteretic deformation loop. Therefore, heat output in the earthquake event increase the temperature of base isolation bearings. In the present

study, additional investigation has been conducted to study the response of variable performance of base isolation system, which is time and temperature dependence. In particular, application of heat conduction technology to different types of base isolation systems, acquiring the accurate temperature value in specified time and finally putting a dynamic properties definition of base isolation systems into use in the seismic analysis.

A further area for research concerns more detailed evaluation of HDR bearing system in cold region, which has better performance than LRB system in this study. As mentioned above, seismic protection capacity should be balanced with deformation, which may be the main problem of application of HDR bearing system.

It is also suggested to develop more temperature independence isolator devices. Since additional constant temperature equipment for base isolation systems is obviously inefficient, temperature independence materials and structures could be a better idea. And this is actually being studied by several manufacturers.